



A RELAY-ROVER DIFFERENTIAL GAME

THESIS

Youngdong Choi, Captain, ROKAF

AFIT/GAE/ENY/11-J06

**DEPARTMENT OF THE AIR FORCE
AIR UNIVERSITY**

AIR FORCE INSTITUTE OF TECHNOLOGY

Wright-Patterson Air Force Base, Ohio

APPROVED FOR PUBLIC RELEASE; DISTRIBUTION UNLIMITED

The views expressed in this thesis are those of the author and do not reflect the official policy or position of the United States Air Force, Department of Defense, or the United States Government. This material is declared a work of the U.S. Government and is not subject to copyright protection in the United States.

AFIT/GAE/ENY/11-J06

A RELAY-ROVER DIFFERENTIAL GAME

THESIS

Presented to the Faculty

Department of Aeronautics and Astronautics

Graduate School of Engineering and Management

Air Force Institute of Technology

Air University

Air Education and Training Command

In Partial Fulfillment of the Requirements for the
Degree of Master of Science in Aeronautical Engineering

Youngdong Choi, BS

Captain, ROKAF

June 2011

APPROVED FOR PUBLIC RELEASE; DISTRIBUTION UNLIMITED

A RELAY-ROVER DIFFERENTIAL GAME

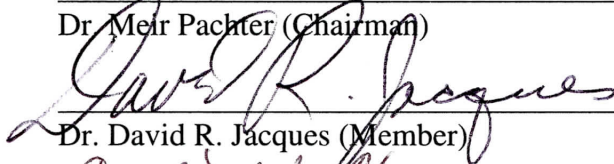
Youngdong Choi, BS

Captain, ROKAF

Approved:



Dr. Meir Pachter (Chairman)



Dr. David R. Jacques (Member)



Frederick G. Harmon, Lt Col (Member)

May 16, 2011
Date

16 MAY 2011
Date

16 May 2011
Date

Abstract

Guidance laws are developed to optimally position a relay Micro-UAV (MAV) to provide an operator at the base with real-time Intelligence, Surveillance, and Reconnaissance (ISR) by relaying communication and video signals when the rover MAV performing the ISR mission is out of radio contact range with the base. The ISR system is comprised of two MAVs, the Relay and the Rover, and a Base. The Relay strives to minimize the radio frequency (RF) power required for maintaining communications, while the Rover performs the ISR mission, which may maximize the required RF power. The optimal control of the Relay MAV entails the solution of a differential game. Suboptimal solutions are also analyzed to gain insight into the solution of the differential game. One suboptimal approach investigated envisages the Rover to momentarily remain stationary and solves for the optimal path for the Relay to minimize the RF power requirement during the planning horizon: the one – sided optimal control problem is solved in closed form. Another suboptimal approach is based upon the geometry of the system: The midpoint between the Rover and the Base is the location which minimizes the RF power required, so the Relay heads toward that point—assuming that the Rover is stationary. At the same time, to maximize the required RF power, the Rover runs away from the Relay. In this work the differential game is fully analyzed. The geometry based suboptimal solution is shown to be the optimal solution in the endgame. Isaac's method is then applied to obtain the optimal trajectories in the differential game.

Acknowledgments

First and foremost I would like to thank Dr. Pachter for his patience and support. He was always willing to share his time with my questions. Without his advice I could not have reached this result in a timely fashion. His mentorship will be unforgettable in my life.

Additionally, I want to thank my lovely wife and daughter. Their sacrifice, encouragement and love inspired me to overcome difficult moments and excel my abilities. Thank you for always being with me.

Lastly, I would like to express my sincere appreciation to the Republic of Korea Air Force for providing me this invaluable opportunity.

Youngdong Choi

Table of Contents

	Page
Abstract	iv
Acknowledgments	v
Table of Contents	vi
List of Figures	viii
List of Symbols	xv
I. Introduction	1
I.1. Background	1
I.2. Research Objectives	1
II. Literature Review	3
II.1. System Definition	4
III. Methodology	10
III.1. The End-Game	10
III.2. Special Case – Optimal Control Problem	13
III.3. Analytic Solution of the Optimal Control Problem	22
III.4. Discussion	28
III.5. Differential Game	30
III.6. Optimal Play	36
IV. Analysis and Results	41
IV.1. Optimal Trajectories of Rover and Relay for different speed ratios α , and	41
IV.2. Optimal Trajectories of Rover and Relay for different r_{E_r} , r_{O_r} , θ_T	54
IV.3. Comparison of the End Game Control Law and Optimal Control Law	58
V. Conclusions and Recommendations	63

V.1. Conclusions	63
V.2. Recommendations for Future Research.....	63
Appendix A – Additional Optimal play.....	65
Appendix B – Geometry	125
Appendix C – New Parameterization of Family of “Endpoints”	128
Appendix D – Suboptimal Solution.....	138
Geometric Approach	138
Numerical Results	141
Bibliography	144

List of Figures

	Page
Figure 1: Schematic of Relay System	5
Figure 2: End Game	12
Figure 3: End Points Manifold.....	19
Figure 4: The Optimal Flow Field	20
Figure 5: Trajectory in Cartesian Plane	22
Figure 6: The domain of definition of the value function.....	28
Figure 7: Pursuit - Evasion	33
Figure 8: Optimal Relay Trajectories in the State Space.....	36
Figure 9: The Construction of Optimal Trajectories in The Realistic Space.....	38
Figure 10: Optimal trajectories of Rover and Relay for $\xi = 10^\circ$, $\alpha = 0.5$, $r_{O_r} = 1, 2, 3$	41
Figure 11: Optimal trajectories of Rover and Relay for $\xi = 10^\circ$, $\alpha = 0.5$, $1, 1.5$, $r_{O_r} = 1$	42
Figure 12: Optimal trajectories of Rover and Relay as ξ changes	43
Figure 13: Optimal trajectories of Rover and Relay for $\alpha = 0.5$, $\xi = 0^\circ$	44
Figure 14: Time history of the States, Costates and Controls. $\alpha = 0.5$, $\xi = 0^\circ$	45
Figure 15: Optimal trajectories of Rover and Relay. $\alpha = 0.5$, $\xi = 30^\circ$, $r_{O_r} = 1$	46
Figure 16: Time history of the States, Costates and Controls. $\alpha = 0.5$, $\xi = 30^\circ$, $r_{O_r} = 1$	47
Figure 17: Time history of the States, Costates and Controls. $\alpha = 1$, $\xi = 0^\circ$, $r_{O_r} = 1$	51

Figure 18: Time history of the States, Costates and Controls. $\alpha = 2$, $\xi = 180^\circ$, $r_{O_T} = 1$.. 53

Figure 19: Optimal Trajectory of Relay When $r_{E_T} = \frac{1}{4}$, $r_{O_T} = \frac{3}{4}$, $\alpha = 0$, $\theta_T = 20^\circ$ 54

Figure 20: Optimal Trajectories of Rover and Relay When

$r_{E_T} = \frac{1}{4}$, $r_{O_T} = 1$, $\alpha = 1$, $\theta_T = 1^\circ, 2^\circ, 20^\circ, 30^\circ, 40^\circ$ 55

Figure 21: Optimal Trajectories of Rover and Relay When

$r_{E_T} = \frac{3}{4}$, $r_{O_T} = 1$, $\alpha = 1$, $\theta_T = 1^\circ, 2^\circ, 20^\circ, 30^\circ, 40^\circ$ 56

Figure 22: Optimal Trajectories of Rover and Relay When

$r_{E_T} = \frac{1}{4}$, $r_{O_T} = \frac{3}{4}$, $\alpha = 1$, $\theta_T = 20^\circ$ 57

Figure 23: Comparison of the End Game Control Law and Optimal Control Law

$r_{E_T} = 0.5$, $r_{O_T} = 1$, $\alpha = 1$, $\xi = 0^\circ$ 58

Figure 24: Comparison of the End Game Control Law and Optimal Control Law

$r_{E_T} = 0.5$, $r_{O_T} = 1$, $\alpha = 1$, $\xi = 30^\circ$ 59

Figure 25: Comparison of the End Game Control Law and Optimal Control Law

$r_{E_T} = 0.5$, $r_{O_T} = 1$, $\alpha = 1$, $\xi = 60^\circ$ 59

Figure 26: Comparison of the End Game Control Law and Optimal Control Law

$r_{E_T} = 0.5$, $r_{O_T} = 1$, $\alpha = 1$, $\xi = 90^\circ$ 60

Figure 27: Comparison of the End Game Control Law and Optimal Control Law

$r_{E_T} = 0.5$, $r_{O_T} = 1$, $\alpha = 1$, $\xi = 120^\circ$ 60

Figure 28: Comparison of the End Game Control Law and Optimal Control Law

$r_{E_T} = 0.5, r_{O_T} = 1, \alpha = 1, \xi = 150^\circ$ 61

Figure 29: Comparison of the End Game Control Law and Optimal Control Law

$r_{E_T} = 0.5, r_{O_T} = 1, \alpha = 1, \xi = 180^\circ$ 61

Figure 30: Comparison of the End Game Control Law and Optimal Relay Control Law

$r_{E_T} = 0.5, r_{O_T} = 1, \alpha = 0, \xi = 90^\circ$ 62

Figure A. 1: Optimal trajectories of Rover and Relay. $\alpha = 0.5, \xi = 60^\circ, r_{O_T} = 1$ 65

Figure A. 2: Time history of the States, Costates and Controls. $\alpha = 0.5, \xi = 60^\circ, r_{O_T} = 1$
..... 66

Figure A. 3: Optimal trajectories of Rover and Relay. $\alpha = 0.5, \xi = 90^\circ, r_{O_T} = 1$ 67

Figure A. 4: Time history of the States, Costates and Controls. $\alpha = 0.5, \xi = 90^\circ, r_{O_T} = 1$
..... 68

Figure A. 5: Optimal trajectories of Rover and Relay. $\alpha = 0.5, \xi = 150^\circ, r_{O_T} = 1$ 69

Figure A. 6: Time history of the States, Costates and Controls $\alpha = 0.5, \xi = 150^\circ, r_{O_T} = 1$
..... 70

Figure A. 7: Optimal trajectories of Rover and Relay. $\alpha = 0.5, \xi = 180^\circ, r_{O_T} = 1$ 71

Figure A. 8: Time history of the States, Costates and Controls $\alpha = 0.5, \xi = 180^\circ, r_{O_T} = 1$
..... 72

Figure A. 9: Optimal trajectories of Rover and Relay. $\alpha = 1, \xi = 30^\circ, r_{O_T} = 1$ 73

Figure A. 10: Time history of the States, Costates and Controls. $\alpha = 1, \xi = 30^\circ, r_{O_r} = 1$	
.....	74
Figure A. 11: Optimal trajectories of Rover and Relay. $\alpha = 1, \xi = 60^\circ, r_{O_r} = 1$	75
Figure A. 12: Time history of the States, Costates and Controls. $\alpha = 1, \xi = 60^\circ, r_{O_r} = 1$	
.....	76
Figure A. 13: Optimal trajectories of Rover and Relay. $\alpha = 1, \xi = 90^\circ, r_{O_r} = 1$	77
Figure A. 14: Time history of the States, Costates and Controls. $\alpha = 1, \xi = 90^\circ, r_{O_r} = 1$	
.....	78
Figure A. 15: Optimal trajectories of Rover and Relay. $\alpha = 1, \xi = 120^\circ, r_{O_r} = 1$	79
Figure A. 16: Time history of the States, Costates and Controls. $\alpha = 1, \xi = 120^\circ, r_{O_r} = 1$	
.....	80
Figure A. 17: Optimal trajectories of Rover and Relay. $\alpha = 1, \xi = 150^\circ, r_{O_r} = 1$	81
Figure A. 18: Time history of the States, Costates and Controls. $\alpha = 1, \xi = 150^\circ, r_{O_r} = 1$	
.....	82
Figure A. 19: Optimal trajectories of Rover and Relay. $\alpha = 1, \xi = 180^\circ, r_{O_r} = 1$	83
Figure A. 20: Time history of the States, Costates and Controls. $\alpha = 1, \xi = 180^\circ, r_{O_r} = 1$	
.....	84
Figure A. 21: Optimal trajectories of Rover and Relay. $\alpha = 1.5, \xi = 0^\circ, r_{O_r} = 1$	85
Figure A. 22: Time history of the States, Costates and Controls. $\alpha = 1.5, \xi = 0^\circ, r_{O_r} = 1$	
.....	86

Figure A. 23: Optimal trajectories of Rover and Relay. $\alpha = 1.5$, $\xi = 30^\circ$, $r_{O_r} = 1$	87
Figure A. 24: Time history of the States, Costates and Controls. $\alpha = 1.5$, $\xi = 30^\circ$, $r_{O_r} = 1$	88
Figure A. 25: Optimal trajectories of Rover and Relay. $\alpha = 1.5$, $\xi = 60^\circ$, $r_{O_r} = 1$	89
Figure A. 26: Time history of the States, Costates and Controls. $\alpha = 1.5$, $\xi = 60^\circ$, $r_{O_r} = 1$	90
Figure A. 27: Optimal trajectories of Rover and Relay. $\alpha = 1.5$, $\xi = 90^\circ$, $r_{O_r} = 1$	91
Figure A. 28: Time history of the States, Costates and Controls. $\alpha = 1.5$, $\xi = 90^\circ$, $r_{O_r} = 1$	92
Figure A. 29: Optimal trajectories of Rover and Relay. $\alpha = 1.5$, $\xi = 120^\circ$, $r_{O_r} = 1$	93
Figure A. 30: Time history of the States, Costates and Controls $\alpha = 1.5$, $\xi = 120^\circ$, $r_{O_r} = 1$	94
Figure A. 31: Optimal trajectories of Rover and Relay. $\alpha = 1.5$, $\xi = 150^\circ$, $r_{O_r} = 1$	95
Figure A. 32: Time history of the States, Costates and Controls $\alpha = 1.5$, $\xi = 150^\circ$, $r_{O_r} = 1$	96
Figure A. 33: Optimal trajectories of Rover and Relay. $\alpha = 1.5$, $\xi = 180^\circ$, $r_{O_r} = 1$	97
Figure A. 34: Time history of the States, Costates and Controls $\alpha = 1.5$, $\xi = 180^\circ$, $r_{O_r} = 1$	98
Figure A. 35: Optimal trajectories of Rover and Relay. $\alpha = 1.9$, $\xi = 0^\circ$, $r_{O_r} = 1$	99

Figure A. 36: Time history of the States, Costates and Controls. $\alpha = 1.9$, $\xi = 0^\circ$, $r_{O_r} = 1$	100
Figure A. 37: Optimal trajectories of Rover and Relay. $\alpha = 1.9$, $\xi = 30^\circ$, $r_{O_r} = 1$	101
Figure A. 38: Time history of the States, Costates and Controls $\alpha = 1.9$, $\xi = 30^\circ$, $r_{O_r} = 1$	102
Figure A. 39: Optimal trajectories of Rover and Relay. $\alpha = 1.9$, $\xi = 60^\circ$, $r_{O_r} = 1$	103
Figure A. 40: Time history of States, Costates and Controls. $\alpha = 1.9$, $\xi = 60^\circ$, $r_{O_r} = 1$	104
Figure A. 41: Optimal trajectories of Rover and Relay. $\alpha = 1.9$, $\xi = 90^\circ$, $r_{O_r} = 1$	105
Figure A. 42: Time history of the States, Costates and Controls $\alpha = 1.9$, $\xi = 90^\circ$, $r_{O_r} = 1$	106
Figure A. 43: Optimal trajectories of Rover and Relay. $\alpha = 1.9$, $\xi = 120^\circ$, $r_{O_r} = 1$	107
Figure A. 44: Time history of the States, Costates and Controls $\alpha = 1.9$, $\xi = 120^\circ$, $r_{O_r} = 1$	108
Figure A. 45: Optimal trajectories of Rover and Relay. $\alpha = 1.9$, $\xi = 150^\circ$, $r_{O_r} = 1$	109
Figure A. 46: Time history of the States, Costates and Controls $\alpha = 1.9$, $\xi = 150^\circ$, $r_{O_r} = 1$	110
Figure A. 47: Optimal trajectories of Rover and Relay. $\alpha = 1.9$, $\xi = 180^\circ$, $r_{O_r} = 1$	111
Figure A. 48: Time history of the States, Costates and Controls $\alpha = 1.9$, $\xi = 180^\circ$, $r_{O_r} = 1$	112

Figure A. 49: Optimal trajectories of Rover and Relay. $\alpha = 2$, $\xi = 0^\circ$, $r_{O_r} = 1$	113
Figure A. 50: Time history of the States, Costates and Controls. $\alpha = 2$, $\xi = 0^\circ$, $r_{O_r} = 1$	114
Figure A. 51: Optimal trajectories of Rover and Relay. $\alpha = 2$, $\xi = 30^\circ$, $r_{O_r} = 1$	115
Figure A. 52: Time history of the States, Costates and Controls. $\alpha = 2$, $\xi = 30^\circ$, $r_{O_r} = 1$	116
Figure A. 53: Optimal trajectories of Rover and Relay. $\alpha = 2$, $\xi = 60^\circ$, $r_{O_r} = 1$	117
Figure A. 54: Time history of the States, Costates and Controls. $\alpha = 2$, $\xi = 60^\circ$, $r_{O_r} = 1$	118
Figure A. 55: Optimal trajectories of Rover and Relay. $\alpha = 2$, $\xi = 90^\circ$, $r_{O_r} = 1$	119
Figure A. 56: Time history of the States, Costates and Controls. $\alpha = 2$, $\xi = 90^\circ$, $r_{O_r} = 1$	120
Figure A. 57: Optimal trajectories of Rover and Relay. $\alpha = 2$, $\xi = 120^\circ$, $r_{O_r} = 1$	121
Figure A. 58: Time history of the States, Costates and Controls. $\alpha = 2$, $\xi = 120^\circ$, $r_{O_r} = 1$	122
Figure A. 59: Optimal trajectories of Rover and Relay. $\alpha = 2$, $\xi = 150^\circ$, $r_{O_r} = 1$	123
Figure A. 60: Time history of the States, Costates and Controls. $\alpha = 2$, $\xi = 150^\circ$, $r_{O_r} = 1$	124
Figure B. 1: Schematic of Fixed Points Showing Isocost Circle.....	126
Figure C. 1: End States' Manifold	128

Figure C. 2: State Space.....	129
Figure D. 1: Schematic of Relay System Showing the Midpoint.....	138
Figure D. 2: Schematic of Relay System Showing Isocost Circle.....	139
Figure D. 3: Relative Spatial Results for $T = .25$, $\alpha = 1$, $r_{E_0} = .5$, $r_{O_0} = 1$ and $\theta_0 = \frac{\pi}{6}$	142
Figure D. 4: Relative Spatial Results for $T = 1$, $\alpha = 1$, $r_{E_0} = .5$, $r_{O_0} = 1$ and $\theta_0 = \frac{\pi}{3}$	143

List of Symbols

B = Base

E = Relay MAV

\mathcal{H} = Hamiltonian of System

M = Midpoint Between Rover and Base

O = Rover MAV

r_E = Distance of Relay MAV from Base

r_O = Distance of Rover MAV from Base

T = Planning Horizon of Algorithm

V_E = Velocity of Relay

V_O = Velocity of Rover

\mathcal{y} = Objective Function

α = Non-dimensional Speed Ratio ($\alpha = V_O / V_E$)

θ = Included Angle of the Radials from the Base to the Relay and the Rover

λ = General Reference to All Co-States of a System

λ_X = Co-State of State X

φ = Relative Course Angle of Relay

ψ = Relative Course Angle of Rover

ξ = Angle of approach of mid-point(“Sweet Spot”)

A RELAY-ROVER DIFFERENTIAL GAME

I. Introduction

I.1. Background

Unmanned Aerial Vehicles (UAVs) are prevalent in current military operations. UAVs vary in size and mission. While some UAVs are the same size as aircraft, others are man-portable and can be carried in a backpack. These man-portable Micro-UAVs (MAVs) utilized by small tactical units are not supported by satellite communications and use radio frequency (RF) modems. High frequency radio communications are range limited. The MAVs considered in this paper are utilized for Intelligence, Surveillance and Reconnaissance (ISR) and will therefore be referred to as ISR MAVs or as Rovers [1].

The Base may lose communication (and controllability) with deployed ISR MAVs/Rovers if the Rovers stray far away. In this thesis guidance laws are developed to optimally position a Relay MAV to provide the operator at the Base with real-time ISR by relaying communication and sensor data while allowing for extended range Rover operations. The Relay-Rover interaction is modeled as a differential game whose solution yields the optimal Relay strategy.

I.2. Research Objectives

The ISR mission is considered where a rover MAV is controlled by an operator and tasked to fly to locations where targets need to be inspected. Since the rover MAV might get out of radio communication range with the base station where the operator is

located, it is envisaged that a relay MAV will be interposed between the rover and the base station, so that connectivity will be maintained.

In order to reduce the workload of the operator, the relay MAV will be autonomous. In other words, a guidance law for the relay MAV will be developed such that the relay MAV will automatically position itself between the rover and the base, with a view to reducing the RF power required for communications – this, despite the maneuvers of the rover. The worst case scenario is considered, where the rover is “giving a hard time” to the relay MAV. This calls for a min–max optimal control formulation, a differential game formulation.

II. Literature Review

To better appreciate the nature of the thesis research, it is necessary to first discuss previous relevant works. Recent studies have produced two general designs for a reliable and robust communication network utilizing mobile communication nodes. The first design consists of one or more mobile communication nodes which form a single chain to relay information between the source and the destination. This is referred to as a “single-flow network.” Many designs for single-flow networks use a fixed source and fixed destination, though they do not discount the possibility of a mobile destination (Dixon and Frew, 2007; Goldenberg et al., 2004). The second design consists of multiple mobile communication nodes which form a “mesh-like network”. This configuration adds fault-tolerance for a more robust network (Basu and Redi, 2004; Floreano et al., 2007). However, a “mesh-like network” would be ill suited for the envisioned ISR and engagement system due to desired unit covertness while engaging a high value target. In this respect, Brown et al. have developed the Ad-hoc UAV Ground Network (AUGNet) test bed, showing the practicality of UAV-based mobile communication nodes using IEEE 802.11b wireless routers (Brown et al., 2004). The proposed ISR and engagement system may have a network design similar to AUGNet but the Relay must still have an optimal mobility control law in order optimize network communications.

Dixon and Frew have utilized the AUGNet system with an extremum seeking controller to study cooperative electronic chaining while maximizing the signal-to-noise ratio between the nodes of the multi-hop network (Dixon and Frew, 2007). Goldenberg et al. have shown that communication nodes should be evenly spaced on the line between the source and

destination in order to minimize the energy cost of communicating between the two (Goldenberg et al., 2004).

This line of research was initiated by Lt. John H. Hansen in 2008, in his thesis ‘Optimal Guidance of A Relay MAV for ISR Support Beyond Line-Of-Sight’[7]. In this thesis, the basic system definition from his work will be introduced again and used for further research. Additional work, including limited experimentation and hardware testing was done by the students of Dr. David R. Jacques.

Building on these foundations, in this thesis the underlying differential game theory is further developed.

II.1. System Definition

It is assumed that the rElay (E) MAV is cognizant of the rOver’s (O) instantaneous position and, obviously, own ship position. As far as the RF power requirements are concerned, this is determined by their distance from the Base (B) and the rOver-rElay separation. Thus, the state is the distance r_E of the rElay from the Base, the distance r_O of the rOver to the Base, and the angle θ included between the radials from the Base to the rElay and the rOver. This angle is measured clockwise. The MAVs have simple motion. The control for each MAV is its relative heading angle measured clock-wise from its radial from the Base. Figure 1 provides a visualization of the kinematics. The differential equations of motion are

$$\left. \begin{aligned} \dot{r}_E &= V_E \cos \varphi & , r_E(0) &= r_{E_0} \\ \dot{r}_O &= V_O \cos \psi & , r_O(0) &= r_{O_0} \\ \dot{\theta} &= \frac{1}{r_O} V_O \sin \psi - \frac{1}{r_E} V_E \sin \varphi & , \theta(0) &= \theta_0, 0 \leq t \leq T \end{aligned} \right\} \quad (1)$$

T is the planning horizon utilized by the control algorithm. The cost functional is indicative of the RF power required and is the time averaged sum of the squares of the distance between the rElay and the rOver and between the rElay and the Base:

$$\mathcal{Y} = \int_0^T \left(\overline{EO}^2(t) + \overline{BE}^2(t) \right) dt$$

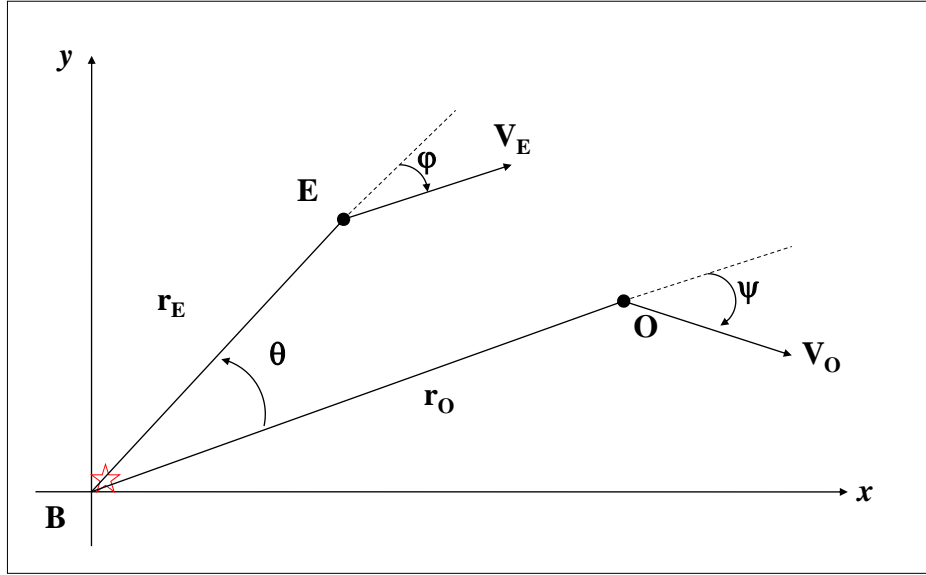


Figure 1: Schematic of Relay System

The points E , B and O in \mathbb{R}^2 represent the positions of the rElay, Base and rOver respectively. These three points form a triangle which can be utilized to calculate the distance \overline{EO} by the law of cosines.

$$\overline{EO}^2(t) = r_E^2 + r_O^2 - 2r_E r_O \cos \theta$$

Hence the cost functional is

$$\mathcal{Y} = \int_0^T (2r_E^2 + r_O^2 - 2r_E r_O \cos \theta) dt \quad (2)$$

The objective is to minimize the average RF power required for maintaining communications. The control available to accomplish this task is limited to setting the course angle φ of the rElay, while the rOver performs the ISR mission: in a worst case scenario, one might assume that the rOver is working to maximize the cost functional. The optimization problem is then a differential game [2] where the rElay's control is its relative heading φ and the rOver's control is its relative heading ψ .

The system is analyzed by first non-dimensionalizing the states and the parameters. The velocities are scaled by the velocity of the rElay (V_E), yielding a non-dimensional speed ratio α . The distances are scaled by d , where d is a characteristic length, say $d = V_E T$. Set $r_E := \frac{r_E}{d}$, $r_O := \frac{r_O}{d}$, $t := \frac{V_E}{d} \cdot t$, $T := \frac{V_E}{d} \cdot T$ and the speed ratio $\alpha \equiv \frac{V_O}{V_E}$. Using these non-dimensional variables and parameters, the two sided optimization problem now becomes

$$\left. \begin{aligned} \min_{\varphi} \max_{\psi} \mathcal{Y} &= \int_0^T (2r_E^2 + r_O^2 - 2r_E r_O \cos \theta) dt \\ s.t. \quad & \left. \begin{aligned} \dot{r}_E &= \cos \varphi & , \quad r_E(0) &= r_{E_0} \\ \dot{r}_O &= \alpha \cos \psi & , \quad r_O(0) &= r_{O_0} \\ \dot{\theta} &= \frac{1}{r_O} \alpha \sin \psi - \frac{1}{r_E} \sin \varphi & , \quad \theta(0) &= \theta_0, \quad 0 \leq t \leq T \end{aligned} \right\} \end{aligned} \right\} \quad (3)$$

The problem parameters are the speed ratio $\alpha \geq 0$ and the planning horizon $T > 0$.

Since the optimal control problem only makes sense if the rOver is closer to the rElay than to the Base (B), the following must hold.

$$r_E \leq 2r_O \cos \theta.$$

Thus, since the problem is symmetric about the $\theta = 0$ axis, the state space is

$$\left\{ (r_E, r_O, \theta) \mid 0 \leq \theta \leq \frac{\pi}{2}, 0 \leq r_E \leq 2r_O \cos \theta \right\}$$

To solve the differential game, the Hamiltonian is introduced in eq. (4),

$$\mathcal{H} = -2r_E^2 - r_O^2 + 2r_E r_O \cos \theta + \lambda_{r_E} \cos \varphi + \lambda_{r_O} \alpha \cos \psi + \lambda_\theta \left(\frac{1}{r_O} \alpha \sin \psi - \frac{1}{r_E} \sin \varphi \right) \quad (4)$$

where λ_{r_E} , λ_{r_O} and λ_θ are the system co-states.

According to the Pontryagin Maximum Principle (PMP) [3], the differential equations for the co-states are

$$\left. \begin{aligned} \dot{\lambda}_{r_E} &= 4r_E - 2r_O \cos \theta - \frac{\lambda_\theta \sin \varphi}{r_E^2}, \quad \lambda_{r_E}(T) = 0 \\ \dot{\lambda}_{r_O} &= 2r_O - 2r_E \cos \theta + \alpha \frac{\lambda_\theta \sin \psi}{r_O^2}, \quad \lambda_{r_O}(T) = 0 \\ \dot{\lambda}_\theta &= 2r_E r_O \sin \theta, \quad \lambda_\theta(T) = 0 \end{aligned} \right\} \quad (5)$$

and the optimality condition is given by $\max_{\varphi} \min_{\psi} \mathcal{H}$, namely

$$\begin{aligned} \frac{\partial \mathcal{H}}{\partial \varphi} &= -\lambda_{r_E} \sin \varphi - \frac{\lambda_\theta \cos \varphi}{r_E} = 0 \\ \Rightarrow \tan \varphi^* &= -\frac{\lambda_\theta}{\lambda_{r_E} r_E}, \end{aligned} \quad (6)$$

or,

$$\sin \varphi^* = -\frac{\lambda_\theta}{\sqrt{\lambda_{r_E}^2 r_E^2 + \lambda_\theta^2}}, \quad \cos \varphi^* = \frac{r_E \lambda_{r_E}}{\sqrt{\lambda_{r_E}^2 r_E^2 + \lambda_\theta^2}} \quad (7)$$

$$\frac{\partial \mathfrak{H}}{\partial \psi} = -\lambda_{r_O} \alpha \sin \psi + \frac{\lambda_\theta \alpha \cos \psi}{r_O} = 0$$

$$\Rightarrow \tan \psi^* = \frac{\lambda_\theta}{\lambda_{r_O} r_O},$$

or,

$$\sin \psi^* = -\frac{\lambda_\theta}{\sqrt{r_O^2 \lambda_{r_O}^2 + \lambda_\theta^2}}, \quad \cos \psi^* = \frac{r_O \lambda_{r_O}}{\sqrt{r_O^2 \lambda_{r_O}^2 + \lambda_\theta^2}} \quad (8)$$

The second-order sufficiency condition for φ is

$$\frac{\partial^2 \mathfrak{H}}{\partial \varphi^2} = -\lambda_{r_E} \cos \varphi + \frac{\lambda_\theta \sin \varphi}{r_E} < 0$$

and inserting the expression for φ^* from (7) yields

$$\begin{aligned} \lambda_\theta + \frac{(r_E \lambda_{r_E})^2}{\lambda_\theta} &< 0 \\ \Rightarrow \lambda_\theta(t) &< 0 \quad \forall \quad 0 \leq t < T \end{aligned}$$

Similarly,

$$\frac{\partial^2 \mathfrak{H}}{\partial \psi^2} = -\lambda_{r_O} \alpha \cos \psi - \frac{\lambda_\theta \alpha \sin \psi}{r_O} > 0$$

and inserting the expression for ψ^* from (7) yields

$$\lambda_\theta + \frac{(r_o \lambda_{r_o})^2}{\lambda_\theta} < 0 \quad (9)$$

$$\Rightarrow \lambda_\theta(t) < 0 \quad \forall \quad 0 \leq t < T$$

The expressions for φ^* and ψ^* given in Equations (7) and (8) can also be used to rewrite the state and co-state equations only in terms of the states and co-states. A standard, albeit nonlinear, Two-Point Boundary Value Problem (TPBVP) on the interval $t \in [0, T]$ is obtained:

$$\left. \begin{aligned} \dot{r}_E &= \frac{\lambda_{r_E} r_E}{\sqrt{\lambda_{r_E}^2 r_E^2 + \lambda_\theta^2}}, & r_E(0) &= r_{E_0} \\ \dot{r}_O &= \frac{-\alpha \lambda_{r_O} r_O}{\sqrt{\lambda_{r_O}^2 r_O^2 + \lambda_\theta^2}}, & r_O(0) &= r_{O_0} \\ \dot{\theta} &= \frac{\lambda_\theta}{r_E \sqrt{\lambda_{r_E}^2 r_E^2 + \lambda_\theta^2}} - \frac{\alpha \lambda_\theta}{r_O \sqrt{\lambda_{r_O}^2 r_O^2 + \lambda_\theta^2}}, & \theta(0) &= \theta_0 \\ \dot{\lambda}_{r_E} &= 4r_E - 2r_O \cos \theta + \frac{\lambda_\theta^2}{r_E^2 \sqrt{\lambda_{r_E}^2 r_E^2 + \lambda_\theta^2}}, & \lambda_{r_E}(T) &= 0 \\ \dot{\lambda}_{r_O} &= 2r_O - 2r_E \cos \theta - \frac{\alpha \lambda_\theta^2}{r_O^2 \sqrt{\lambda_{r_O}^2 r_O^2 + \lambda_\theta^2}}, & \lambda_{r_O}(T) &= 0 \\ \dot{\lambda}_\theta &= 2r_E r_O \sin \theta, & \lambda_\theta(T) &= 0, \quad 0 \leq t \leq T \end{aligned} \right\} \quad (10)$$

Note: if $\theta_T \neq 0$, the costate $\lambda_\theta(t) < 0 \quad \forall \quad 0 \leq t < T$; also $\sqrt{\lambda_{r_E}^2 r_E^2 + \lambda_\theta^2} \neq 0$,

$$\sqrt{\lambda_{r_O}^2 r_O^2 + \lambda_\theta^2} \neq 0 \quad \forall \quad 0 \leq t < T.$$

III. Methodology

III.1. The End-Game

At time $t=T$ where the co-states vanish, and since the control variables do not explicitly feature in the cost functional, it is impossible to calculate the terminal controls by applying the PMP and maximizing and minimizing the Hamiltonian (4); obviously, equations (10) don't apply because $\sqrt{\lambda_{r_E}^2 r_E^2 + \lambda_\theta^2} = 0$. The end game requires special attention.

Since the end state is free - that's why the co-states vanish at $t=T$ - the rElay's and rOver's optimal strategies at $t=T$ are myopic. Thus, from first principles, the rElay would want the integrand in the cost functional

$$L(r_E, r_O, \theta) = 2r_E^2 + r_O^2 - 2r_E r_O \cos \theta$$

to be minimized. Similarly, the rOver would want the integrand in the cost functional to be maximized. However the control variables φ and ψ do not directly feature in L . Hence the rElay minimizes and the rOver maximizes the temporal derivative of L , evaluated at $t=T$:

$$\begin{aligned} \frac{d}{dt}L &= 2 \left[2r_E \cos \varphi + \alpha r_O \cos \psi - r_O \cos \varphi \cos \theta - \alpha r_E \cos \psi \cos \theta + r_E r_O \sin \theta \left(\alpha \frac{1}{r_O} \sin \psi - \frac{1}{r_E} \sin \varphi \right) \right] \\ &= 2 \left\{ (2r_E - r_O \cos \theta) \cos \varphi - r_O \sin \theta \sin \varphi + \alpha \left[(r_O - r_E \cos \theta) \cos \psi + r_E \sin \theta \sin \psi \right] \right\} \end{aligned}$$

The rElay and rOver solve the respective static optimization problems

$$\min_{\varphi} \left[(2r_E - r_O \cos \theta) \cos \varphi - r_O \sin \theta \sin \varphi \right] \quad (11)$$

and

$$\max_{\psi} \left[(r_o - r_E \cos \theta) \cos \psi + r_E \sin \theta \sin \psi \right] \quad (12)$$

Concerning eq. (11): minimizing in φ the derivative of the integrand at time $t=T$ yields the rElay's optimal terminal control

$$\cos(\varphi^*(T)) = \frac{r_{O_T} \cos \theta_T - 2r_{E_T}}{\sqrt{4r_{E_T}^2 + r_{O_T}^2 - 4r_{E_T} r_{O_T} \cos \theta_T}}, \quad \sin(\varphi^*(T)) = \frac{r_{O_T} \sin \theta_T}{\sqrt{4r_{E_T}^2 + r_{O_T}^2 - 4r_{E_T} r_{O_T} \cos \theta_T}},$$

provided that r_{E_T}, r_{O_T} and θ_T are s.t. the following is not the case: $r_{E_T} = \frac{1}{2}r_{O_T}$ and $\theta_T = 0$.

Here, $(r_{E_T}, r_{O_T}, \theta_T)$ denote the terminal state at time $t=T$.

When $\theta_T = 0$, eq. (11) yields

$$\varphi^*(T) = \begin{cases} 0 & \text{if } r_{E_T} < \frac{1}{2}r_{O_T} \\ \pi & \text{if } r_{E_T} > \frac{1}{2}r_{O_T} \end{cases}$$

An inspection of Fig. 2 tells us that in the end game, at time $t=T$, the rElay heads toward the midpoint M of the segment \overline{BO} .

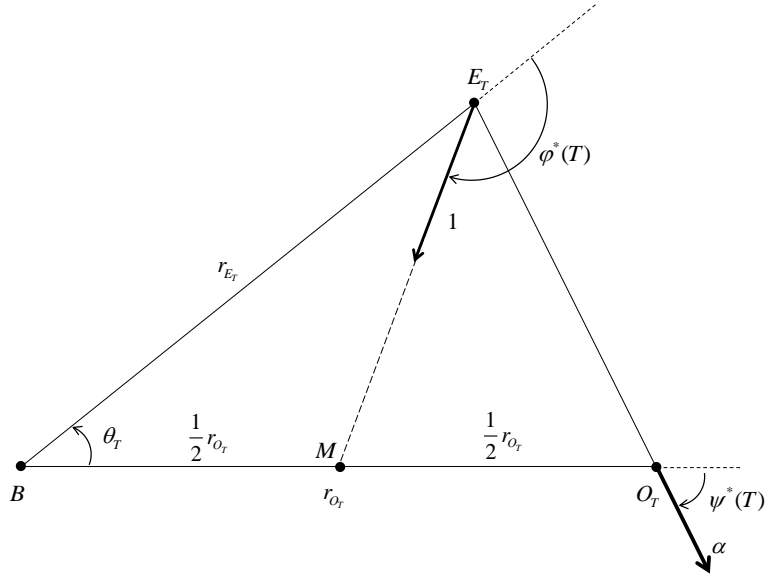


Figure 2: End Game

Concerning eq. (12), maximizing in ψ the derivative of the integrand at time $t=T$ yields the rOver optimal terminal control

$$\cos(\psi^*(T)) = \frac{r_{O_T} - r_{E_T} \cos \theta_T}{\sqrt{r_{E_T}^2 + r_{O_T}^2 - 2r_{E_T}r_{O_T} \cos \theta_T}}, \quad \sin(\psi^*(T)) = \frac{r_{E_T} \sin \theta_T}{\sqrt{r_{E_T}^2 + r_{O_T}^2 - 2r_{E_T}r_{O_T} \cos \theta_T}},$$

provided that r_{E_T} , r_{O_T} and θ_T are s.t. the following is not the case: $r_{O_T} = r_{E_T}$ and $\theta_T = 0$.

When $\theta_T = 0$, eq. (12) yields

$$\psi^*(T) = \begin{cases} 0 & \text{if } r_{O_T} > r_{E_T} \\ \pi & \text{if } r_{O_T} < r_{E_T} \end{cases}$$

An inspection of Fig. 2 tells us that in the end game, at time $t=T$, the rOver runs away from the rElay.

III.2. Special Case – Optimal Control Problem

We are interested in the solution of the zero-sum differential game which, loosely speaking, is a two-sided optimal control problem. When the rOver is stationary the speed ratio parameter $\alpha=0$, and the rElay is faced with a simpler optimal control problem. Subscribing to Polya's [4] dictum: "If you cannot solve the problem on hand, there surely is a simplified version of the problem which you also don't know how to solve – solve that problem first", we consider the case where the rOver is stationary and we first obtain the closed-form solution of the optimal control problem.

The optimal control problem considered is

$$\begin{aligned} & \min_{\varphi} \int_0^T (r_E^2 - r_E r_O \cos \theta) dt \\ & s.t. \\ & \dot{r}_E = V_E \cos \varphi, \quad r_E(0) = r_{E_0} \\ & \dot{\theta} = -\frac{V_E}{r_E} \sin \varphi, \quad \theta(0) = \theta_0, \quad 0 \leq t \leq T \end{aligned}$$

This is equivalent to setting $\alpha=0$ in the differential game (3) the parameter. Without loss of generality we use the characteristic length $d = r_O$, that is, using non dimensional variables, the rOver is stationary at $r_O=1$ and, the optimal control problem is

$$\begin{aligned}
& \min_{\varphi} \int_0^T (r_E^2 - r_E \cos \theta) dt \\
& s.t. \\
& \dot{r}_E = \cos \varphi, \quad r_E(0) = r_{E_0} \\
& \dot{\theta} = -\frac{1}{r_E} \sin \varphi, \quad \theta(0) = \theta_o, \quad 0 \leq t \leq T
\end{aligned}$$

The state space is the half disc of unit radius centered at (1,0),

$$\left\{ (r_E, \theta) \mid 0 \leq \theta \leq \frac{\pi}{2}, \quad 0 \leq r_E \leq 2 \cos \theta \right\}$$

The control $0 \leq \varphi \leq \pi$ and the problem parameter is $T \left(T \equiv \frac{v_E}{r_o} T \right)$

III.2.1. Analysis

In the optimal control problem the Hamiltonian

$$\mathcal{H} = r_E \cos \theta - r_E^2 + \lambda_{r_E} \cos \varphi - \lambda_{\theta} \frac{1}{r_E} \sin \varphi$$

Applying the Pontryagin Maximum Principle (PMP) we obtain

$$\begin{aligned}
\sin \varphi^* &= -\frac{\lambda_{\theta}}{\sqrt{\lambda_{r_E}^2 r_E^2 + \lambda_{\theta}^2}} \\
\cos \varphi^* &= \frac{r_E \lambda_{r_E}}{\sqrt{\lambda_{r_E}^2 r_E^2 + \lambda_{\theta}^2}},
\end{aligned}$$

provided the co-states λ_{θ} and λ_{r_E} don't vanish.

The co-states' differential equations are

$$\begin{aligned}
\dot{\lambda}_{r_E} &= 2r_E - \cos \theta - \frac{\lambda_{\theta} \sin \varphi}{r_E^2}, \quad \lambda_{r_E}(T) = 0 \\
\dot{\lambda}_{\theta} &= r_E \sin \theta, \quad \lambda_{\theta}(T) = 0
\end{aligned}$$

The TPBVP for the optimal control problem is

$$\left. \begin{aligned}
 \dot{r}_E &= \frac{\lambda_{r_E} r_E}{\sqrt{\lambda_{r_E}^2 r_E^2 + \lambda_\theta^2}} & , r_E(0) &= r_{E_0} \\
 \dot{\theta} &= \frac{\lambda_\theta}{r_E \sqrt{\lambda_{r_E}^2 r_E^2 + \lambda_\theta^2}} & , \theta(0) &= \theta_0 \\
 \dot{\lambda}_{r_E} &= 2r_E - \cos \theta + \frac{\lambda_\theta^2}{r_E^2 \sqrt{\lambda_{r_E}^2 r_E^2 + \lambda_\theta^2}} & , \lambda_{r_E}(T) &= 0 \\
 \dot{\lambda}_\theta &= r_E \sin \theta & , \lambda_\theta(T) &= 0, \quad 0 \leq t \leq T
 \end{aligned} \right\} \quad (13)$$

Note: if $\theta_T \neq 0$, the costate $\lambda_\theta(t) < 0 \quad \forall 0 \leq t < T$; also, $\sqrt{\lambda_{r_E}^2 r_E^2 + \lambda_\theta^2} \neq 0 \quad \forall 0 \leq t < T$.

III.2.2. The End-Game in Optimal Control Problem

As in the differential game at time $t=T$ where the co-states vanish, and since the control variable φ does not explicitly feature in the cost functional, it is impossible to calculate the terminal control by applying the PMP and maximizing the Hamiltonian; obviously, equations (13) don't apply because $\sqrt{\lambda_{r_E}^2 r_E^2 + \lambda_\theta^2} = 0$. The end game requires special attention.

Since the end state is free - that's why the co-states vanish at $t=T$ - the rElay's optimal strategy at $t=T$ is myopic. Thus, from first principles it is clear that the rElay would want the integrand in the cost functional,

$$L(r_E, \theta) = r_E^2 - r_E \cos \theta$$

to be minimized. However the control variable φ does not feature in L . Hence the rElay minimizes the temporal derivative of L , evaluated at $t=T$.

$$\begin{aligned}\frac{d}{dt}L &= 2r_E \cos \varphi - \cos \varphi \cos \theta - \sin \theta \sin \varphi \\ &= (2r_E - \cos \theta) \cos \varphi - \sin \theta \sin \varphi\end{aligned}$$

Minimizing in φ the derivative of the integrand at time $t=T$ yields

$$\left. \begin{aligned}\cos(\varphi^*(T)) &= \frac{\cos \theta_T - 2r_{E_T}}{\sqrt{4r_{E_T}^2 + 1 - 4r_{E_T} \cos \theta_T}} \\ \sin(\varphi^*(T)) &= \frac{\sin \theta_T}{\sqrt{4r_{E_T}^2 + 1 - 4r_{E_T} \cos \theta_T}},\end{aligned}\right\} \quad (14)$$

Here $(r_{E_T}, r_{O_T}, \theta_T)$ is the state at time $t=T$.

Note that as in the differential game, when $\theta_T = 0$, the optimal terminal rElay control is

$$\varphi^*(T) = \begin{cases} 0 & \forall \ 0 < r_E < \frac{1}{2} \\ \pi & \forall \ \frac{1}{2} < r_E \leq 2 \end{cases} \quad (15)$$

As in the differential game, an inspection of Fig. 2 and eqs. (14) and (15) tell us that in the end game, at time $t=T$, the rElay heads toward the mid-point $M=(\frac{1}{2}, 0)$.

The analysis yielding the optimal terminal rElay strategy (14) and (15) applies, provided that the end state (r_{E_T}, θ_T) is not

$$\theta_T = 0, r_{E_T} = \frac{1}{2}$$

III.2.3. Retrograde Integration: $t \leq T$

At time $t=T$ the co-states vanish and we cannot use eqs. (13); also, $\sqrt{\lambda_{r_E}^2 r_E^2 + \lambda_\theta^2} = 0$ at $t = T$. At the terminal time $t = T$ where, the maximization of \mathcal{H} does not yield the optimal control according to the PMP, we must use eqs. (14) and (15) derived from first principles. Thus, in the end game at the terminal time $t=T$, the specified rElay control in eqs. (13), is replaced by the rElay control in the end game, namely, eq. (14). Thus, at time $t=T$ eqs. (13) are replaced by

$$\left. \begin{aligned} \dot{r}_E \Big|_T &= \cos(\varphi^*(T)) = \frac{\cos \theta_T - 2r_{E_T}}{\sqrt{4r_{E_T}^2 + 1 - 4r_{E_T} \cos \theta_T}}, \quad r_E(T) = r_{E_T} \\ \dot{\theta} \Big|_T &= -\frac{1}{r_{E_T}} \sin(\varphi^*(T)) = -\frac{1}{r_{E_T}} \frac{\sin \theta_T}{\sqrt{4r_{E_T}^2 + 1 - 4r_{E_T} \cos \theta_T}}, \quad \theta(T) = \theta_T \\ \dot{\lambda}_{r_E} \Big|_T &= 2r_{E_T} - \cos \theta_T - \frac{\lambda_\theta \sin(\varphi^*(T))}{r_{E_T}^2} = 2r_{E_T} - \cos \theta, \quad \lambda_{r_E}(T) = 0 \\ \dot{\lambda}_\theta \Big|_T &= r_{E_T} \sin \theta_T, \quad \lambda_\theta(T) = 0 \end{aligned} \right\} \quad (16)$$

We can now kick start the backward integration at $t = T$, from any end state in the state space, except the special end state $r_{E_T} = \frac{1}{2}, \theta_T = 0$, where the terminal control cannot be calculated. Also recall that the costate $\lambda_\theta(t) < 0 \forall 0 \leq t < T$, provided that $\theta_T > 0$. We are particularly interested in the trajectories which, under optimal play, terminate at the midpoint M of the segment \overline{BO} where $r_E(T) = \frac{1}{2}, \theta(T) = 0$ - referred to as the

“sweet spot”. When the end point is the “sweet spot” $\theta_T = 0$, $r_{E_T} = \frac{1}{2}$ we cannot obtain the optimal rElay control; the terminal optimal control $\varphi^*(T)$ cannot be determined from an examination of the equation

$$\begin{aligned}\frac{d}{dt}L &= (2r_E - \cos \theta) \cos \varphi - \sin \theta \sin \varphi \\ &= 0 \cdot \cos \varphi - 0 \cdot \sin \varphi\end{aligned}$$

The same applies when higher derivatives of L are considered. Eq. (14) does not apply and the retrograde integration of eqs. (13) cannot be “started” at the special “sweet spot” terminal state $r_{E_T} = \frac{1}{2}$, $\theta_T = 0$ using eqs. (16). Yet, as we shall see – see, e.g., Figure 4 in the sequel - it turns out that all the optimal trajectories radiate “out” of the “sweet spot” M where $r_E = \frac{1}{2}$, $\theta = 0$. In other words, for all initial states (r_{E_o}, θ_o) in the state space there exists a planning horizon $T(r_{E_o}, \theta_o)$ s.t. $r_E(T(r_{E_o}, \theta_o)) = \frac{1}{2}$ and $\theta(T(r_{E_o}, \theta_o)) = 0$.

Furthermore, given the initial state (r_{E_o}, θ_o) , if the planning horizon $T > T(r_{E_o}, \theta_o)$, the optimal trajectory is s.t. the “sweet spot” $r_E = \frac{1}{2}$, $\theta = 0$ is reached at time $T(r_{E_o}, \theta_o)$, following which, during the time interval $T(r_{E_o}, \theta_o) \leq t \leq T$, chattering control will be applied and the rElay will stay put at the “sweet spot”. Hence we back off and instead “start” the retrograde integration from a family of end points located on the

circumference of a small semicircle of radius $0 < \varepsilon \ll 1$ centered at the “sweet spot”, namely, the mid-point $M = \left(\frac{1}{2}, 0\right)$ of the segment \overline{OB} - as shown in Fig. 3.

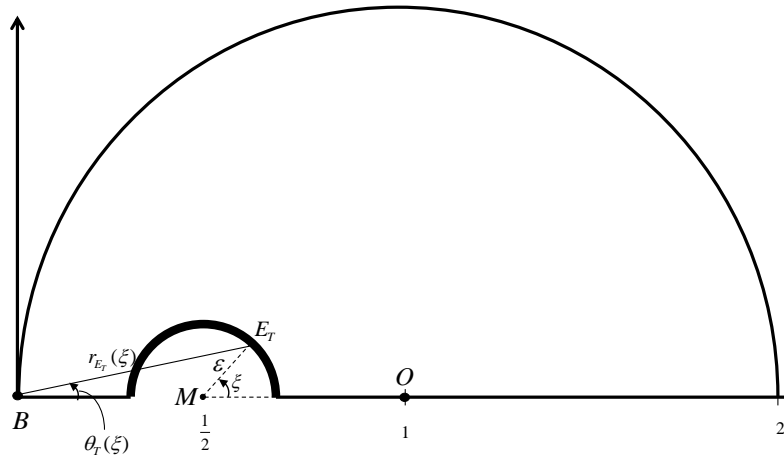


Figure 3: End Points Manifold

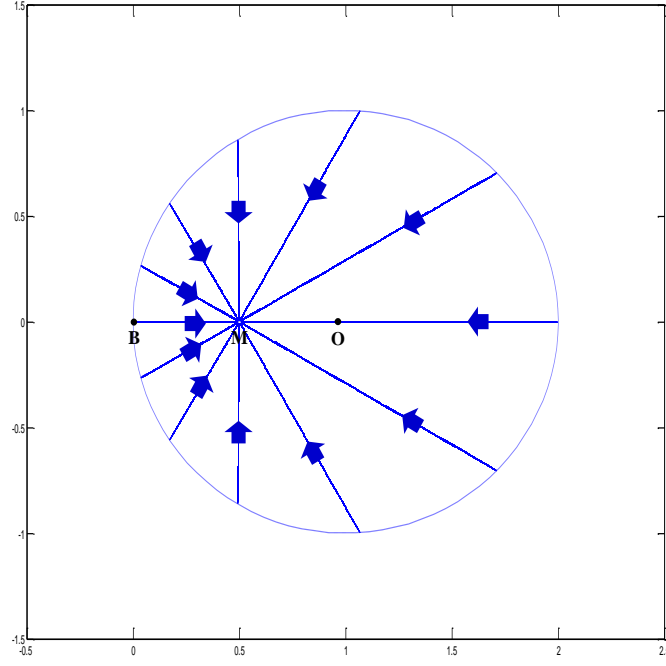


Figure 4: The Optimal Flow Field

The characteristics are integrated in retrograde fashion “starting” out at end-points

$E_T = (r_{E_T}, \theta_T)$, where

$$\left. \begin{aligned} r_{E_T} &= \sqrt{\varepsilon^2 \sin^2 \xi + \left(\frac{1}{2} + \varepsilon \cos \xi \right)^2} = \frac{1}{2} \sqrt{1 + 4\varepsilon \cos \xi + 4\varepsilon^2}, \\ \text{and} \\ \theta_T &= \text{Atan} \left(\frac{\varepsilon \sin \xi}{\frac{1}{2} + \varepsilon \cos \xi} \right), \quad 0 \leq \xi \leq \pi \end{aligned} \right\} \quad (17)$$

One proceeds as follows. One “starts out” from a point E_T on the terminal semicircular manifold shown in Fig. 3. Eqs. (17) are inserted into the R.H.S. of eqs. (16) where the optimal control in the end game is used and equations (16) are then used to step back one

time increment to time $T - \Delta T$. From that point on, having gotten away from the end state, and, in particular, the critical end state $r_{E_T} = \frac{1}{2}$, $\theta_T = 0$, eqs. (13) where the optimal control specified by the PMP is used are integrated in retrograde fashion $\forall T - \Delta T \geq t \geq 0$. The integration is stopped when the condition $r_E \leq 2 \cos \theta$ is violated, that is, the boundary of the state space is reached. The end points manifold is the thick line semicircle of radius ε centered at $\left(\frac{1}{2}, 0\right)$, as shown in Fig. 3. The family of end points E_T is parameterized by the angle ξ , $0 \leq \xi \leq \pi$.

The rElay's optimal strategy in the end game is in fact the optimal strategy throughout, as proven in Section 3.4 in the sequel. Hence the optimal trajectories leading into the semicircular terminal manifold are straight lines. Also note that if $\theta_T \equiv 0$, that is, $\xi = 0$ or $\xi = \pi$, the rElay stays on the horizontal line BO – the symmetry axis of the disc shaped state space – and heads toward the mid-point M of the segment \overline{OB} .

Consequently, the optimal flow field consists of straight line trajectories which converge at the “sweet spot” M. This results in the optimal flow field shown in Fig. 4: the optimal state feedback strategy is

$$\cos(\varphi^*(r_E, \theta)) = \frac{\cos \theta - 2r_E}{\sqrt{4r_E^2 + 1 - 4r_E \cos \theta}}, \quad \sin(\varphi^*(r_E, \theta)) = \frac{\sin \theta}{\sqrt{4r_E^2 + 1 - 4r_E \cos \theta}}$$

and the ensuing optimal straight line trajectories, all converge to the “sweet spot” M = $\left(\frac{1}{2}, 0\right)$.

III.3. Analytic Solution of the Optimal Control Problem

In the optimal control problem there are just two state variables, r_E and θ . It is therefore instructive to use Cartesian coordinates (x, y) as shown below.

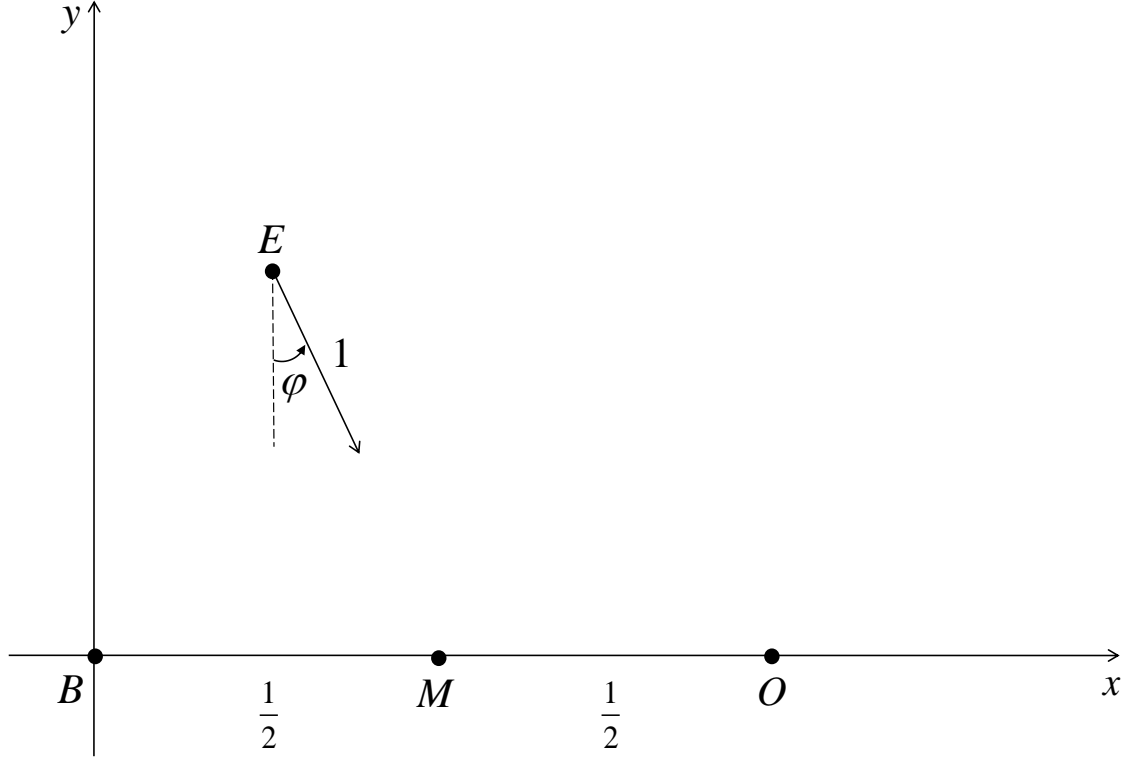


Figure 5: Trajectory in Cartesian Plane

The dynamics now are

$$\begin{aligned}\dot{x} &= \sin \varphi, \quad x(0) = x_0 \\ \dot{y} &= -\cos \varphi, \quad y(0) = y_0, \quad 0 \leq t \leq T,\end{aligned}$$

and the cost functional is

$$J = 2 \int_0^T (x^2 + y^2 - x) dt$$

The state space is the set

$$S = \{(x, y) \mid x^2 + y^2 - 2x \leq 0\},$$

namely, a disc of radius 1 centered at (1,0).

The Hamiltonian is

$$\mathcal{H} = 2x - 2x^2 - 2y^2 + \lambda_x \sin \varphi - \lambda_y \cos \varphi$$

The Hamiltonian is maximized on φ , which yields the optimal controls

$$\sin \varphi^* = \frac{\lambda_x}{\sqrt{\lambda_x^2 + \lambda_y^2}}, \quad \cos \varphi^* = -\frac{\lambda_y}{\sqrt{\lambda_x^2 + \lambda_y^2}} \quad (18)$$

Hence, we must solve the TPBVP

$$\dot{x} = \frac{\lambda_x}{\sqrt{\lambda_x^2 + \lambda_y^2}}, \quad x(0) = x_0 \quad (19)$$

$$\dot{y} = \frac{\lambda_y}{\sqrt{\lambda_x^2 + \lambda_y^2}}, \quad y(0) = y_0 \quad (20)$$

$$\dot{\lambda}_x = 4x - 2, \quad \lambda_x(T) = 0 \quad (21)$$

$$\dot{\lambda}_y = 4y, \quad \lambda_y(T) = 0 \quad (22)$$

III.3.1. The End Game in the Cartesian Plane

The controls don't directly feature in the cost functional. Hence we minimize the derivative of the integrand in the cost functional:

$$\frac{d}{dt}(x^2 + y^2 - x) \rightarrow \min_{\varphi}$$

\Rightarrow

$$2x \sin \varphi - 2y \cos \varphi - \sin \varphi \rightarrow \min_{\varphi}$$

\Rightarrow

$$\left(x - \frac{1}{2}\right) \sin \varphi - y \cos \varphi \rightarrow \min_{\varphi}$$

\Rightarrow

$$\sin(\varphi^*(T)) = \frac{\frac{1}{2} - x}{\sqrt{x^2 + y^2 - x + \frac{1}{4}}}, \quad \cos(\varphi^*(T)) = \frac{y}{\sqrt{x^2 + y^2 - x + \frac{1}{4}}} \quad (23)$$

Have obtained the optimal controls in the end game.

- In the end game E heads toward the \overline{BO} midpoint M.

Proposition A The following holds.

$$\frac{\lambda_x(t)}{\lambda_y(t)} = \text{const.} = c, \quad 0 \leq t \leq T.$$

□

Proposition A \Rightarrow

$$\varphi^*(t) \equiv \text{const.}, \quad 0 \leq t \leq T$$

\Rightarrow

$$x(t) = x_0 + \sin \varphi^* \cdot t$$

$$y(t) = y_0 - \cos \varphi^* \cdot t$$

\Rightarrow

$$\dot{\lambda}_x = 4x_0 + 4 \sin \varphi^* \cdot t - 2$$

$$\dot{\lambda}_y = 4y_0 - 4 \cos \varphi^* \cdot t$$

\Rightarrow

$$\lambda_x(t) = 2(2x_0 - 1)t + 2 \sin \varphi^* \cdot t^2 - a$$

$$\lambda_y(t) = 4y_0t - 2\cos\varphi^* \cdot t^2 + b$$

where a and b are integration constants.

Furthermore, Proposition A \Rightarrow

$$\frac{(2x_0 - 1)t + \sin\varphi^* \cdot t^2 - a}{2y_0t - \cos\varphi^* \cdot t^2 + b} = c \quad \forall 0 \leq t \leq T$$

\Rightarrow

$$(\sin\varphi^* + c \cdot \cos\varphi^*)t^2 + (2x_0 - 1 - 2y_0 \cdot c)t + a - bc = 0 \quad \forall 0 \leq t \leq T$$

\Rightarrow

$$\begin{aligned} \varphi^* &= -A \tan c, \\ \frac{\frac{1}{2} - x_0}{y_0} &= \tan\varphi^*, \\ b &= \frac{a}{c} \end{aligned}$$

We conclude that the rElay heads in a straight line toward the midpoint M.

Finally, given the initial state (x_0, y_0) , we calculate

$$T_{\max} = \sqrt{x_0^2 + y_0^2 - x_0 + \frac{1}{4}}.$$

Note Since $\lambda_x(T_{\max}) = 0$, we calculate the constant

$$a = (1 - 2x_0)T_{\max} - \sin\varphi^* \cdot T_{\max}^2$$

\Rightarrow

$$b = (2x_0 - 1)T_{\max} \frac{\cos\varphi^*}{\sin\varphi^*} + \cos\varphi^* \cdot T_{\max}^2$$

Now

$$\begin{aligned}\lambda_y(T_{\max}) &= 2 \left[2y_0 T_{\max} - \cos \varphi^* \cdot T_{\max}^2 + (2x_0 - 1) T_{\max} \frac{\cos \varphi^*}{\sin \varphi^*} + \cos \varphi^* \cdot T_{\max}^2 \right] \\ &= 4T_{\max} \left[y_0 - \left(\frac{1}{2} - x_0 \right) \cot \varphi^* \right]\end{aligned}$$

But

$$\frac{\frac{1}{2} - x_0}{y_0} = \tan \varphi^*$$

\Rightarrow

$$\lambda_y(T_{\max}) = 0.$$

and the “transversality conditions” $\lambda_y(T_{\max}) = 0$, $\lambda_y(T_{\max}) = 0$ hold.

- The optimal trajectories are straight lines.

III.3.2. Value Function

The optimal trajectories are

$$\begin{aligned}x(\tau) &= x + \sin \varphi^* \cdot \tau, \quad x(t) = x \\ y(\tau) &= y - \cos \varphi^* \cdot \tau, \quad y(t) = y, \quad t \leq \tau \leq T\end{aligned}$$

and the (constant) optimal controls

$$\sin \varphi^* = \frac{\frac{1}{2} - x}{\sqrt{x^2 + y^2 - x + \frac{1}{4}}}, \quad \cos \varphi^* = \frac{y}{\sqrt{x^2 + y^2 - x + \frac{1}{4}}}$$

Now

$$\begin{aligned}x^2(\tau) + y^2(\tau) - x(\tau) &= \tau^2 + 2 \left[\left(x - \frac{1}{2} \right) \sin \varphi^* - y \cos \varphi^* \right] \cdot \tau + x^2 + y^2 - x \\ &= \tau^2 - 2 \sqrt{x^2 + y^2 - x + \frac{1}{4}} \cdot \tau + x^2 + y^2 - x\end{aligned}$$

Therefore, the value function is

$$\begin{aligned} V(t, x, y; T) &= 2 \int_t^T \left[\tau^2 - 2 \sqrt{x^2 + y^2 - x + \frac{1}{4}} \cdot \tau + x^2 + y^2 - x \right] d\tau \\ &= 2 \left[\frac{1}{3} (T^3 - t^3) - \sqrt{x^2 + y^2 - x + \frac{1}{4}} \cdot (T^2 - t^2) + (x^2 + y^2 - x)(T - t) \right] \end{aligned}$$

Hence, have obtained the explicit value function

$$\begin{aligned} V(t, x, y; T) &= 2(T - t) \cdot \left[x^2 + y^2 - x - \sqrt{x^2 + y^2 - x + \frac{1}{4}} \cdot (T + t) + \frac{1}{3} (T^2 + Tt + t^2) \right], \\ (x, y) &\in S_T, \quad 0 \leq t \leq T \end{aligned}$$

The domain of definition of the value function $V(t, x, y; T)$ is the set

$$S = \left\{ (x, y) \mid (x-1)^2 + y^2 \leq 1, \left(x - \frac{1}{2} \right)^2 + y^2 \geq T^2 \right\}.$$

shown in Fig. 6

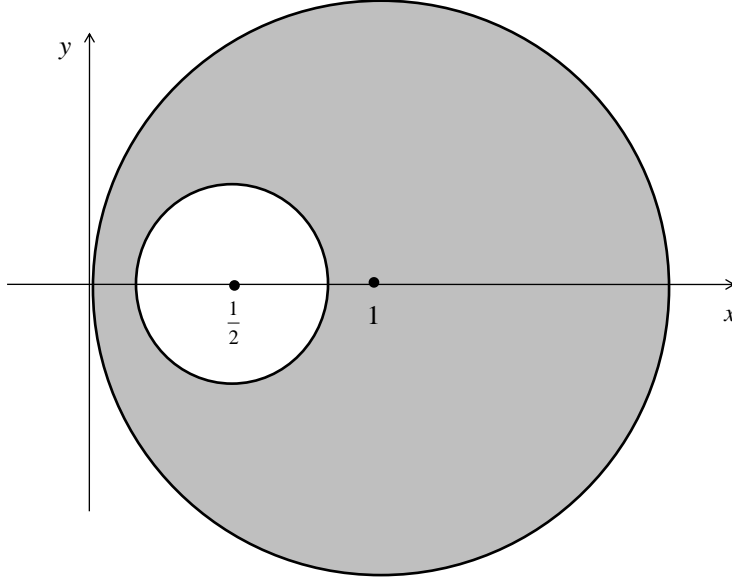


Figure 6: The domain of definition of the value function

In particular,

$$V(x_0, y_0; T) = 2T \left(x_0^2 + y_0^2 - x_0 - \sqrt{x_0^2 + y_0^2 - x_0 + \frac{1}{4}} \cdot T + \frac{1}{3} T^2 \right), \quad (x_0, y_0) \in S_T$$

Note:

$$\text{When } T = \sqrt{x_0^2 + y_0^2 - x_0 + \frac{1}{4}}, \quad y(x_0, y_0) = \frac{2}{3} \left(x_0^2 + y_0^2 - x_0 - \frac{1}{2} \right) \sqrt{x_0^2 + y_0^2 - x_0 + \frac{1}{4}}.$$

III.4. Discussion

This is an interesting optimal control problem: The end state is free and the control does not explicitly feature in the cost functional, which requires us to consider the end game. Furthermore, if the planning horizon T is long enough, all the optimal

trajectories in the state space will terminate at the “sweet spot” $r_E = \frac{1}{2}$, $\theta = 0$. At the same time, to solve the optimal control problem we employ the method of characteristics - also referred to as Isaacs method [2], which requires us to integrate the characteristics equations/state and co-state equations in a retrograde manner, "starting out" from an end state. But there is only one end state, the critical "sweet spot". Now, recall that the optimal control provided by the solution of the end game does not apply at the “sweet spot” and one is at a loss of how to kickstart the backward integration. This indicates a strong singularity at this critical end state, the "sweet spot".

Indeed the complete optimal flow field/solution "emanates" from the special sweet spot, and this has the appearance of a Big Bang type situation. It would appear that since a family of characteristics, and not just a single characteristic, emanates from the sweet spot, the solution of the characteristics equation is not unique, and Isaacs method is not applicable to the solution of the rElay optimal control problem. This difficulty was overcome by slightly backing off from the sweet spot. The sweet spot was replaced by the family of terminal states shown in Fig. 3, namely the small semicircle centered at the sweet spot and indicated by the thick line; the radius of the semicircle is $\varepsilon \ll 1$.

When “starting” the integration from, say, point E_T on the circumference of the semicircle, the first step in the retrograde integration entails the use of the optimal strategy (14) for the end game; the end states E_T on the circumference of the small semicircle are parameterized by the angle ξ , $0 \leq \xi \leq \pi$. This kicks off the integration, and from this point on, one uses the characteristics’ eqs. (13). The integration is stopped when

the boundary of the state space is approached, where the condition $r_E \leq 2r_O \cos \theta$ is violated.

III.5. Differential Game

To solve the differential game we employ the method of characteristics, a.k.a., the method of Isaacs. The partial derivatives of the value function are related to the costates according to

$$V_{r_E} \equiv -\lambda_{r_E}, \quad V_{r_O} \equiv -\lambda_{r_O}, \quad V_\theta \equiv -\lambda_\theta$$

Hence, in view of eqs. (3), (5), (7) and (8), the equations of the characteristics are

$$\frac{d}{dt} V_{r_E} = 2r_O \cos \theta - 4r_E - \frac{V_\theta^2}{r_E^2 \sqrt{V_{r_E}^2 r_E + V_\theta^2}}, \quad V_{r_E}(T) = 0$$

$$\frac{d}{dt} V_{r_O} = 2r_E \cos \theta - 2r_O + \alpha \frac{V_\theta^2}{r_O^2 \sqrt{V_{r_O}^2 r_O + V_\theta^2}}, \quad V_{r_O}(T) = 0$$

$$\frac{d}{dt} V_\theta = -2r_E r_O \sin \theta, \quad V_\theta(T) = 0$$

$$\frac{d}{dt} r_E = -\frac{r_E V_{r_E}}{\sqrt{V_{r_E}^2 r_E + V_\theta^2}}, \quad r_E(T) = r_{E_T}, \quad r_{E_T} \geq 0$$

$$\frac{d}{dt} r_O = \alpha \frac{r_O V_{r_O}}{\sqrt{V_{r_O}^2 r_O + V_\theta^2}}, \quad r_O(T) = r_{O_T}, \quad r_{O_T} > 0$$

$$\frac{d\theta}{dt} = \alpha \frac{V_\theta}{r_O \sqrt{V_{r_O}^2 r_O + V_\theta^2}} - \frac{V_\theta}{r_E \sqrt{V_{r_E}^2 r_E + V_\theta^2}}, \quad \theta(T) = \theta_T, \quad 0 \leq \theta_T \leq \cos^{-1}\left(\frac{1}{2} \frac{r_{E_T}}{r_{O_T}}\right), \quad 0 \leq t \leq T$$

According to Isaac's method [2], the characteristic equations are integrated in retrograde fashion "starting" out at r_{E_T} , r_{O_T} , θ_T . To this end set $\tau \triangleq T - t$. Thus

$$\left. \begin{aligned} \frac{d}{d\tau} r_E &= \frac{r_E V_{r_E}}{\sqrt{V_{r_E}^2 r_E^2 + V_\theta^2}}, r_E(0) = r_{E_T} \\ \frac{d}{d\tau} r_O &= -\alpha \frac{r_O V_{r_O}}{\sqrt{V_{r_O}^2 r_O^2 + V_\theta^2}}, r_O(0) = r_{O_T} \\ \frac{d\theta}{d\tau} &= \left(\frac{1}{r_E \sqrt{V_{r_E}^2 r_E^2 + V_\theta^2}} - \alpha \frac{1}{r_O \sqrt{V_{r_O}^2 r_O^2 + V_\theta^2}} \right) V_\theta, \theta(0) = \theta_T \\ \frac{d}{d\tau} V_{r_E} &= 4r_E - 2r_O \cos \theta + \frac{V_\theta^2}{r_E^2 \sqrt{V_{r_E}^2 r_E^2 + V_\theta^2}}, V_{r_E}(0) = 0 \\ \frac{d}{d\tau} V_{r_O} &= 2r_O - 2r_E \cos \theta - \alpha \frac{V_\theta^2}{r_O^2 \sqrt{V_{r_O}^2 r_O^2 + V_\theta^2}}, V_{r_O}(0) = 0 \\ \frac{d}{d\tau} V_\theta &= 2r_E r_O \sin \theta, V_\theta(0) = 0, 0 \leq \tau \leq T \end{aligned} \right\} (24)$$

Now, the first step in the retrograde integration of the equations of the characteristics requires us to use the controls from the end game. Thus, the first integration step is

$$\left. \begin{aligned} r_E(\Delta T) &= r_{E_T} + \Delta T \cdot \frac{2r_{E_T} - r_{O_T} \cos \theta_T}{\sqrt{4r_{E_T}^2 + r_{O_T}^2 - 4r_{E_T} r_{O_T} \cos \theta_T}} \\ r_O(\Delta T) &= r_{O_T} + \alpha \Delta T \cdot \frac{r_{E_T} \cos \theta_T - r_{O_T}}{\sqrt{r_{E_T}^2 + r_{O_T}^2 - 2r_{E_T} r_{O_T} \cos \theta_T}} \\ \theta(\Delta T) &= \theta_T + \Delta T \cdot \sin \theta_T \left(\frac{r_{O_T}}{r_{E_T}} \cdot \frac{\sin \theta_T}{\sqrt{4r_{E_T}^2 + r_{O_T}^2 - 4r_{E_T} r_{O_T} \cos \theta_T}} - \alpha \frac{r_{E_T}}{r_{O_T}} \cdot \frac{\sin \theta_T}{\sqrt{r_{E_T}^2 + r_{O_T}^2 - 2r_{E_T} r_{O_T} \cos \theta_T}} \right) \\ V_{r_E}(\Delta T) &= 2\Delta T(2r_{E_T} - r_{O_T} \cos \theta_T) \\ V_{r_O}(\Delta T) &= 2\Delta T(r_{O_T} - r_{E_T} \cos \theta_T) \\ V_\theta(\Delta T) &= 2\Delta T r_{E_T} r_{O_T} \sin \theta_T \end{aligned} \right\} (25)$$

Equations (25) are obtained from eqs. (24) by using therein the terminal optimal controls derived in Section 2.1.

Since $V_{r_E}(0)=0$, $V_{r_O}(0)=0$ and $V_\theta(0)=0$, the first step (25) is required and the integration of the equations of the characteristics (24) starts at time $\tau=\Delta T$ with the “initial” condition $(r_E(\Delta T), r_O(\Delta T), \theta(\Delta T), V_{r_E}(\Delta T), V_{r_O}(\Delta T), V_\theta(\Delta T))$.

The following holds.

PROPOSITION When the speed ratio $0 \leq \alpha < 2$, the rElay can always reach the midpoint M, provided that the game horizon

$$T > \frac{1}{(2-\alpha)} \sqrt{4r_E^2 + r_O^2 - 4r_E r_O \cos \theta}$$

Proof

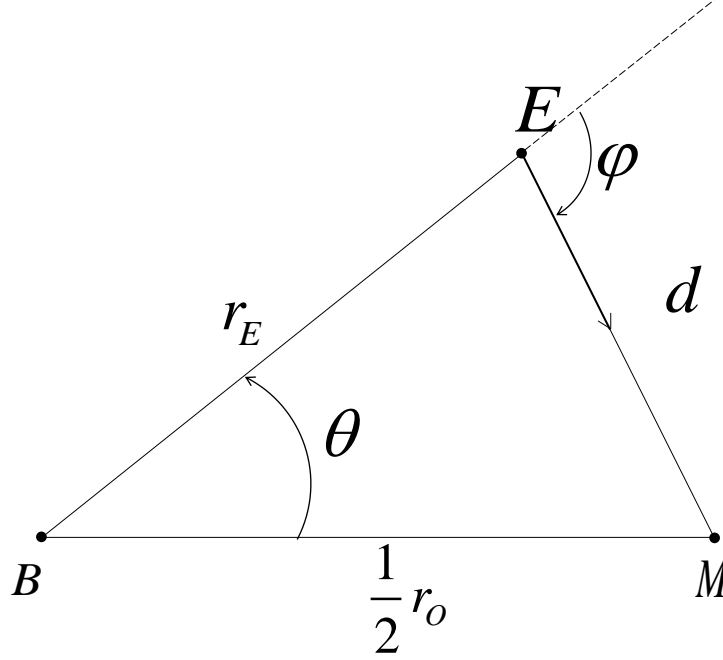


Figure 7: Pursuit - Evasion

From Fig. 7, the instantaneous distance EM is

$$d = \frac{1}{2} \sqrt{4r_E^2 + r_o^2 - 4r_E r_o \cos \theta}$$

and

$$\begin{aligned} \dot{d} &= \frac{1}{2d} \left[2r_E \cos \varphi + \frac{\alpha}{2} r_o \cos \psi - r_o \cos \theta \cos \varphi - \alpha r_E \cos \theta \cos \psi + r_E r_o \sin \theta \left(\frac{\alpha}{r_o} \sin \psi - \frac{1}{r_E} \sin \varphi \right) \right] \\ &= \frac{1}{2d} \left(2r_E \cos \varphi + \frac{\alpha}{2} r_o \cos \psi - r_o \cos \theta \cos \varphi - \alpha r_E \cos \theta \cos \psi + \alpha r_E \sin \theta \sin \psi - r_o \sin \theta \sin \varphi \right) \\ &= \frac{1}{2d} \left\{ (2r_E - r_o \cos \theta) \cos \varphi - r_o \sin \theta \sin \varphi + \frac{\alpha}{2} \left[(r_o - 2r_E \cos \theta) \cos \psi + 2r_E \sin \theta \sin \psi \right] \right\} \end{aligned}$$

Now $\min_{\varphi} \max_{\psi} \dot{d}$ yields the rElay pursuit strategy

$$\cos \varphi = \frac{r_o \cos \theta - 2r_E}{\sqrt{4r_E^2 + r_o^2 - 4r_E r_o \cos \theta}}, \quad \sin \varphi = \frac{r_o \sin \theta}{\sqrt{4r_E^2 + r_o^2 - 4r_E r_o \cos \theta}}$$

The rElay heads toward the midpoint M of the segment \overline{BO} .

The motion of the midpoint M is exclusively controlled by the rOver and the rOver's evasion strategy is

$$\cos \psi = \frac{r_o - 2r_E \cos \theta}{\sqrt{4r_E^2 + r_o^2 - 4r_E r_o \cos \theta}}, \quad \sin \psi = \frac{2r_E \sin \theta}{\sqrt{4r_E^2 + r_o^2 - 4r_E r_o \cos \theta}}$$

Hence, we calculate

$$\begin{aligned} \dot{d} &= \frac{1}{2d} \left(-\sqrt{4r_E^2 + r_o^2 - 4r_E r_o \cos \theta} + \frac{1}{2} \alpha \sqrt{4r_E^2 + r_o^2 - 4r_E r_o \cos \theta} \right) \\ &= \frac{1}{4d} (\alpha - 2) \sqrt{4r_E^2 + r_o^2 - 4r_E r_o \cos \theta} \\ &= \frac{1}{2} (\alpha - 2) < 0 \end{aligned}$$

and therefore the time-to-go

$$\begin{aligned} T(r_E, r_o, \theta) &= \frac{2}{2 - \alpha} d \\ &= \frac{1}{2 - \alpha} \sqrt{4r_E^2 + r_o^2 - 4r_E r_o \cos \theta} \end{aligned}$$

□

In general, optimal trajectories do not terminate s.t. a configuration where B, E and O in Fig. 2 are collinear is achieved. If however the game horizon T is sufficiently long and the speed ratio parameters $0 \leq \alpha < 2$, at some point in time a state s.t. $r_E = \frac{1}{2} r_O$ and $\theta = 0$ will be reached under optimal control, after which the game is rectilinear and the trajectory arc is singular. – strictly speaking the rElay will reduce its speed to $\frac{1}{2} \alpha$ and follow the rOver s.t. $r_E(t) \equiv \frac{1}{2} r_O(t)$. Hence we are interested in the trajectories which “emanate” in retrograde fashion from “sweet spots” ($r_E = \frac{1}{2} r_O$, $\theta = 0$).

It is however impossible to kick start the retrograde integration of the equation of the characteristics using eqs. (25) when starting out from a “sweet spot”. Therefore, similar to the optimal control problem, we “start out” from the family of “initial states” parameterized by ξ , as shown in Fig. 3. Thus, in eqs. (25)

$$r_{E_T} = \sqrt{\left(\frac{1}{2} r_{O_T} + \varepsilon \cos \xi\right)^2 + \varepsilon^2 \sin^2 \xi} \quad , \quad r_{O_T} = r_{O_r} \quad , \quad \theta_T = A \tan \left(\frac{\varepsilon \sin \xi}{\frac{1}{2} r_{O_T} + \varepsilon \cos \xi} \right)$$

where $0 < \varepsilon \ll 1$. In other words, in eqs. (25)

$$r_{E_T}(\xi; r_{O_T}) = \sqrt{\frac{1}{4} r_{O_T}^2 + r_{O_T} \varepsilon \cos \xi + \varepsilon^2} \quad , \quad r_{O_T} = r_{O_r} \quad ,$$

$$\theta_T(\xi; r_{O_T}) = A \tan \left(\frac{\varepsilon \sin \xi}{\frac{1}{2} r_{O_T} + \varepsilon \cos \xi} \right) \quad , \quad 0 \leq \xi \leq \pi$$

III.6. Optimal Play

In Fig. 8 optimal trajectories in the state space are shown.

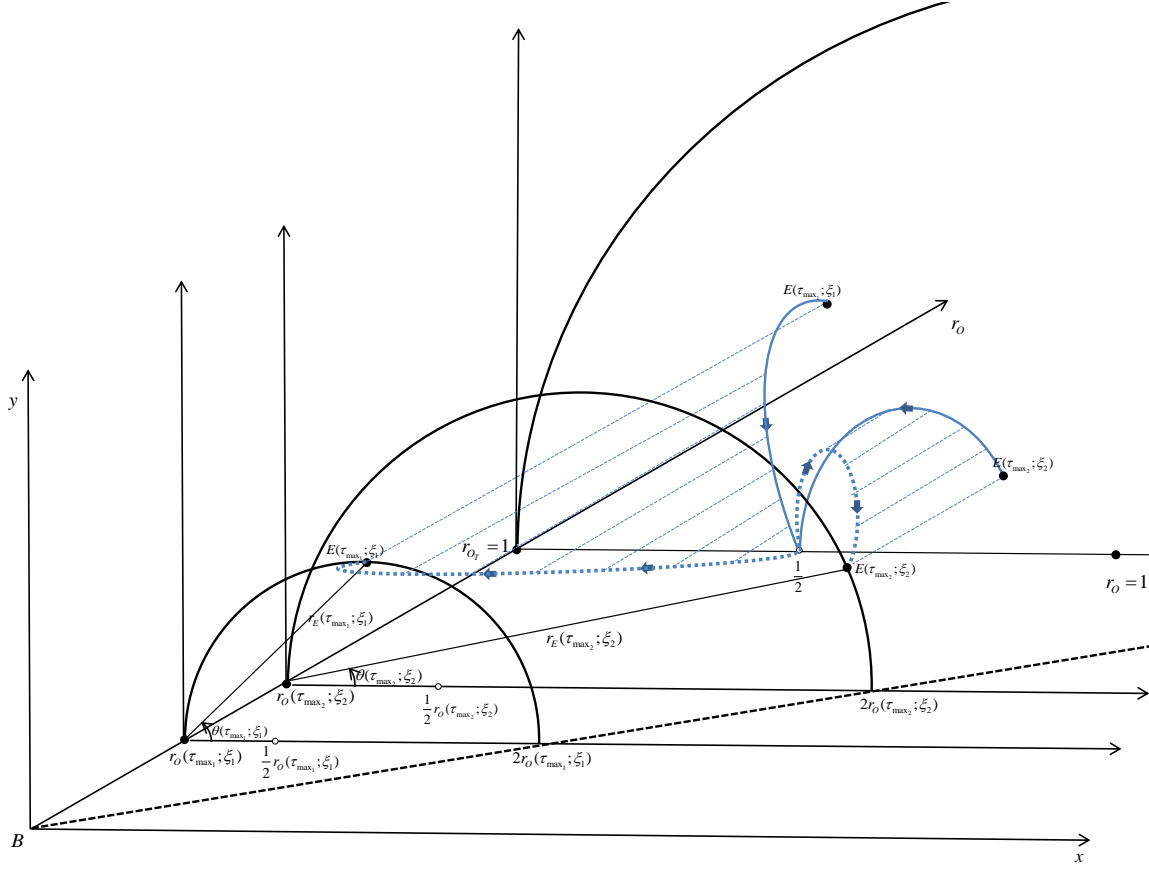


Figure 8: Optimal Relay Trajectories in the State Space

The broken lines are rElay trajectories in the state space which terminate at $r_{O_r} = 1$ and the full lines are their projection onto the half disc at $r_o = 1$. Optimal trajectories which terminate at $r_{O_r} = 1$ are constructed. The retrograde integration of the equations of the characteristics yields $r_E(\tau; \xi)$, $r_O(\tau; \xi)$ and $\theta(\tau; \xi)$. τ_{\max} is determined by the condition $r_E(\tau_{\max}; \xi) = 2r_O(\tau_{\max}; \xi) \cdot \cos(\theta(\tau_{\max}; \xi))$, that is, the boundary of the

state space is reached, or, $\theta(\tau_{\max}; \xi) = 0$, that is, the plane of symmetry of the state space is reached. To plot the trajectory in the state space, are calculated

$$\begin{aligned} x(\tau; \xi) &= r_E(\tau; \xi) \cdot \cos \theta(\tau; \xi), \\ y(\tau; \xi) &= r_E(\tau; \xi) \cdot \sin \theta(\tau; \xi), \\ r_o(\tau; \xi) \\ 0 \leq \tau &\leq \tau_{\max} \end{aligned}$$

III.6.1. The Optimal Trajectories in the Realistic Space

The retrograde integration of the equations of the characteristics yields the optimal trajectories $r_E(\tau)$, $r_o(\tau)$, $\theta(\tau)$, $0 \leq \tau \leq \tau_{\max}$.

We have used a reduced state space (r_E, r_o, θ) and have obtained the trajectory and optimal controls' time histories in a rotating frame of reference. Specifically, the sequences $r_{E_k} \triangleq r_E(k\Delta T)$, $r_{O_k} \triangleq r_o(k\Delta T)$, $\theta_k \triangleq \theta(k\Delta T)$, $k=1, \dots, N$ are calculated, where

$$N = \frac{\tau_{\max}}{\Delta T}; \quad r_{E_o} = \frac{1}{2} \sqrt{1 + 4\varepsilon \cos \xi + 4\varepsilon^2}, \quad r_{O_o} = r_{O_r} = 1, \quad \theta_o = A \tan \left(\frac{\varepsilon \sin \xi}{\frac{1}{2} + \varepsilon \cos \xi} \right).$$

In addition, the optimal control sequences $\varphi_k^* \triangleq \varphi^*(k\Delta T)$, $\psi_k^* \triangleq \psi^*(k\Delta T)$, $k=0, \dots, N-1$ are also calculated. To better visualize the optimal trajectories, they are plotted in the realistic plane. We proceed as follows.

Set

$$E(k\Delta T) := E((N-k)\Delta T), \quad O(k\Delta T) := O((N-k)\Delta T), \quad k=0, \dots, N-1$$

and

$$\varphi^*(k\Delta T) := \varphi^*((N-1-k)\Delta T), \quad \psi^*(k\Delta T) := \psi^*((N-1-k)\Delta T), \quad k=0, \dots, N-1.$$

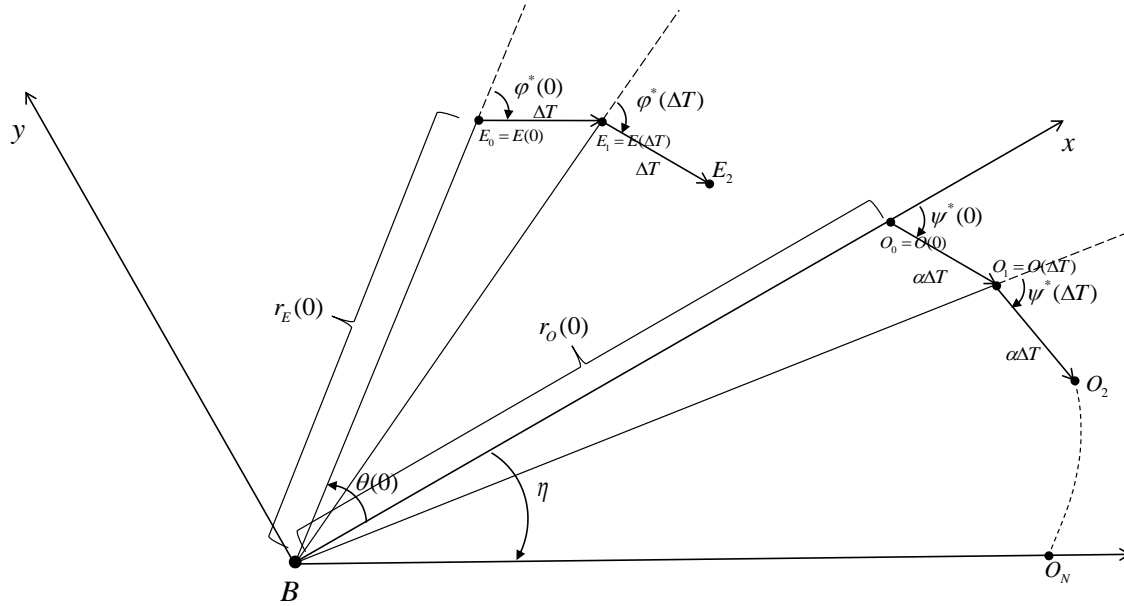


Figure 9: The Construction of Optimal Trajectories in The Realistic Space

The origin of the realistic plane is at B and the x-axis of the realistic plane is aligned with the segment $\overline{BO(0)}$. Thus, the coordinates of the rOver and rElay at time t=0 are

$$\begin{aligned} E(0) &= (r_E(0) \cos(\theta(0)), r_E(0) \sin(\theta(0))) \\ O(0) &= (r_o(0), 0) \end{aligned}$$

cAt time $t=0$, the rElay and rOver start out from

$$O_o \triangleq O(0) = (r_o(0), 0) \text{ and } E_o \triangleq E(0) = (r_E(0)\cos(\theta(0)), r_E(0)\sin(\theta(0))).$$

Using the position of E at $t=0$, $E_o \triangleq E(0)$, and the optimal control of E at time $t=0$, $\varphi^*(0)$, we obtain $E_1 \triangleq E(\Delta T)$ as shown in Fig. 9. Likewise, using the position of O at $t=0$, $O_o \triangleq O(0)$, and the optimal control of O at time $t=0$, $\psi^*(0)$, we obtain $O_1 \triangleq O(\Delta T)$, as shown in Fig. 9. Having obtained $E_1 \triangleq E(\Delta T)$, construct the line $\overline{BE_1}$ and use the rElay's optimal control $\varphi^*(\Delta T)$ to obtain $E_2 \triangleq E(2\Delta T)$. Similarly, having obtained $O_1 \triangleq O(\Delta T)$, construct the line $\overline{BO_1}$ and use the rOver's optimal control $\psi^*(\Delta T)$ to obtain $O_2 \triangleq O(2\Delta T)$.

This process terminates at time N, where $N = \frac{\tau_{\max}}{\Delta T}$. One thus obtains the trajectories

$$E_k \triangleq (x_E(k\Delta T), y_E(k\Delta T)), \text{ and } O_k \triangleq (x_O(k\Delta T), y_O(k\Delta T)), k = 0, \dots, N.$$

We want these trajectories to be presented in an (x, y) frame where the x-axis is aligned with the segment $\overline{BO_N}$.

Having obtained O_N namely, (x_{O_N}, y_{O_N}) , calculate the angle $\eta \triangleq \text{atan}\left(\frac{y_{O_N}}{x_{O_N}}\right)$,

Note : $\sqrt{x_{O_N}^2 + y_{O_N}^2} = r_o(N) = 1$

To get the rElay and rOver's trajectories in the new (x, y) frame, rotate the rElay and rOver trajectories η degrees, namely

$$\begin{aligned}x_E &:= x_E \cos \eta + y_E \sin \eta \\y_E &:= -x_E \sin \eta + y_E \cos \eta\end{aligned}$$

and

$$\begin{aligned}x_O &:= x_O \cos \eta + y_O \sin \eta \\y_O &:= -x_O \sin \eta + y_O \cos \eta\end{aligned}$$

IV. Analysis and Results

IV.1. Optimal Trajectories of Rover and Relay for different speed ratios α , and angle of approach of “sweet spot” ξ .

The cases of a speed ratio $\alpha = 0.5$ and angle of approach ξ is illustrated in Fig. 10, for different terminal rOver distances from the base.

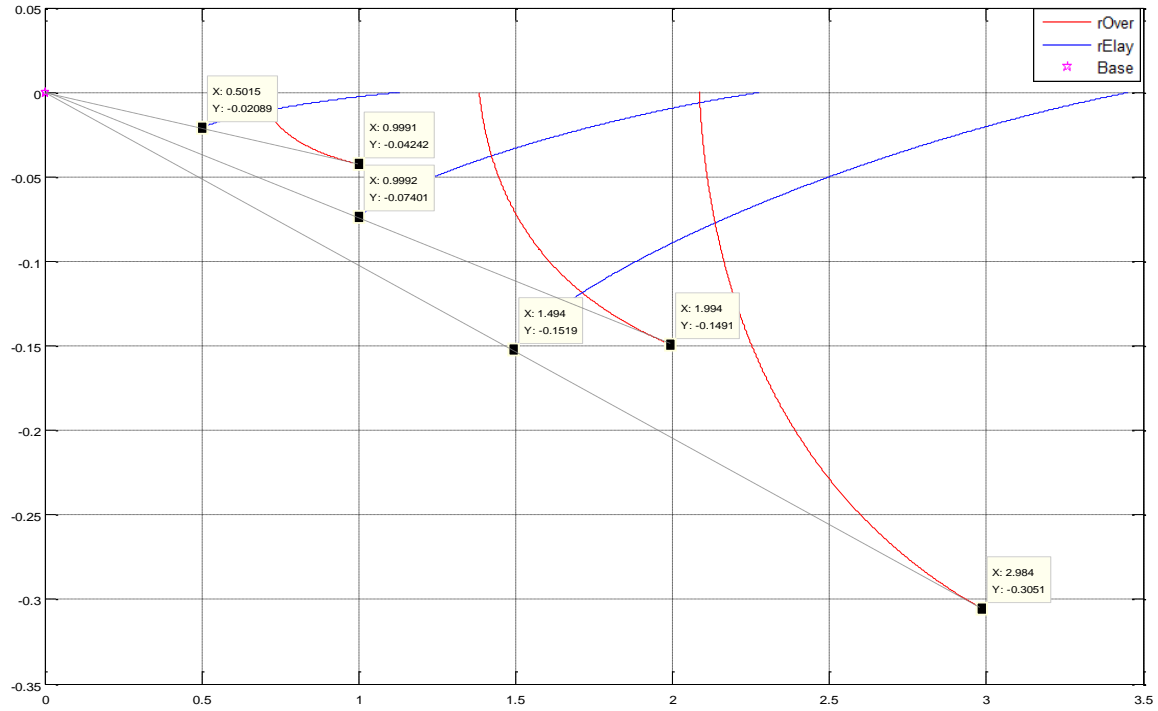


Figure 10: Optimal trajectories of Rover and Relay for $\xi = 10^\circ$, $\alpha = 0.5$, $r_{O_r} = 1, 2, 3$

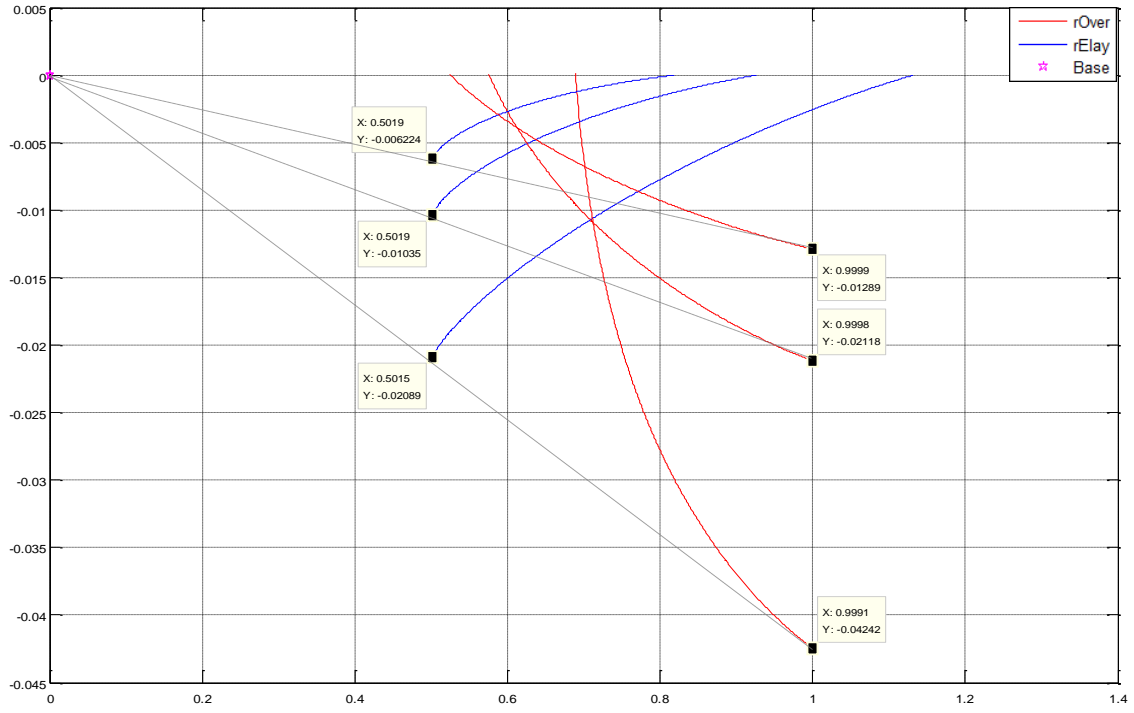


Figure 11: Optimal trajectories of Rover and Relay for

$$\xi = 10^\circ, \alpha = 0.5, 1, 1.5, r_{O_r} = 1$$

Figs. 10 and 11 show that the trajectories don't scale linearly as r_{O_r} and α vary.

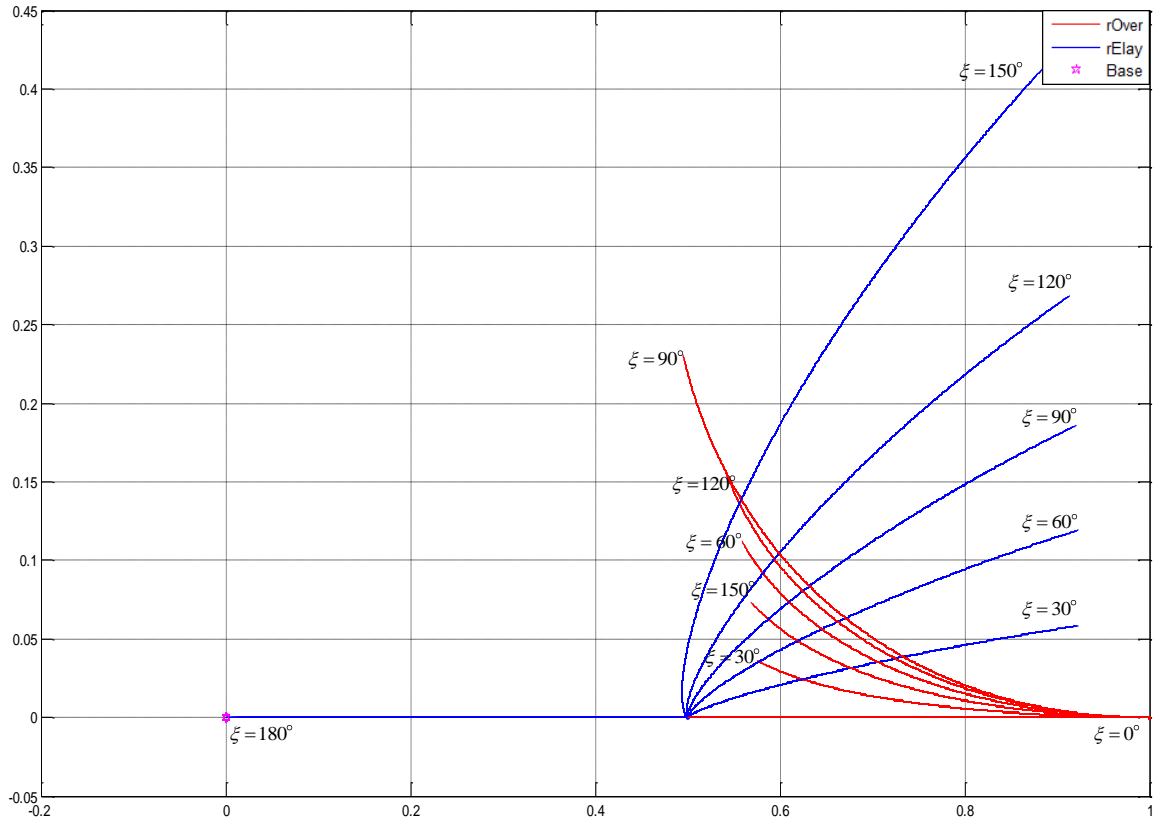


Figure 12: Optimal trajectories of Rover and Relay as ξ changes

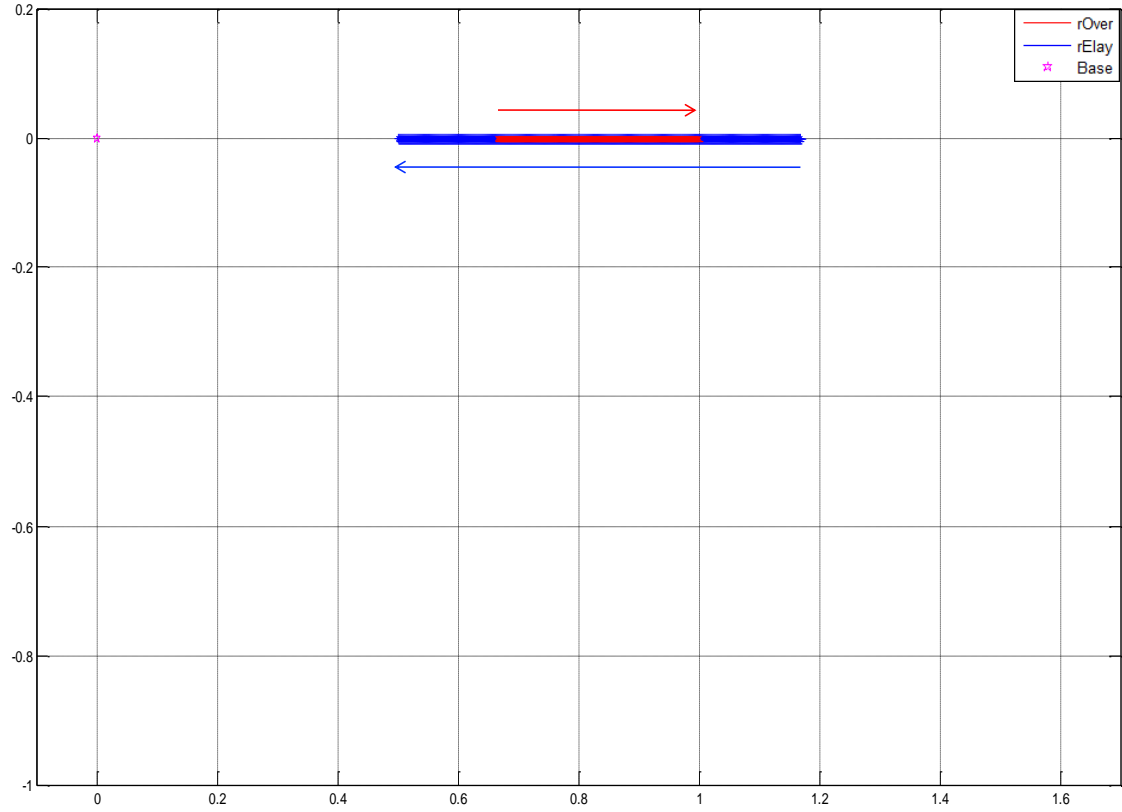


Figure 13: Optimal trajectories of Rover and Relay for $\alpha = 0.5$, $\xi = 0^\circ$

When $\xi = 0^\circ$, the rElay approaches the “sweet spot” at an angle $\theta \equiv 0^\circ$ during the game. The rElay’s displacement is twice of the rOver’s because of the speed ratio $\alpha = \frac{1}{2}$.

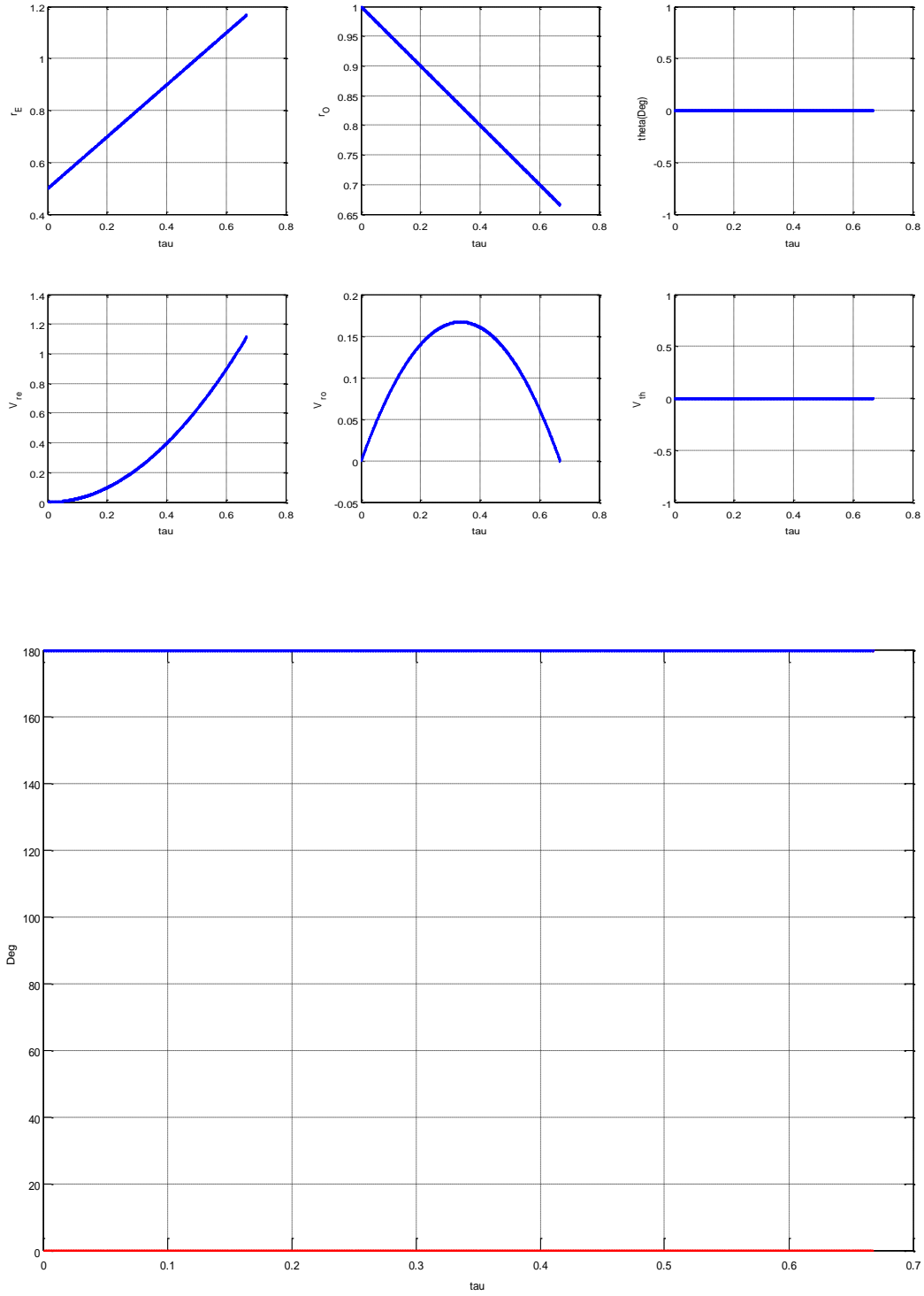


Figure 14: Time history of the States, Costates and Controls. $\alpha = 0.5$, $\xi = 0^\circ$

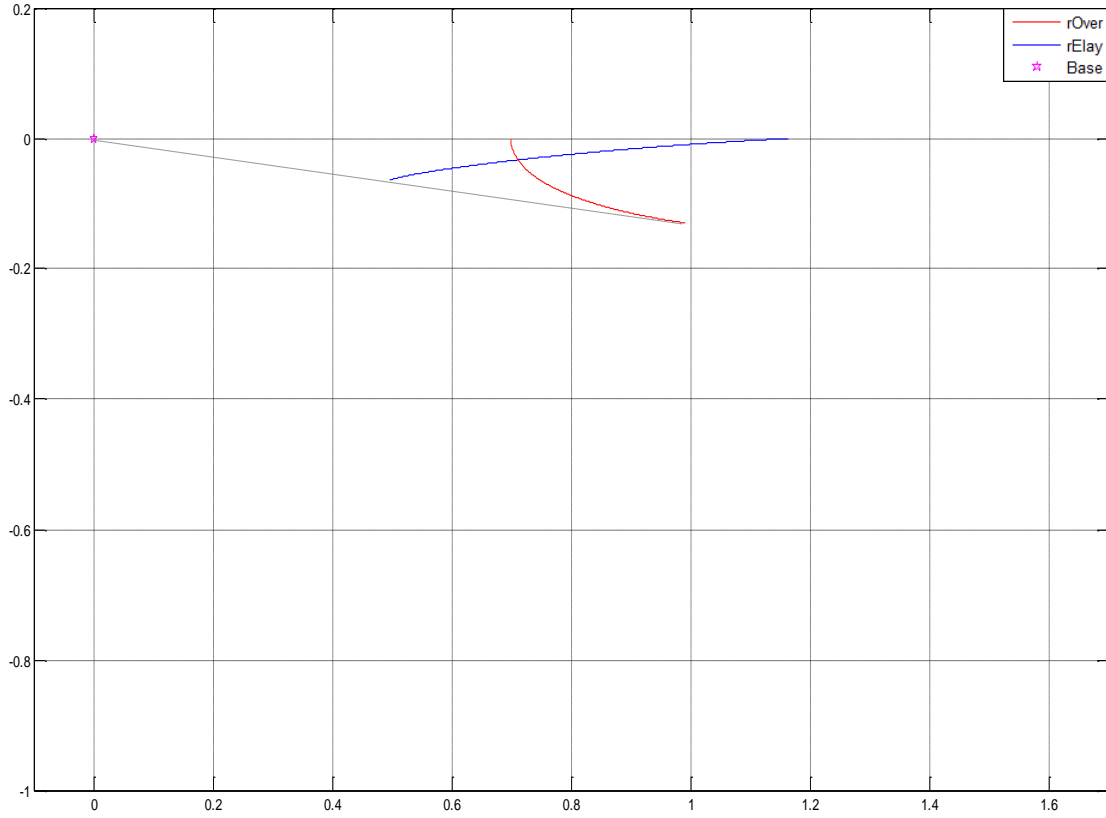


Figure 15: Optimal trajectories of Rover and Relay. $\alpha = 0.5$, $\xi = 30^\circ$, $r_{O_r} = 1$

Unlike the case $\xi = 0^\circ$, when $\xi = 30^\circ$ the rOver and rElay don't move along a straight line. However, even though they didn't stay on the $\theta \equiv 0$ line, eventually they end up s.t. $\theta = 0$. The broken line shows the end position at τ_{\max} , where the three points B, E, O are collinear.

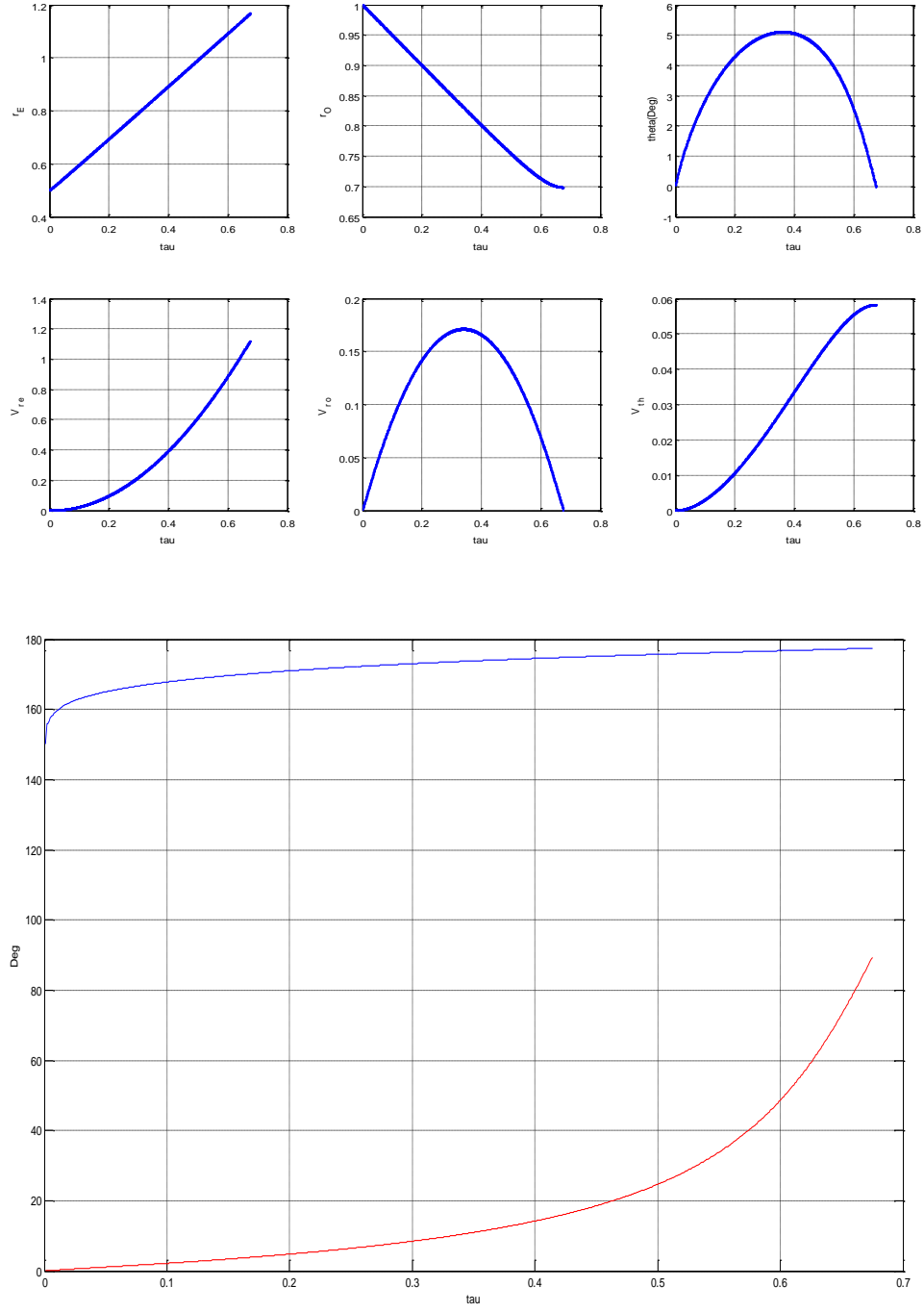


Figure 16: Time history of the States, Costates and Controls. $\alpha = 0.5$, $\xi = 30^\circ$, $r_{O_r} = 1$

At the end point the rElay's control is $\varphi^*(0) = 180^\circ - 30^\circ = 150^\circ$

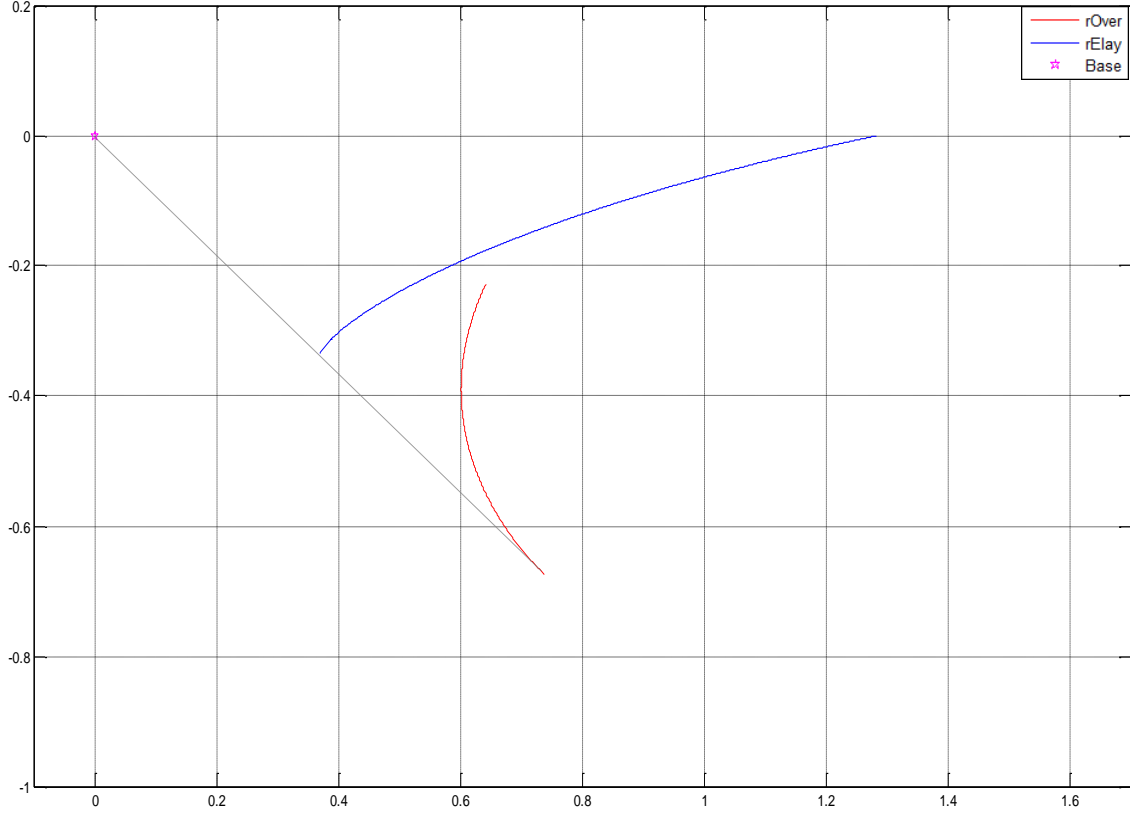


Figure 17: Optimal trajectories of Rover and Relay. $\alpha = 0.5$, $\xi = 120^\circ$, $r_{O_r} = 1$

When $\xi = 120^\circ$ the rOver and rElay start the game at a non zero θ angle. In other words, initially the base, rOver and rElay are not colinear. The optimal trajectory “terminates” on the boundary of the state space s.t. $r_E(\tau_{\max}) = 2r_O(\tau_{\max}) \cdot \cos(\theta(\tau_{\max}))$.

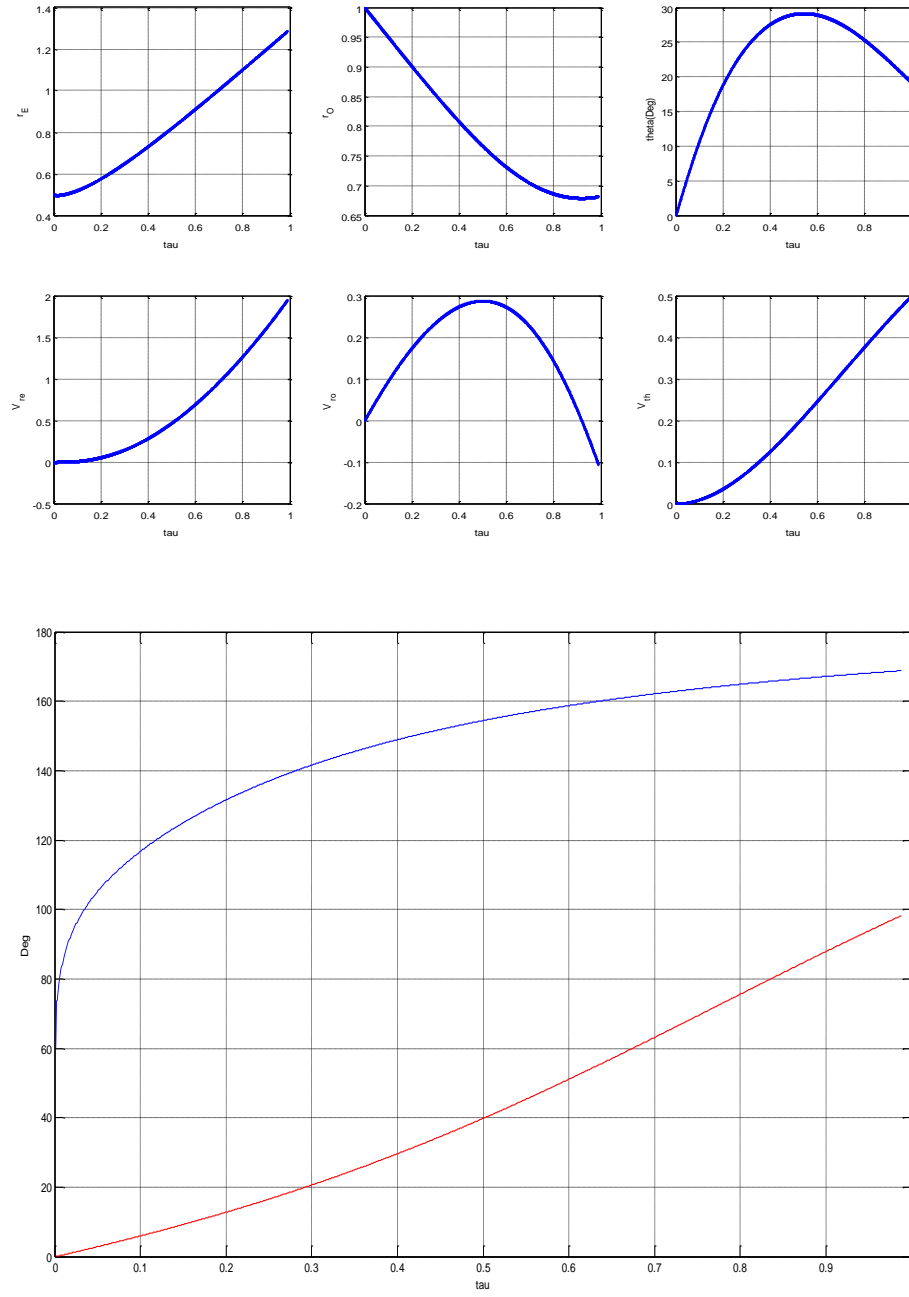


Figure 18: Time history of the States, Costates and Controls.

$$\alpha = 0.5, \quad \xi = 120^\circ, \quad r_{O_r} = 1$$

At the end point the rElay's control is $\varphi^*(0) = 180^\circ - 120^\circ = 60^\circ$

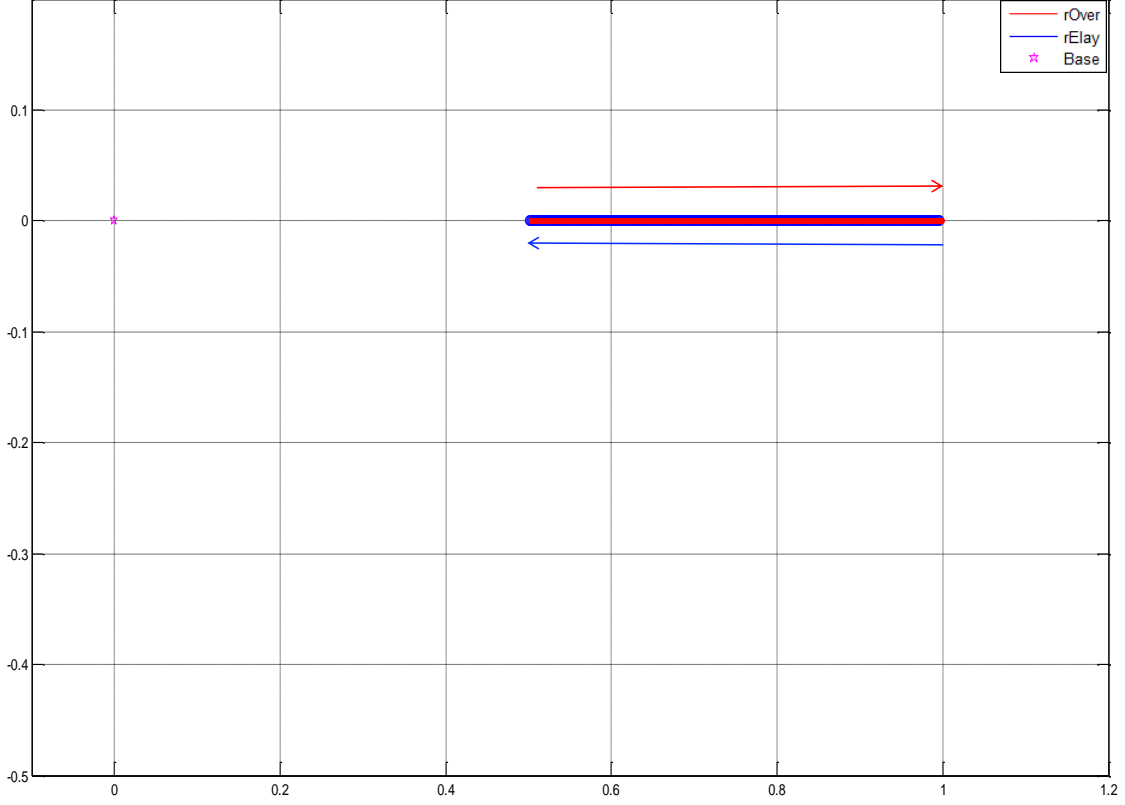


Figure 19: Optimal trajectories of Rover and Relay $\alpha = 1$, $\xi = 0^\circ$, $r_{Or} = 1$

Unlike in the previous cases, when $1 \leq \alpha \leq 2$, the rElay and rOver start and end the game at $\theta = 0$, irrespective of ξ .

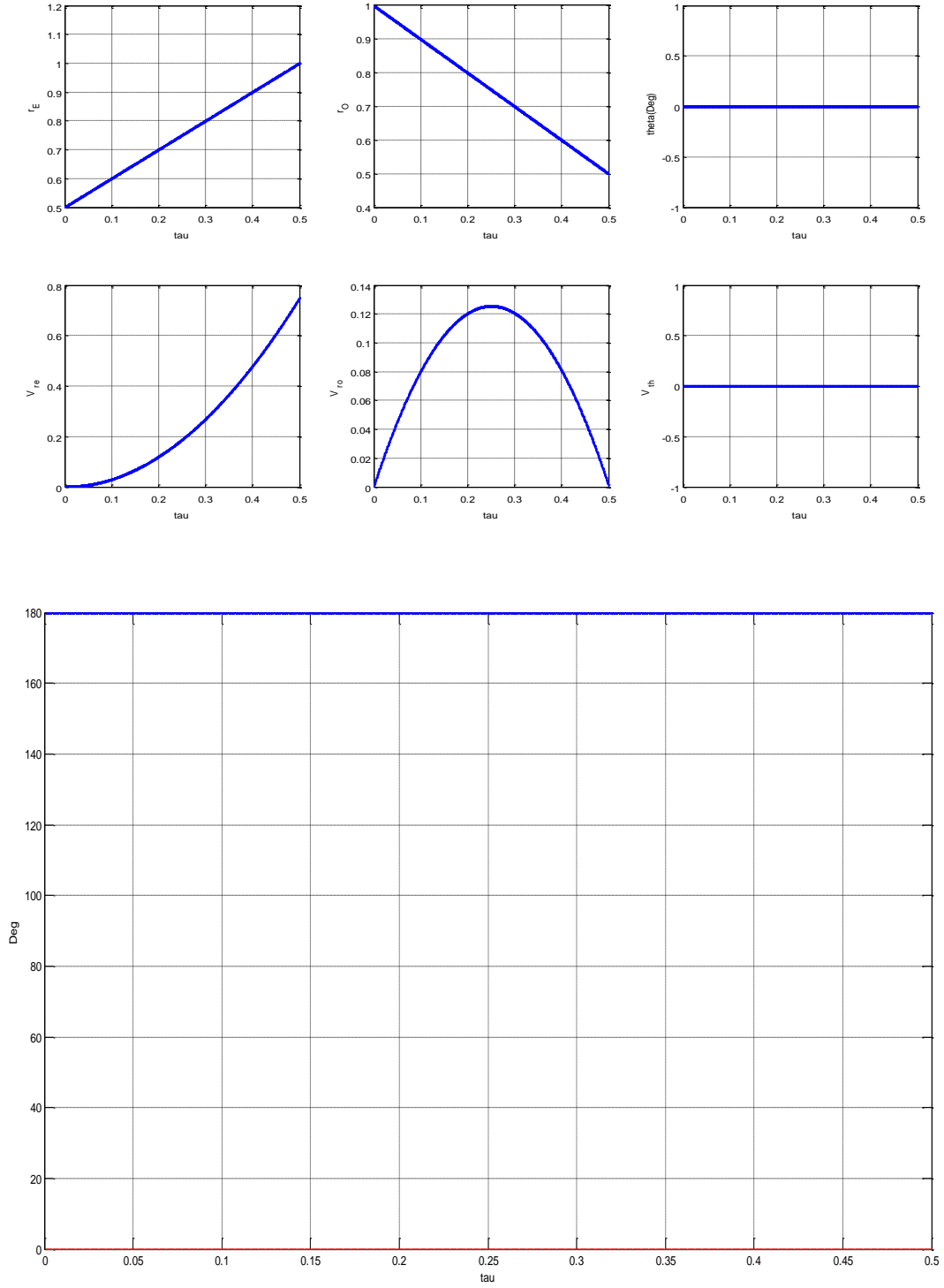


Figure 17: Time history of the States, Costates and Controls. $\alpha = 1$, $\xi = 0^\circ$, $r_{O_r} = 1$

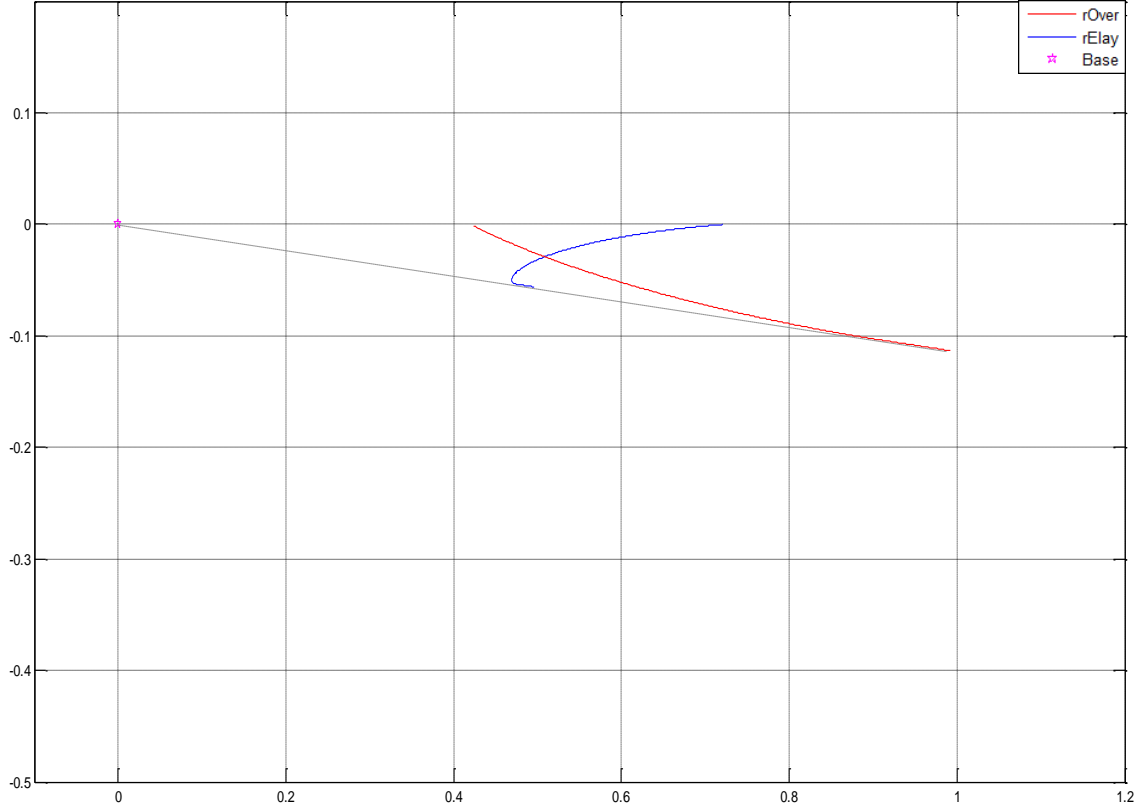


Figure 21: Optimal trajectories of Rover and Relay. $\alpha = 2$, $\xi = 180^\circ$, $r_{O_r} = 1$

The rElay and rOver should start and end on a line since $\xi = 180^\circ$. In other words, they maintain $\theta \equiv 0$. However, as seen in Fig. 21, the simulation didn't show the result we expected. This is because of a small numerical error. Without the error, the rOver and rElay each will start the game at 0.5 and 0.75.

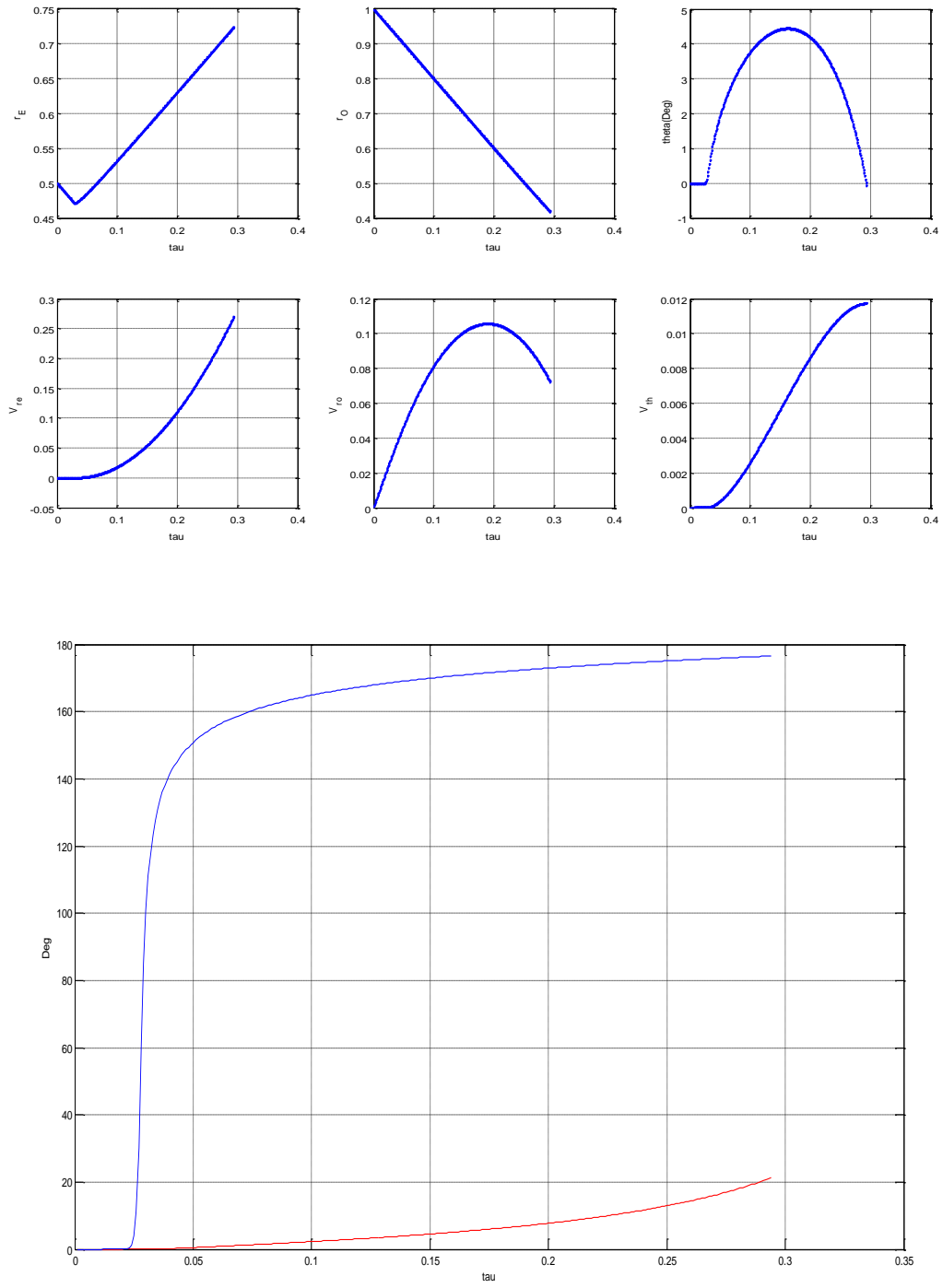


Figure 18: Time history of the States, Costates and Controls. $\alpha = 2$, $\xi = 180^\circ$, $r_{O_T} = 1$

IV.2. Optimal Trajectories of Rover and Relay for different r_{E_T} , r_{O_T} , θ_T

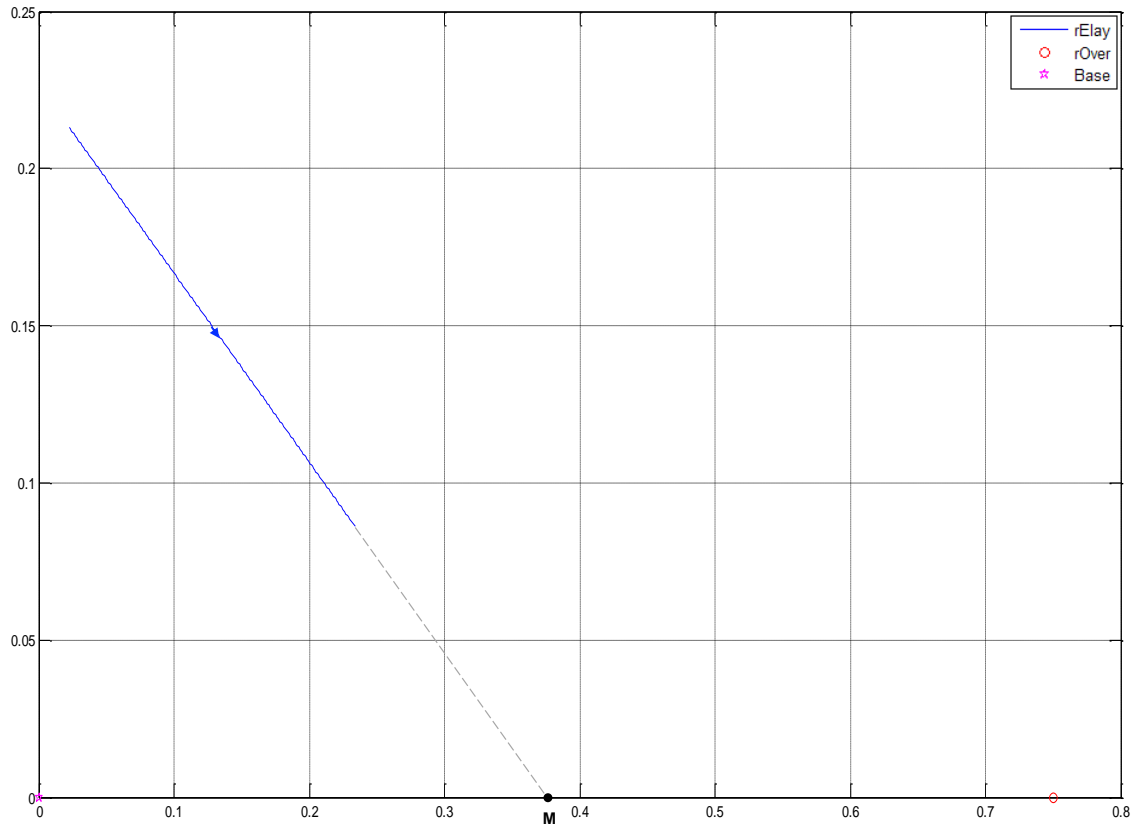


Figure 19: Optimal Trajectory of Relay When $r_{E_T} = \frac{1}{4}$, $r_{O_T} = \frac{3}{4}$, $\alpha = 0$, $\theta_T = 20^\circ$

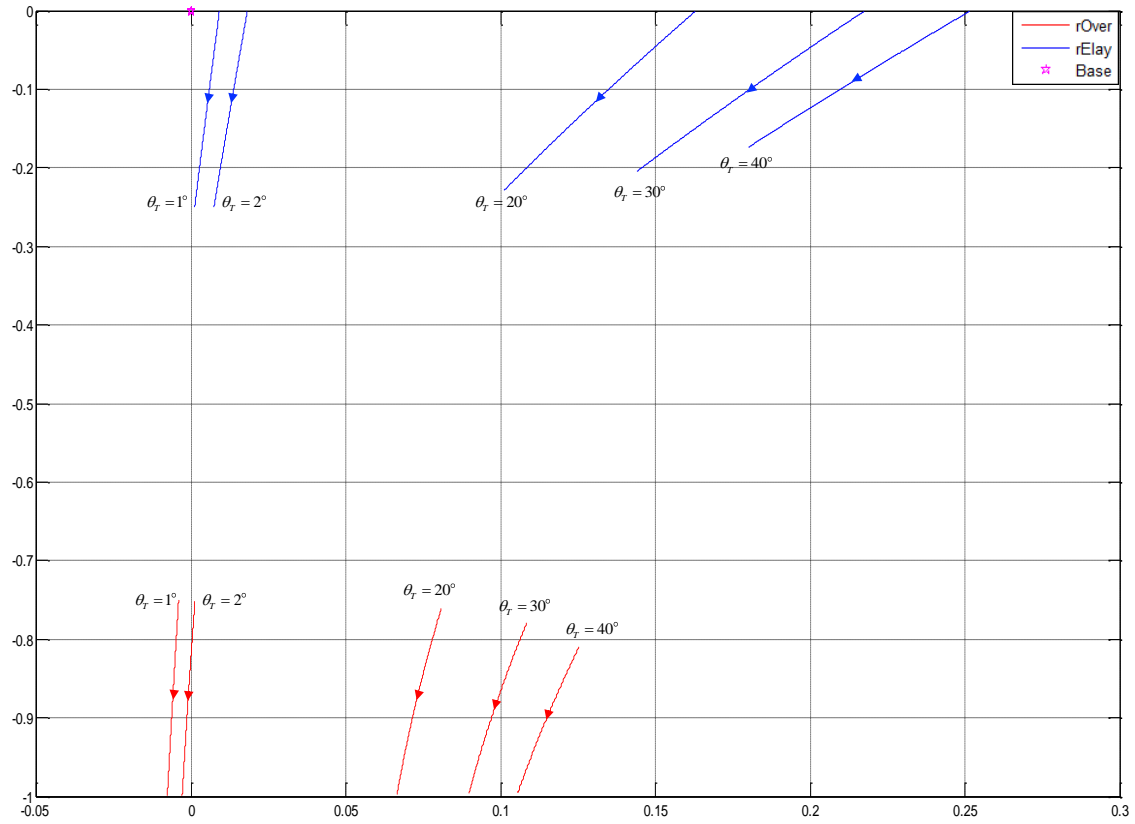


Figure 20: Optimal Trajectories of Rover and Relay When

$$r_{E_T} = \frac{1}{4}, r_{O_T} = 1, \alpha = 1, \theta_T = 1^\circ, 2^\circ, 20^\circ, 30^\circ, 40^\circ$$

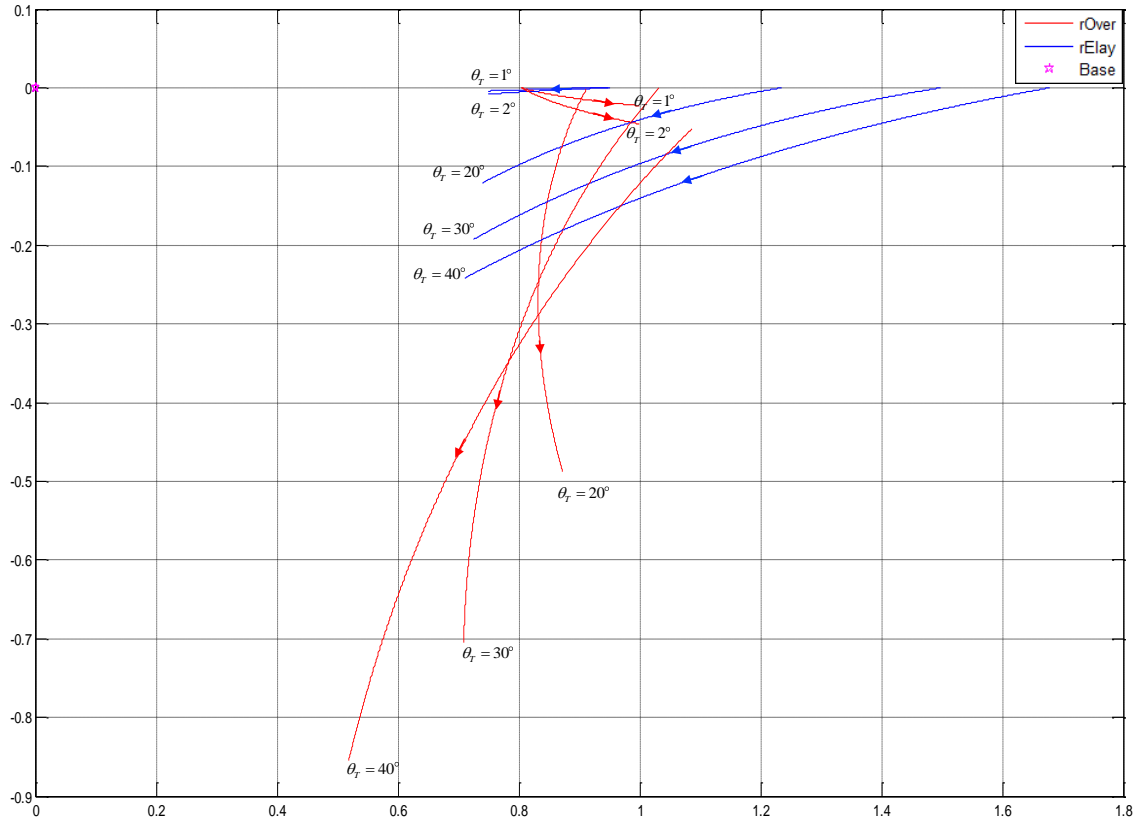


Figure 21: Optimal Trajectories of Rover and Relay When

$$r_{E_T} = \frac{3}{4}, r_{O_T} = 1, \alpha = 1, \theta_T = 1^\circ, 2^\circ, 20^\circ, 30^\circ, 40^\circ$$

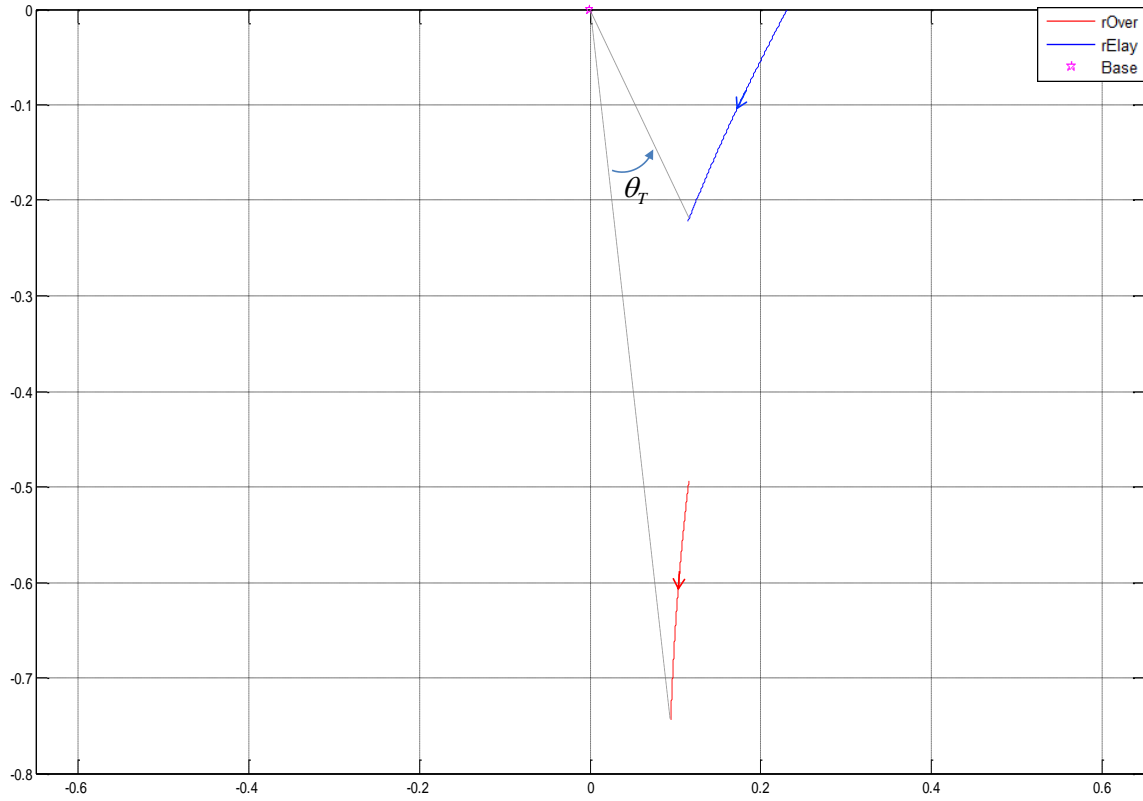


Figure 22: Optimal Trajectories of Rover and Relay When

$$r_{E_r} = \frac{1}{4}, r_{O_r} = \frac{3}{4}, \alpha = 1, \theta_T = 20^\circ$$

Fig. 19 shows the case when the rElay doesn't have enough time to reach to the mid- point. This is the optimal control case when the rOver is stationary. Therefore the rElay moves straight toward the mid-point, however unlike in our previous result, it stops moving at $r_{E_r} = \frac{1}{4}$. Whereas, the rOver is moving and the rElay is tracking its optimal position continuously in fig. 22. In both cases the rElay was not able to reach its optimal position but it's following the guidance of the optimal control law.

From these results now we know we can check if the rElay is optimally positioned. And if it is, even the rElay didn't arrive its optimal point we are able to calculate the estimated location or time it takes until the rElay will reach this position. Moreover, if we know the final position of the rOver and the time we are given, even if the rElay was following the optimal course, we can find the final optimal point of the rElay. Therefore we can control the rElay directly to the intended location.

IV.3. Comparison of the End Game Control Law and Optimal Control Law

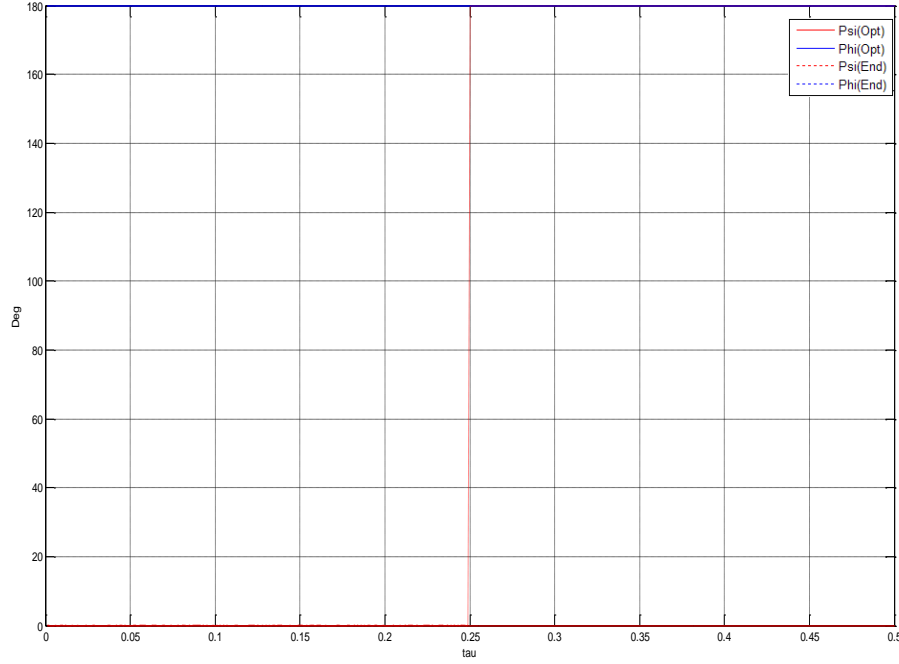


Figure 23: Comparison of the End Game Control Law and Optimal Control Law

$$r_{E_r} = 0.5, r_{O_r} = 1, \alpha = 1, \xi = 0^\circ$$

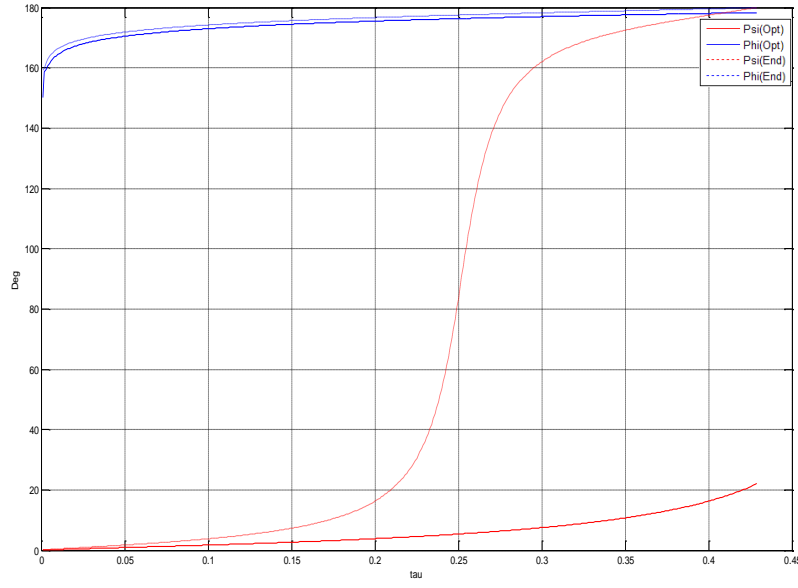


Figure 24: Comparison of the End Game Control Law and Optimal Control Law

$$r_{E_T} = 0.5, r_{O_T} = 1, \alpha = 1, \xi = 30^\circ$$

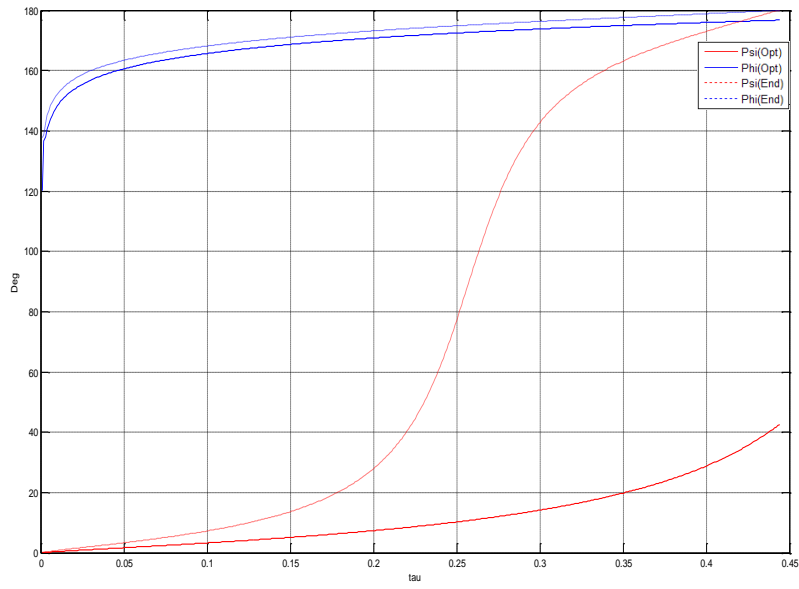


Figure 25: Comparison of the End Game Control Law and Optimal Control Law

$$r_{E_T} = 0.5, r_{O_T} = 1, \alpha = 1, \xi = 60^\circ$$

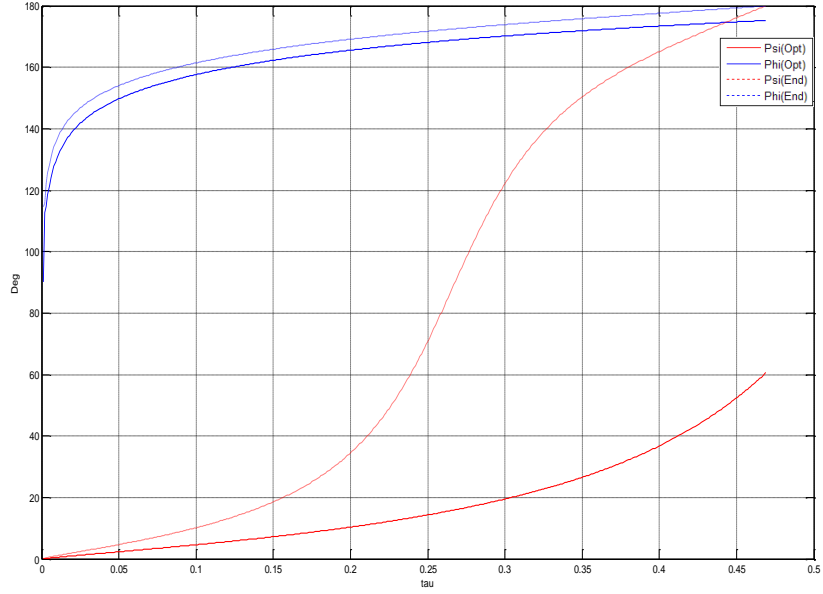


Figure 26: Comparison of the End Game Control Law and Optimal Control Law

$$r_{E_T} = 0.5, r_{O_T} = 1, \alpha = 1, \xi = 90^\circ$$

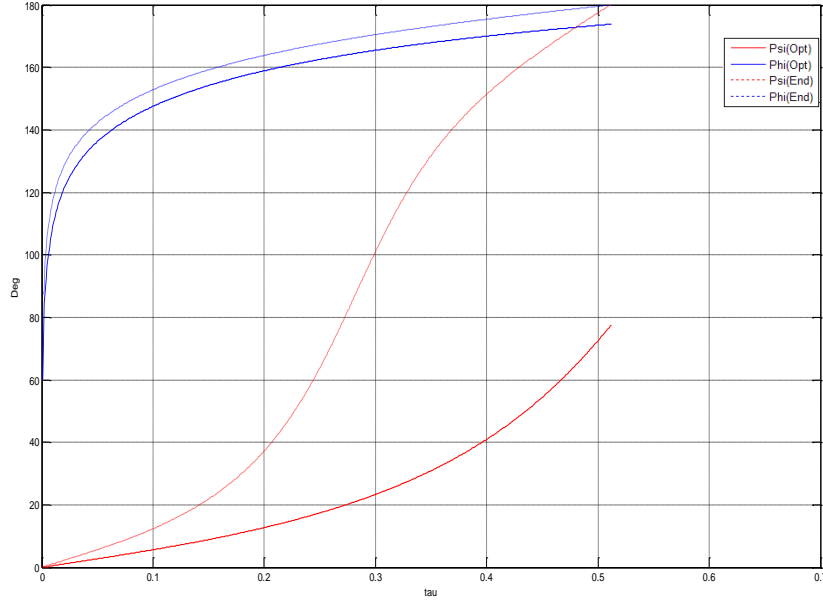


Figure 27: Comparison of the End Game Control Law and Optimal Control Law

$$r_{E_T} = 0.5, r_{O_T} = 1, \alpha = 1, \xi = 120^\circ$$

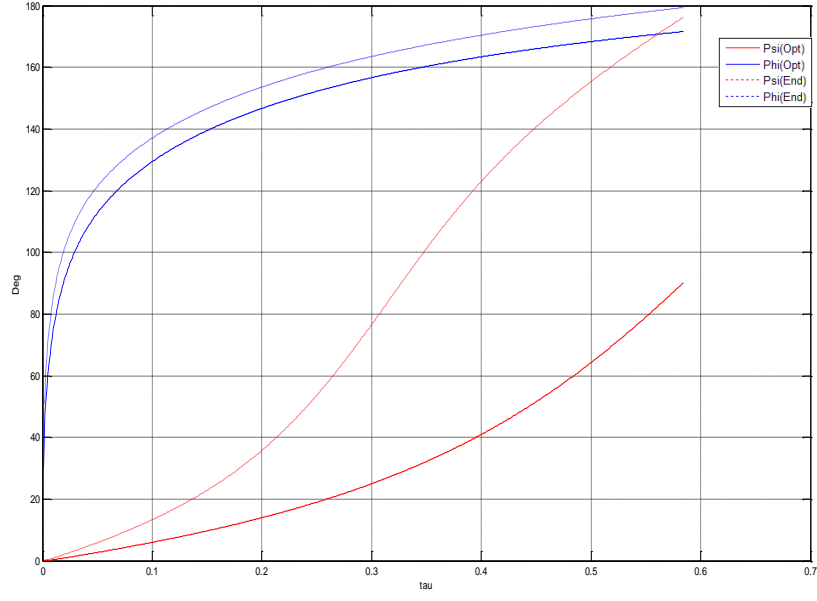


Figure 28: Comparison of the End Game Control Law and Optimal Control Law

$$r_{E_T} = 0.5, r_{O_T} = 1, \alpha = 1, \xi = 150^\circ$$

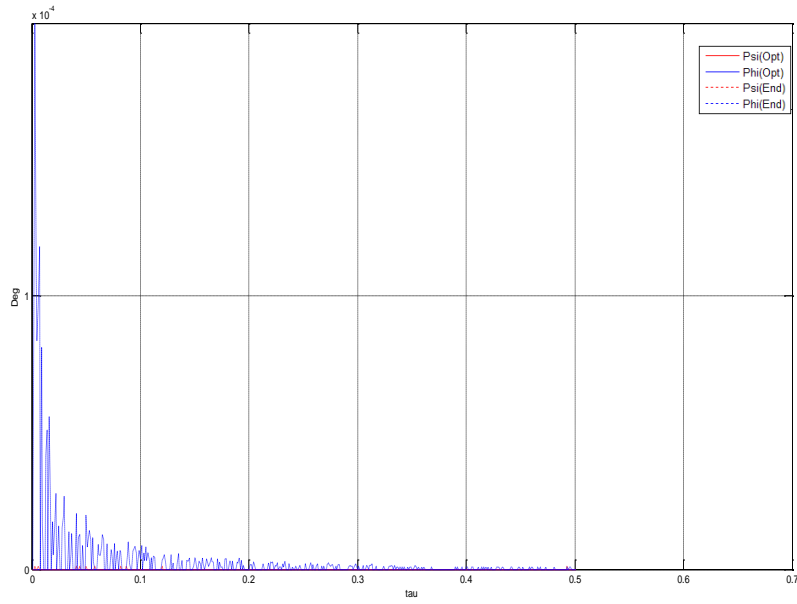


Figure 29: Comparison of the End Game Control Law and Optimal Control Law

$$r_{E_T} = 0.5, r_{O_T} = 1, \alpha = 1, \xi = 180^\circ$$

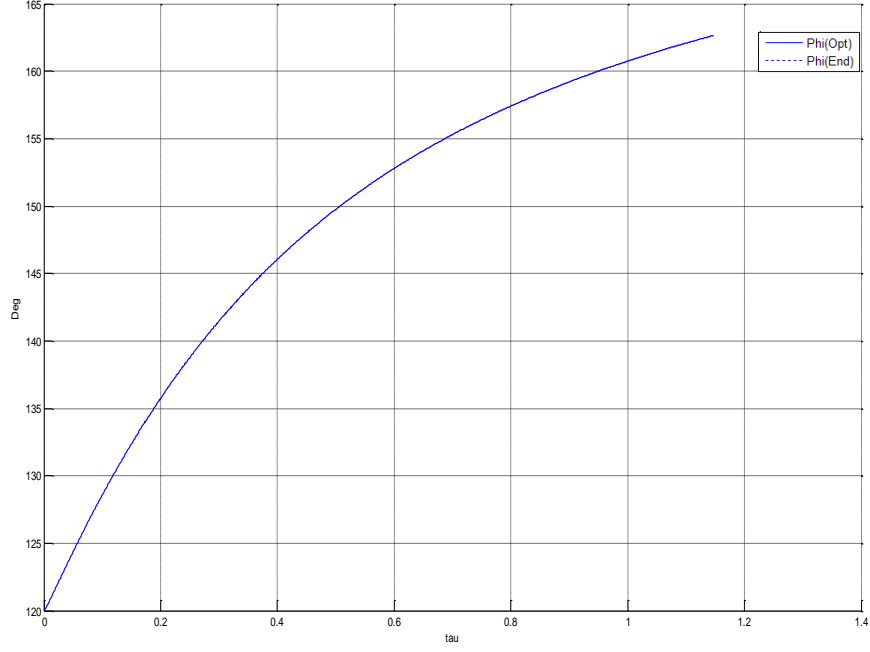


Figure 30: Comparison of the End Game Control Law and Optimal Relay Control

$$\text{Law } r_{E_r} = 0.5, r_{O_r} = 1, \alpha = 0, \xi = 90^\circ$$

As we see from Figs. 23-30, the control of the rElay using the optimal control law and the end game control law look very similar. However, the rOver's control using the end game control law is quite different from the optimal control law.

We are mostly concerned with the control of the rElay. Therefore we can conclude that the end game rElay control law is a good sub-optimal control law.

V. Conclusions and Recommendations

V.1. Conclusions

This thesis develops optimal guidance laws for a rElay MAV in support of extended range ISR operations. The algorithm is based upon the solution of a min-max optimization problem, namely, the solution of the differential game, which represents a worst case scenario. Heuristic rElay guidance strategies are also provided. These are derived using a geometry based (sub) optimality principle, and also the solution of the one-sided rElay optimal control problem, where the rOver is considered stationary. Both methods provided corroborating results which were then employed to gain insight into the solution of the differential game. The optimal control and differential game's solution exhibits interesting behavior: the optimal flow field namely the optimal trajectories will converge to the family of end states $r_E = \frac{1}{2}r_O$, where from the optimal trajectory is a singular optimal trajectory and $r_E(t) = \frac{1}{2}r_O(t) \forall t$. A parametric investigation was conducted and optimal trajectories were generated for speed ratio parameters $0 \leq \alpha < 2$. When the speed ratio $\alpha \geq 2$, a “sweet spot” won't be reached. Obviously, the most interesting case is $\alpha = 1$.

V.2. Recommendations for Future Research

The interesting cases of

1. Higher-order-dynamics of the rElay MAV must be modeled, including a time delay in the control loop.

2. Multi player scenarios must be addressed: One rElay MAV, multiple rOver MAVs needs to be considered.
3. Multiple relay MAVs and multiple rOver MAV scenarios must be considered.
4. Investigate different RF power requirements for Rover and Relay

Appendix A – Additional Scenarios

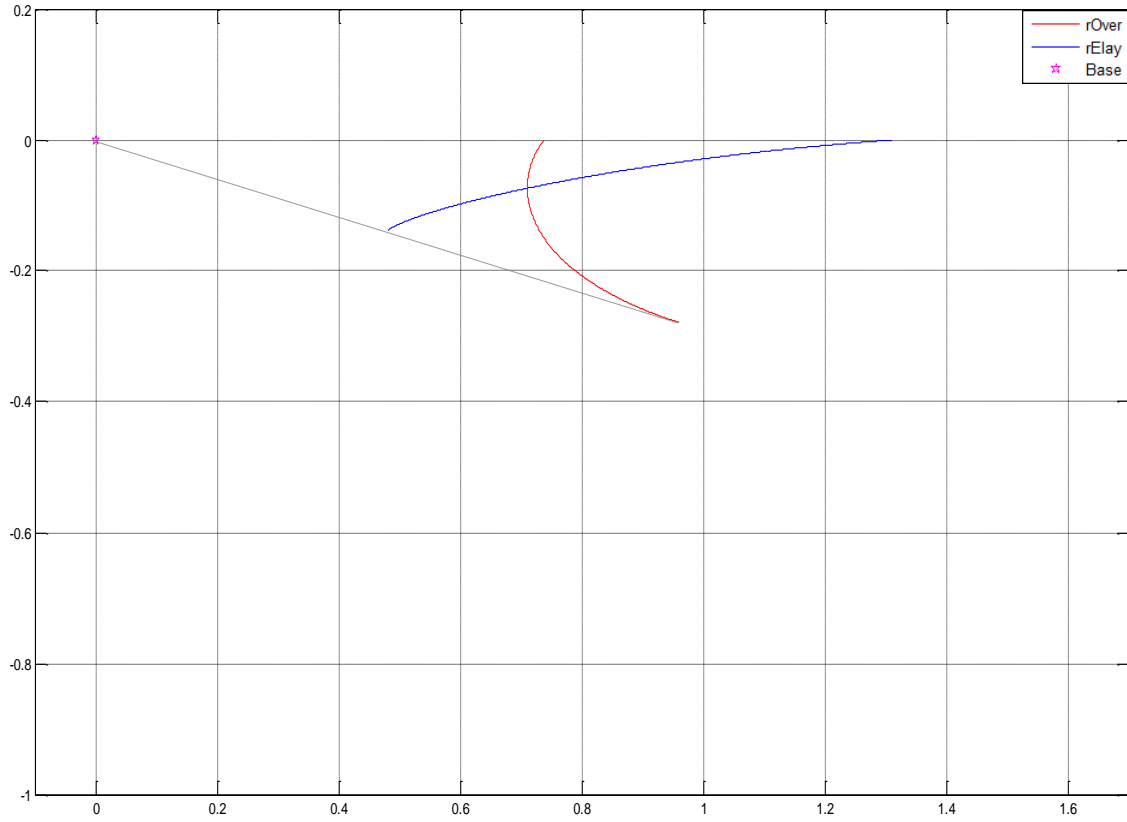


Figure A. 1: Optimal trajectories of Rover and Relay. $\alpha = 0.5$, $\xi = 60^\circ$, $r_{O_r} = 1$

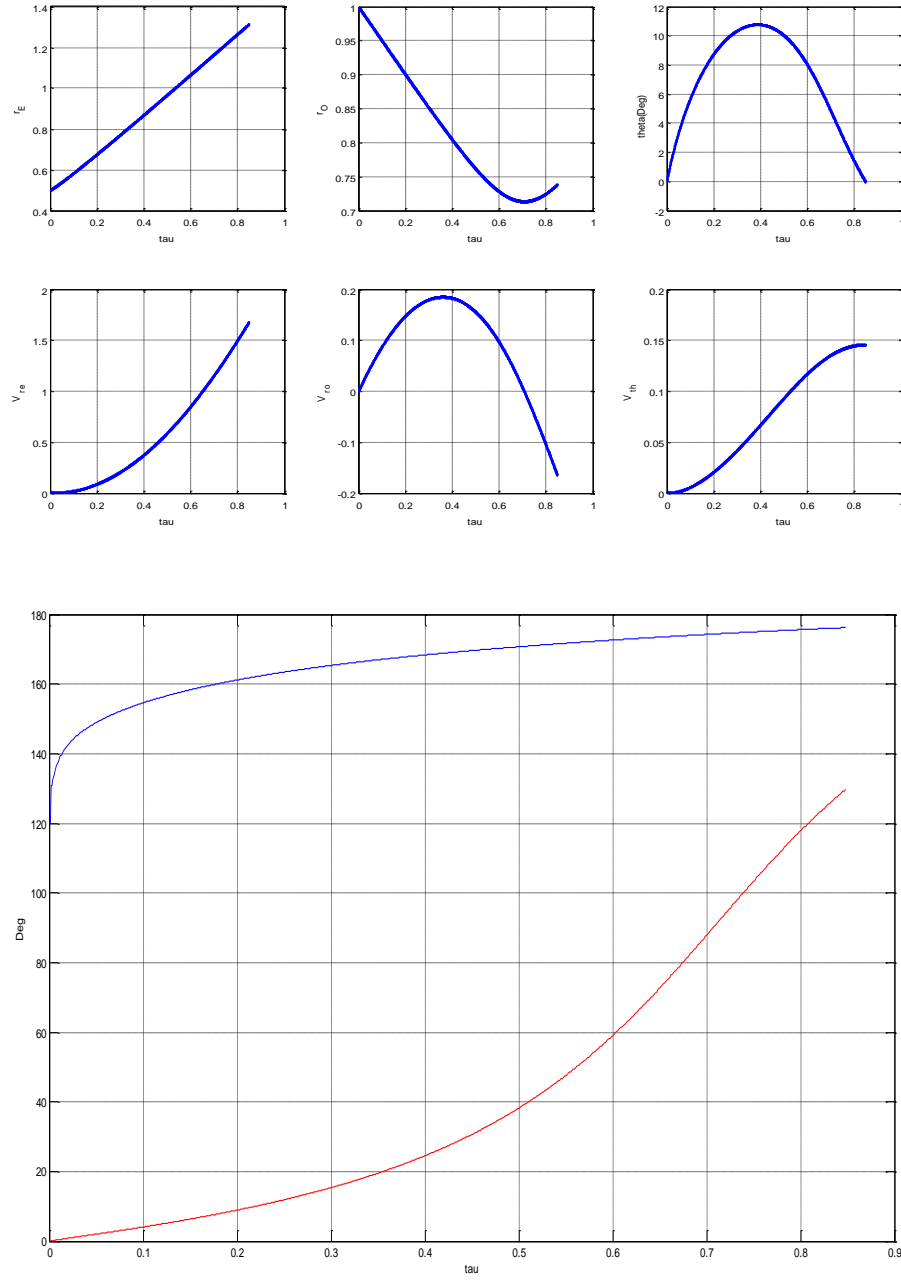


Figure A. 2: Time history of the States, Costates and Controls.

$$\alpha = 0.5, \quad \xi = 60^\circ, \quad r_{O_T} = 1$$

At the end point the rElay's control is $\varphi^*(0) = 180^\circ - 60^\circ = 120^\circ$

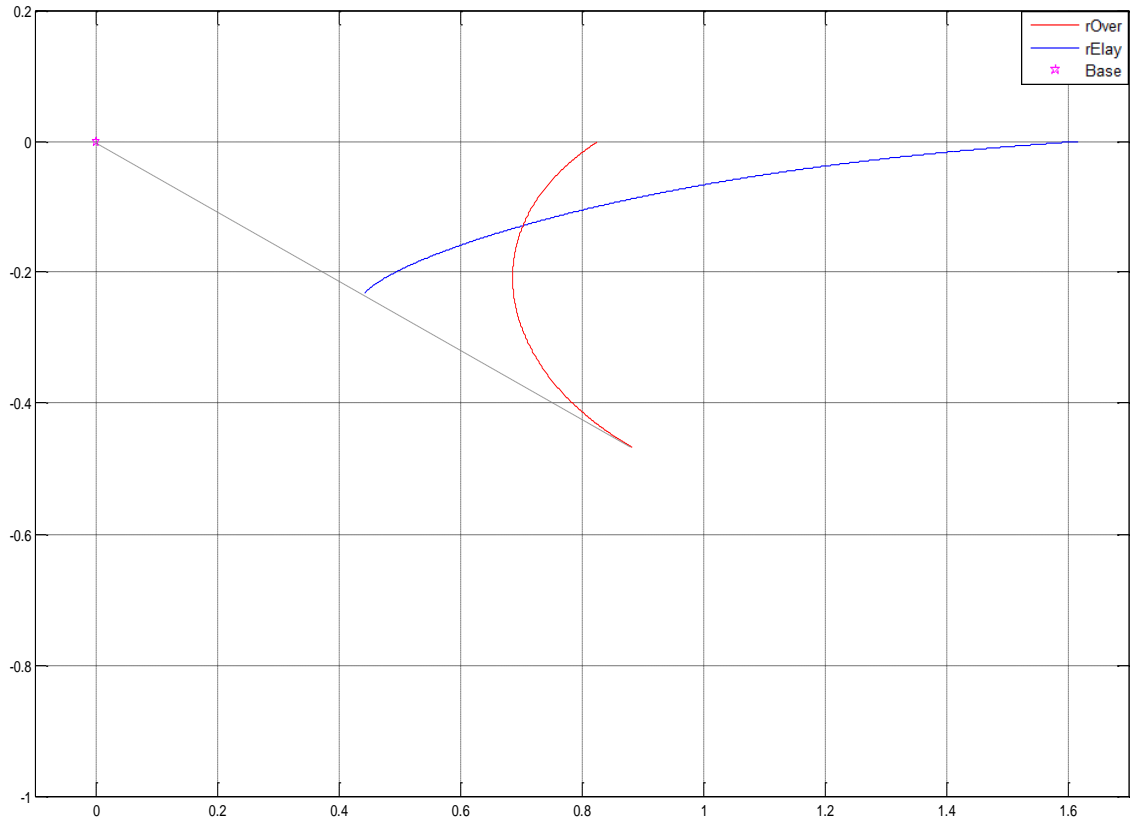


Figure A. 3: Optimal trajectories of Rover and Relay. $\alpha = 0.5$, $\xi = 90^\circ$, $r_{O_r} = 1$

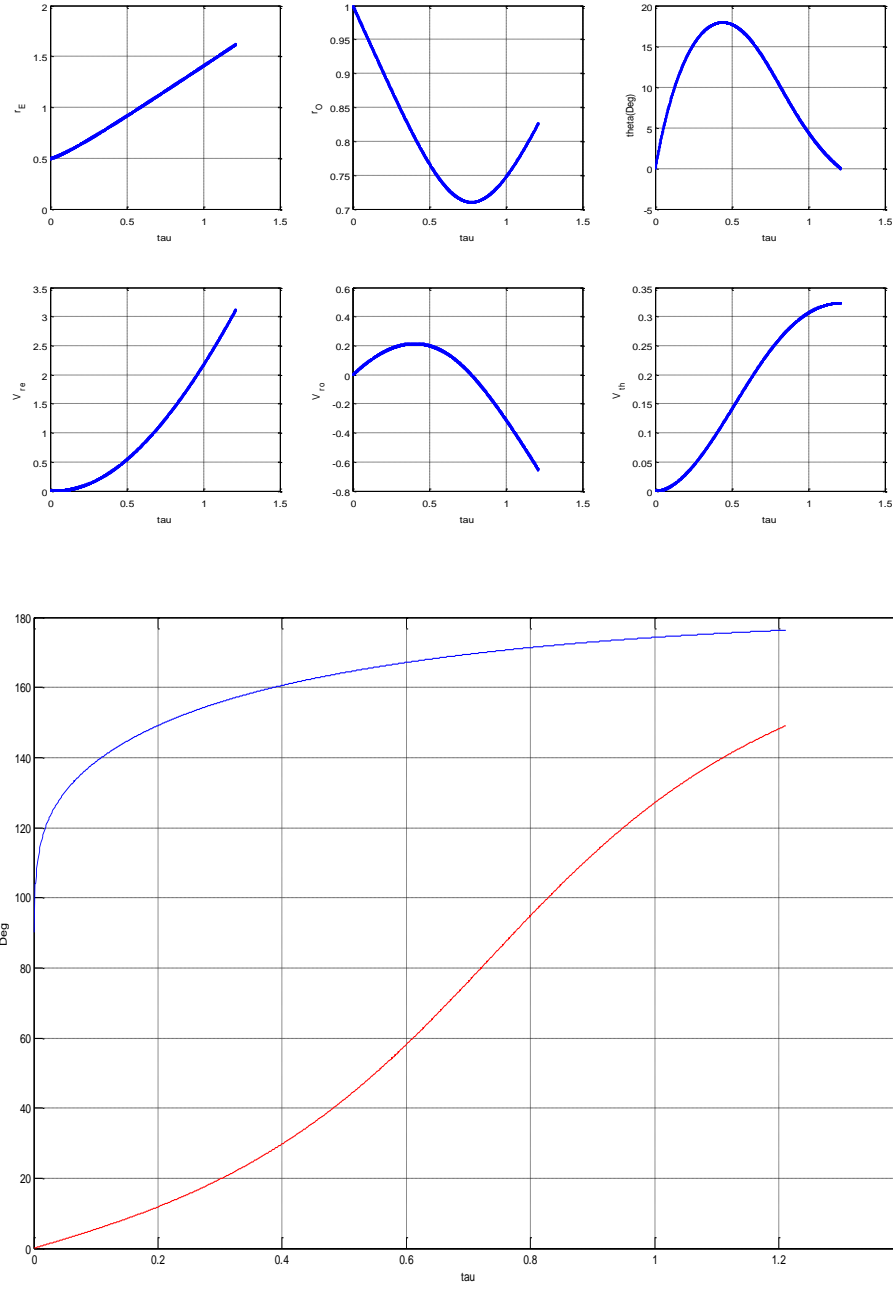


Figure A. 4: Time history of the States, Costates and Controls.

$$\alpha = 0.5, \xi = 90^\circ, r_{O_T} = 1$$

At the end point the rElay's control is $\varphi^*(0) = 180^\circ - 90^\circ = 90^\circ$

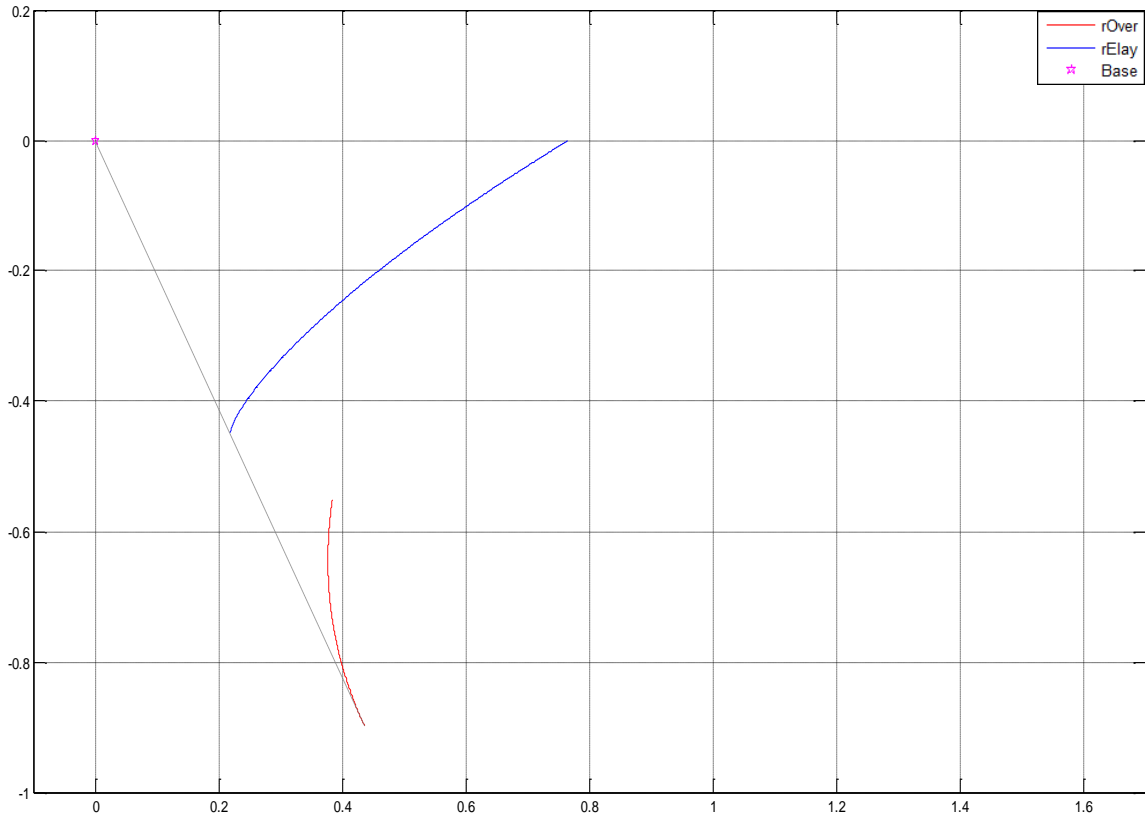


Figure A. 5: Optimal trajectories of Rover and Relay. $\alpha = 0.5$, $\xi = 150^\circ$, $r_{O_r} = 1$

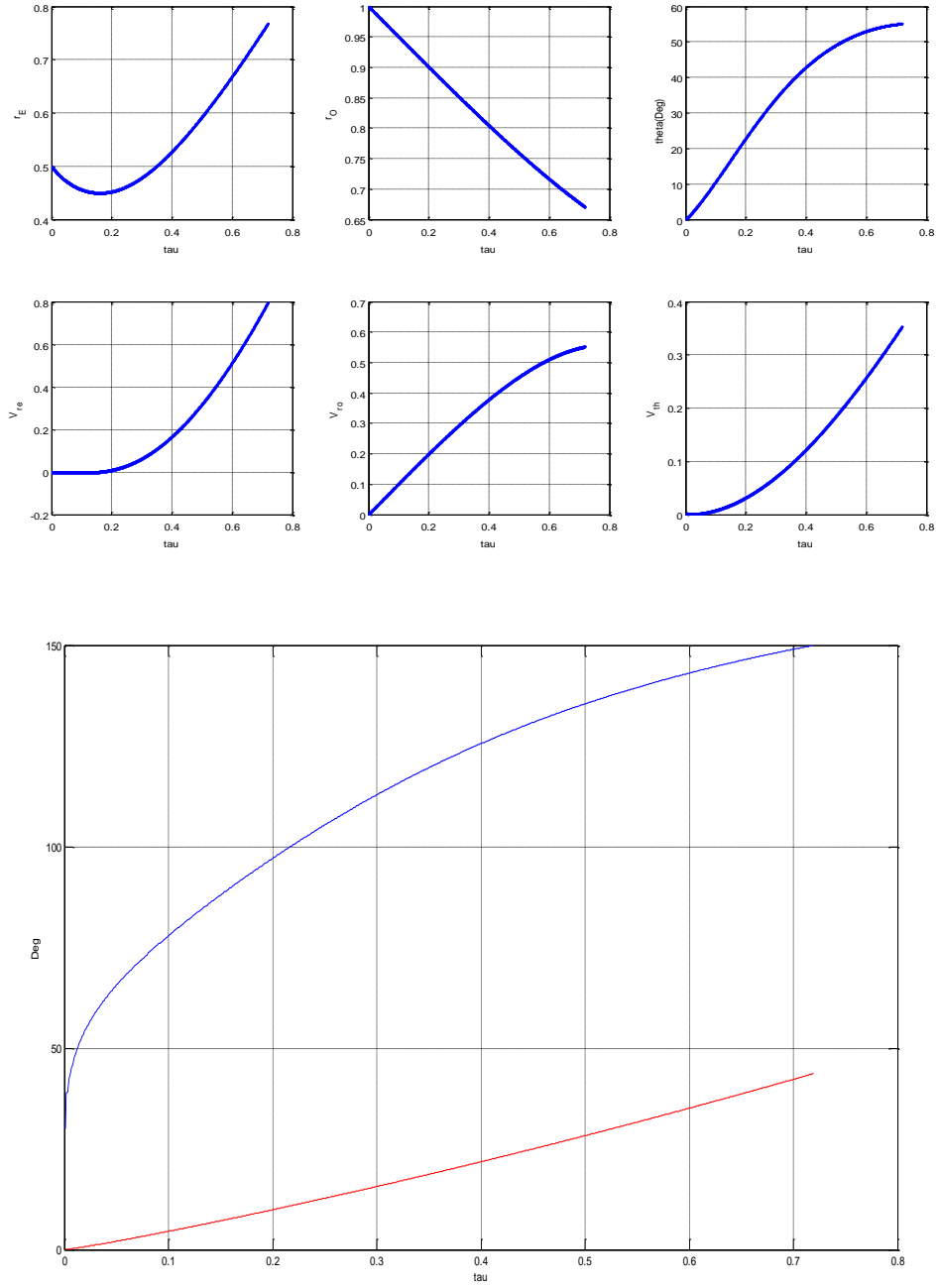


Figure A. 6: Time history of the States, Costates and Controls

$$\alpha = 0.5, \xi = 150^\circ, r_{O_T} = 1$$

At the end point the rElay's control is $\varphi^*(0) = 180^\circ - 150^\circ = 30^\circ$

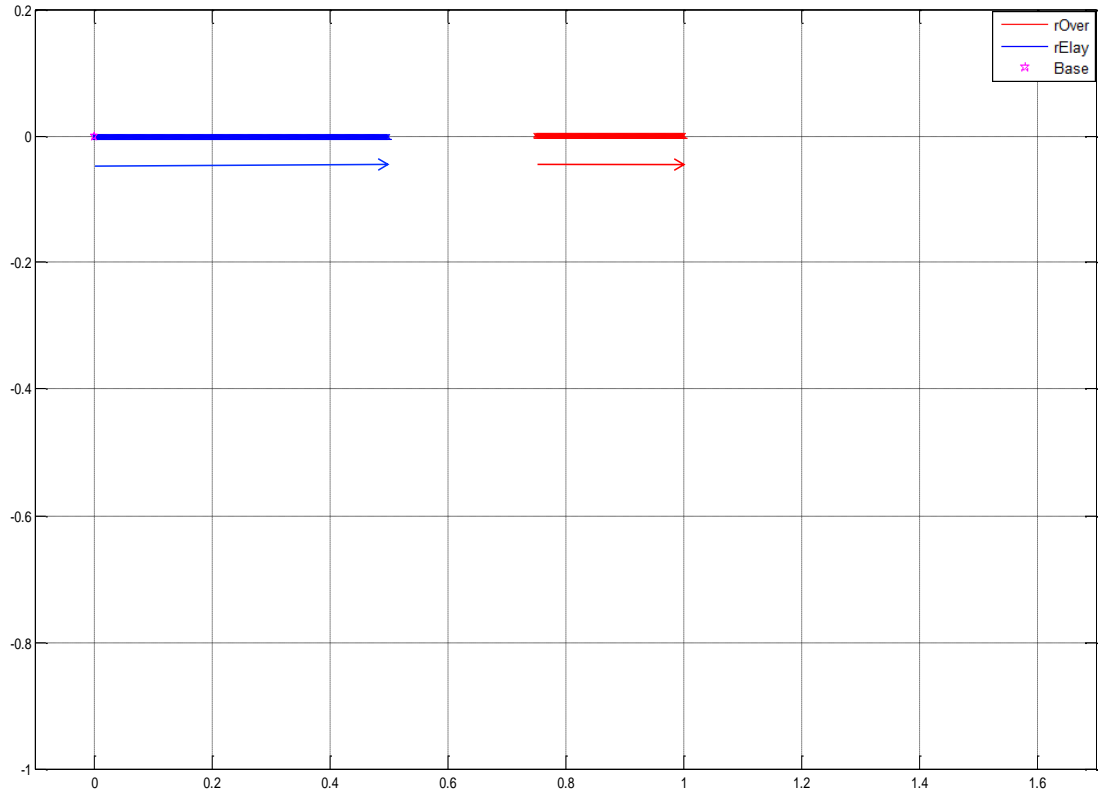


Figure A. 7: Optimal trajectories of Rover and Relay. $\alpha = 0.5$, $\xi = 180^\circ$, $r_{O_r} = 1$

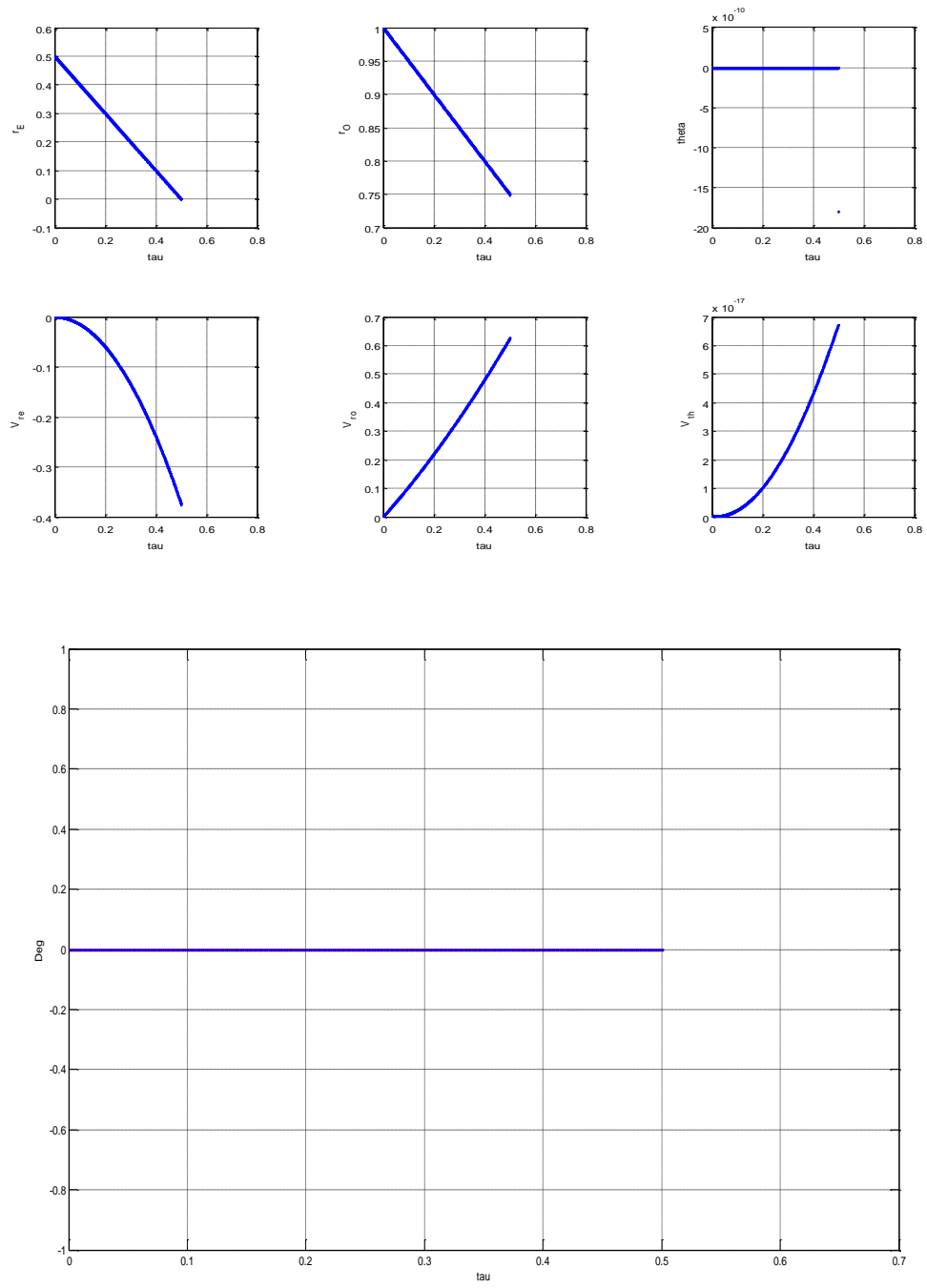


Figure A. 8: Time history of the States, Costates and Controls

$$\alpha = 0.5, \quad \xi = 180^\circ, \quad r_{O_r} = 1$$

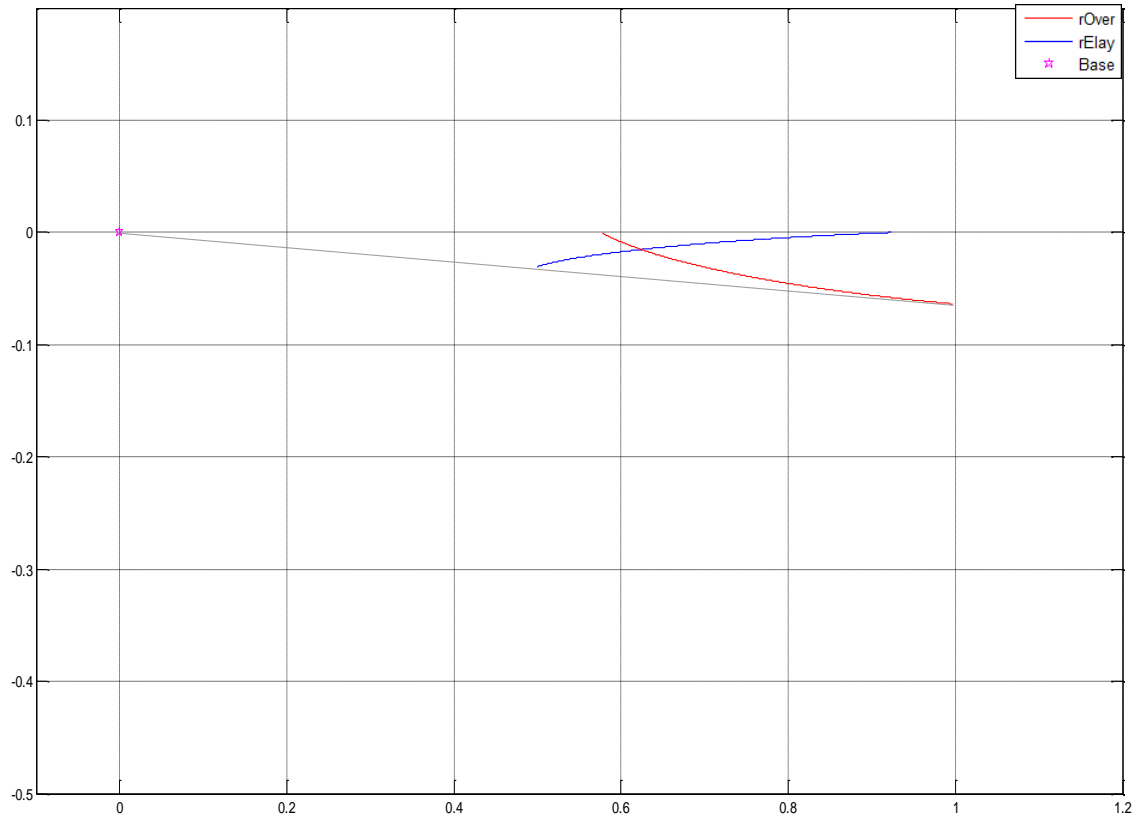


Figure A. 9: Optimal trajectories of Rover and Relay. $\alpha = 1$, $\xi = 30^\circ$, $r_{O_r} = 1$

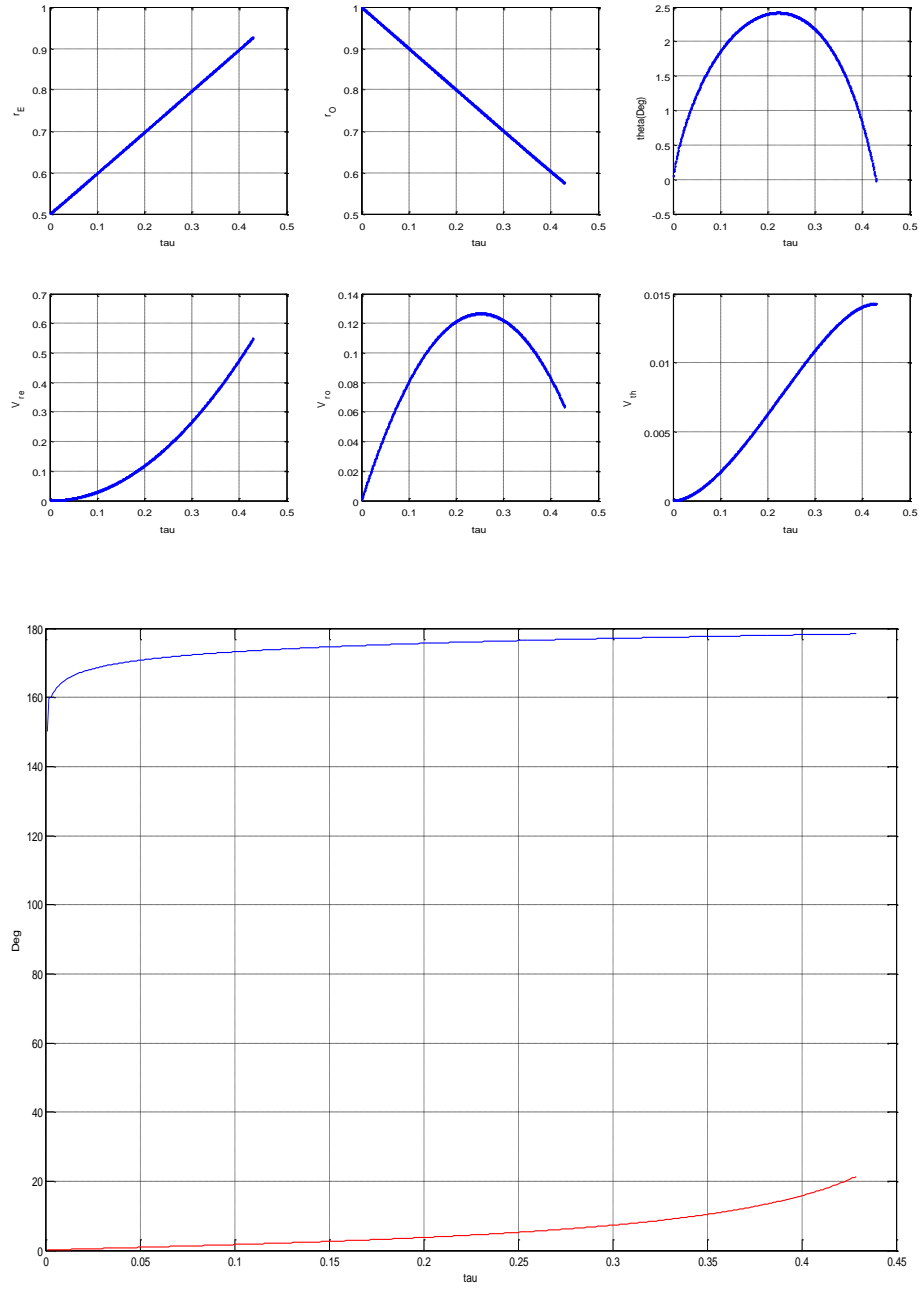


Figure A. 10: Time history of the States, Costates and Controls.

$$\alpha = 1, \xi = 30^\circ, r_{O_T} = 1$$

At the end point the rElay's control is $\varphi^*(0) = 180^\circ - 30^\circ = 150^\circ$

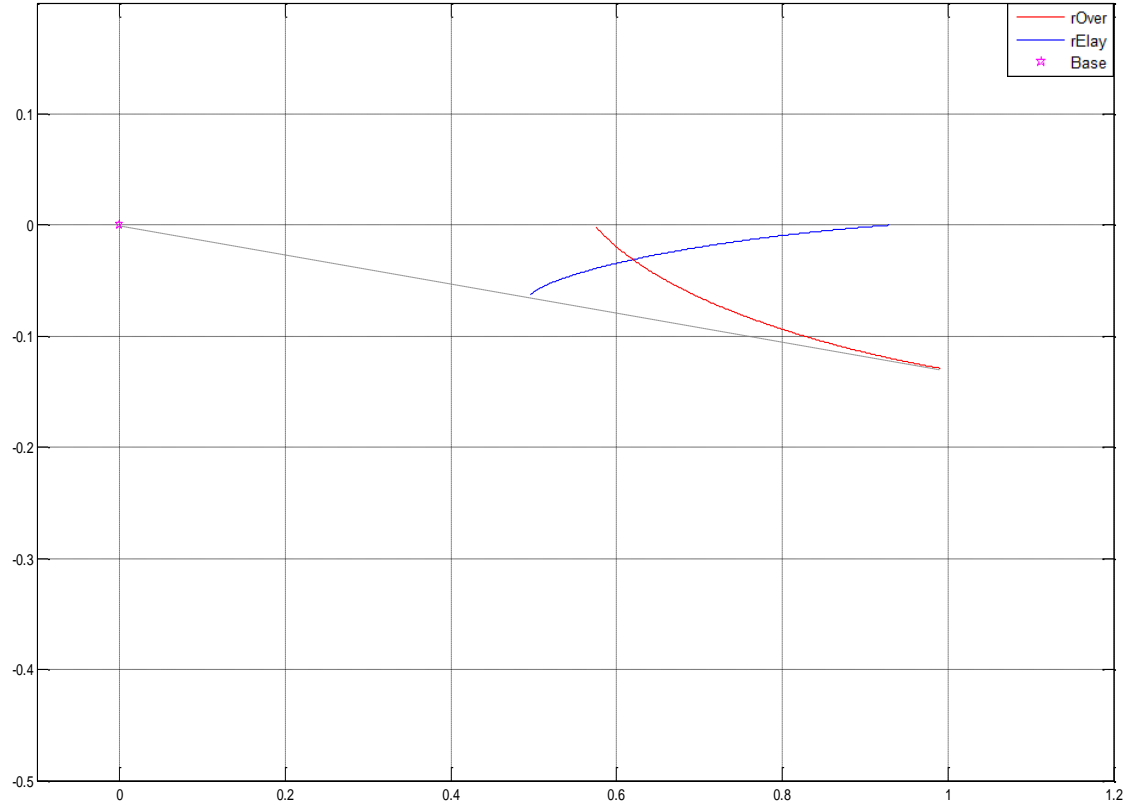


Figure A. 11: Optimal trajectories of Rover and Relay. $\alpha = 1$, $\xi = 60^\circ$, $r_{O_r} = 1$

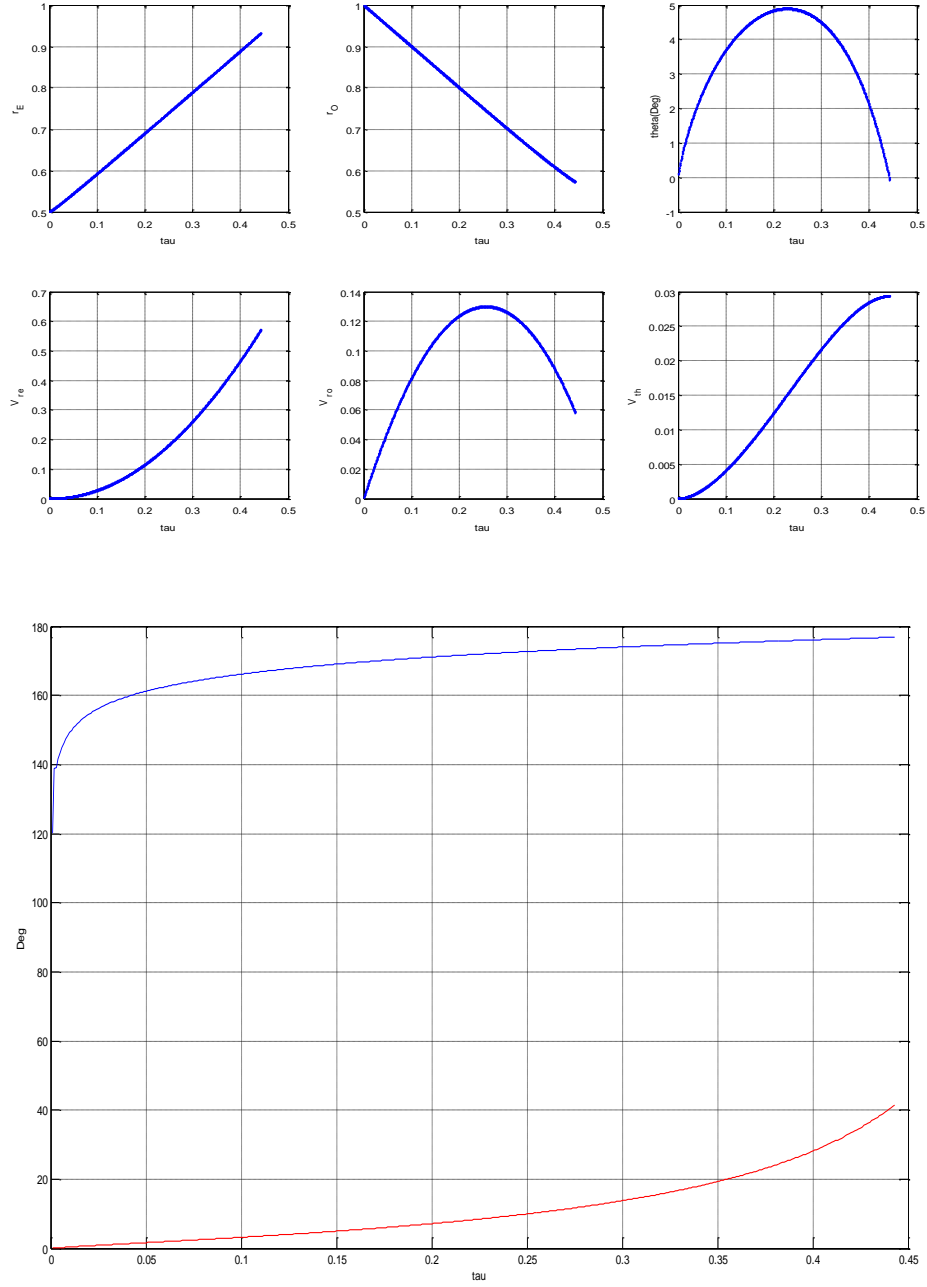


Figure A. 12: Time history of the States, Costates and Controls.

$$\alpha = 1, \xi = 60^\circ, r_{O_T} = 1$$

At the end point the rElay's control is $\varphi^*(0) = 180^\circ - 60^\circ = 120^\circ$

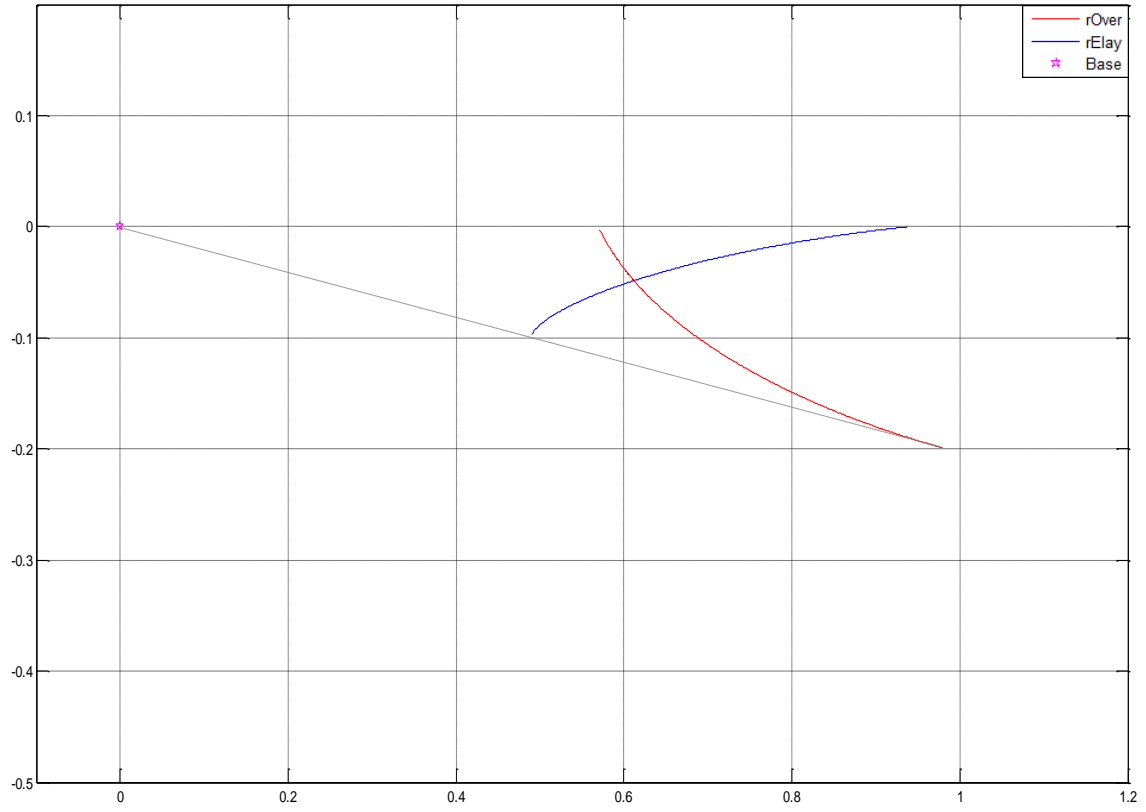


Figure A. 13: Optimal trajectories of Rover and Relay. $\alpha = 1$, $\xi = 90^\circ$, $r_{O_r} = 1$

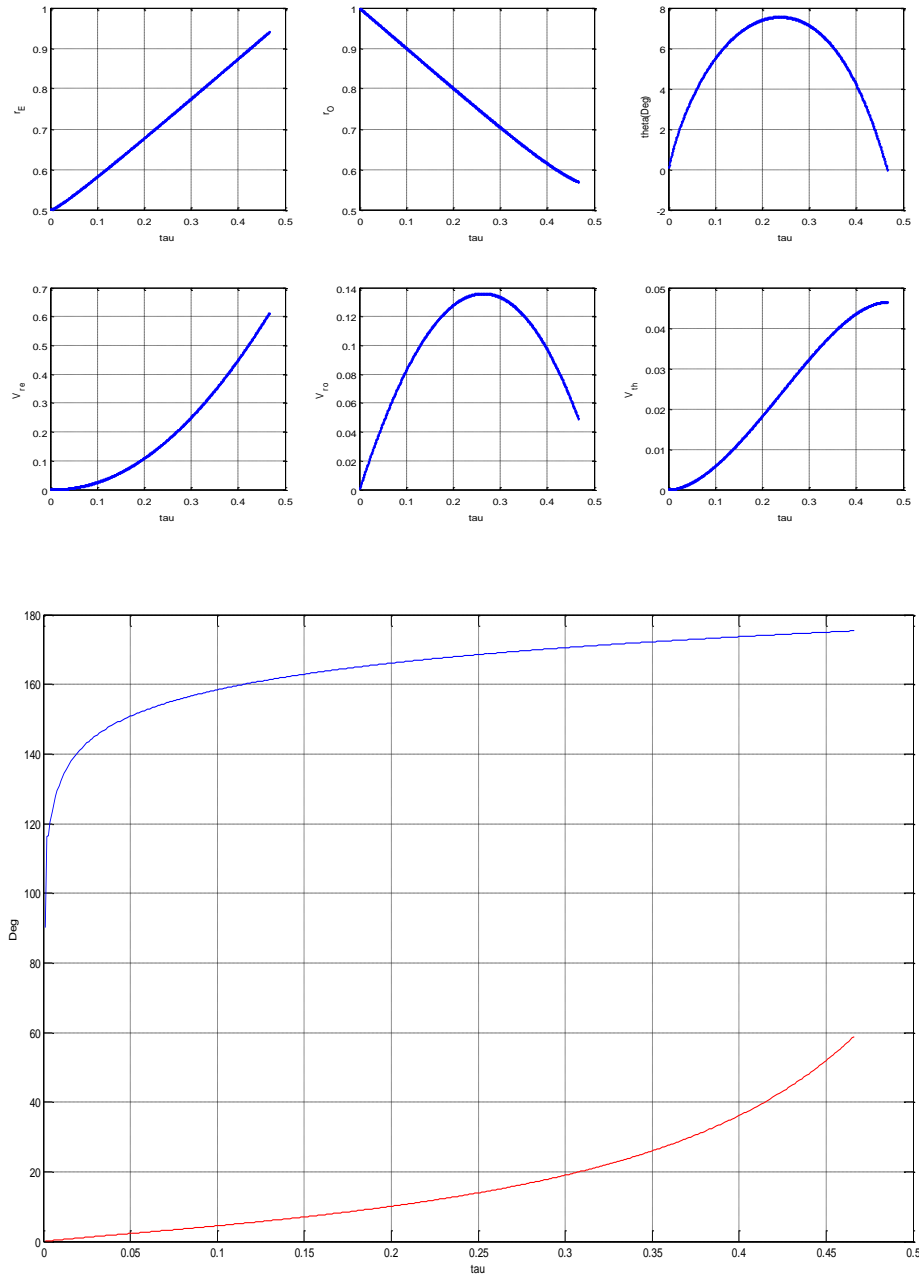


Figure A. 14: Time history of the States, Costates and Controls.

$$\alpha = 1, \quad \xi = 90^\circ, \quad r_{O_r} = 1$$

At the end point the rElay's control is $\varphi^*(0) = 180^\circ - 90^\circ = 90^\circ$

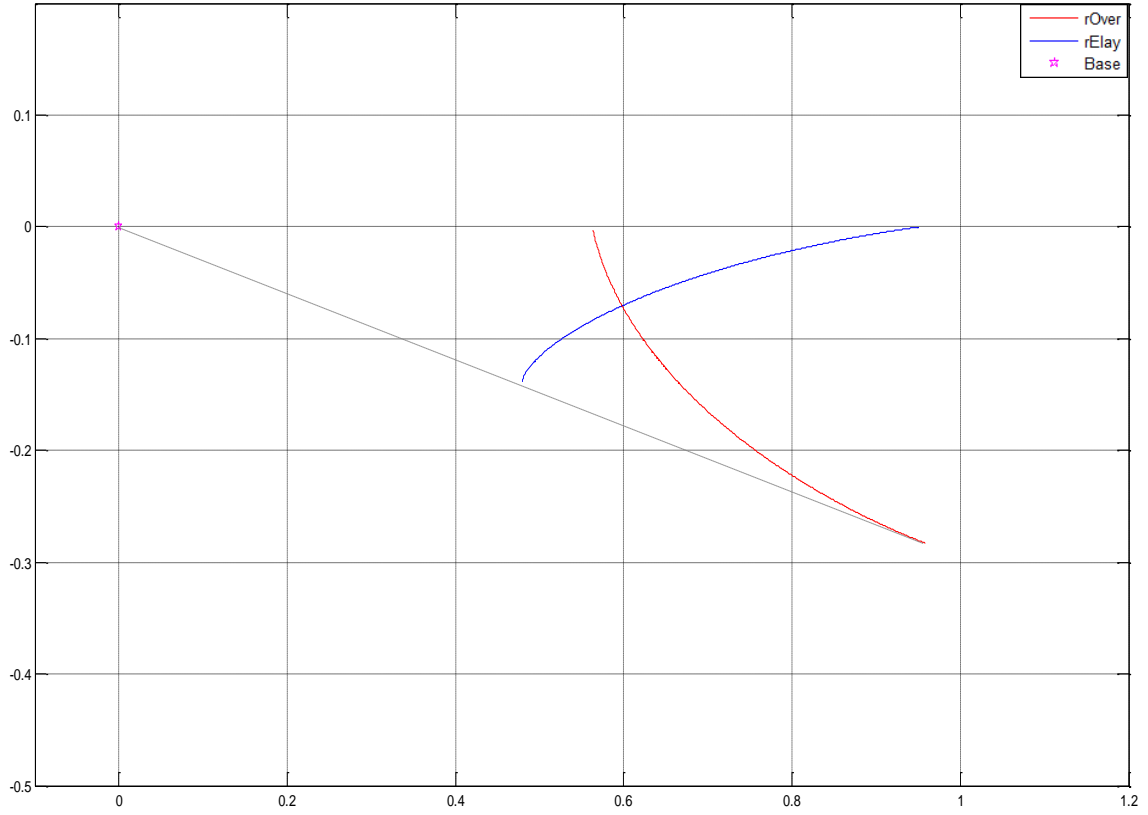


Figure A. 15: Optimal trajectories of Rover and Relay. $\alpha = 1$, $\xi = 120^\circ$, $r_{O_r} = 1$

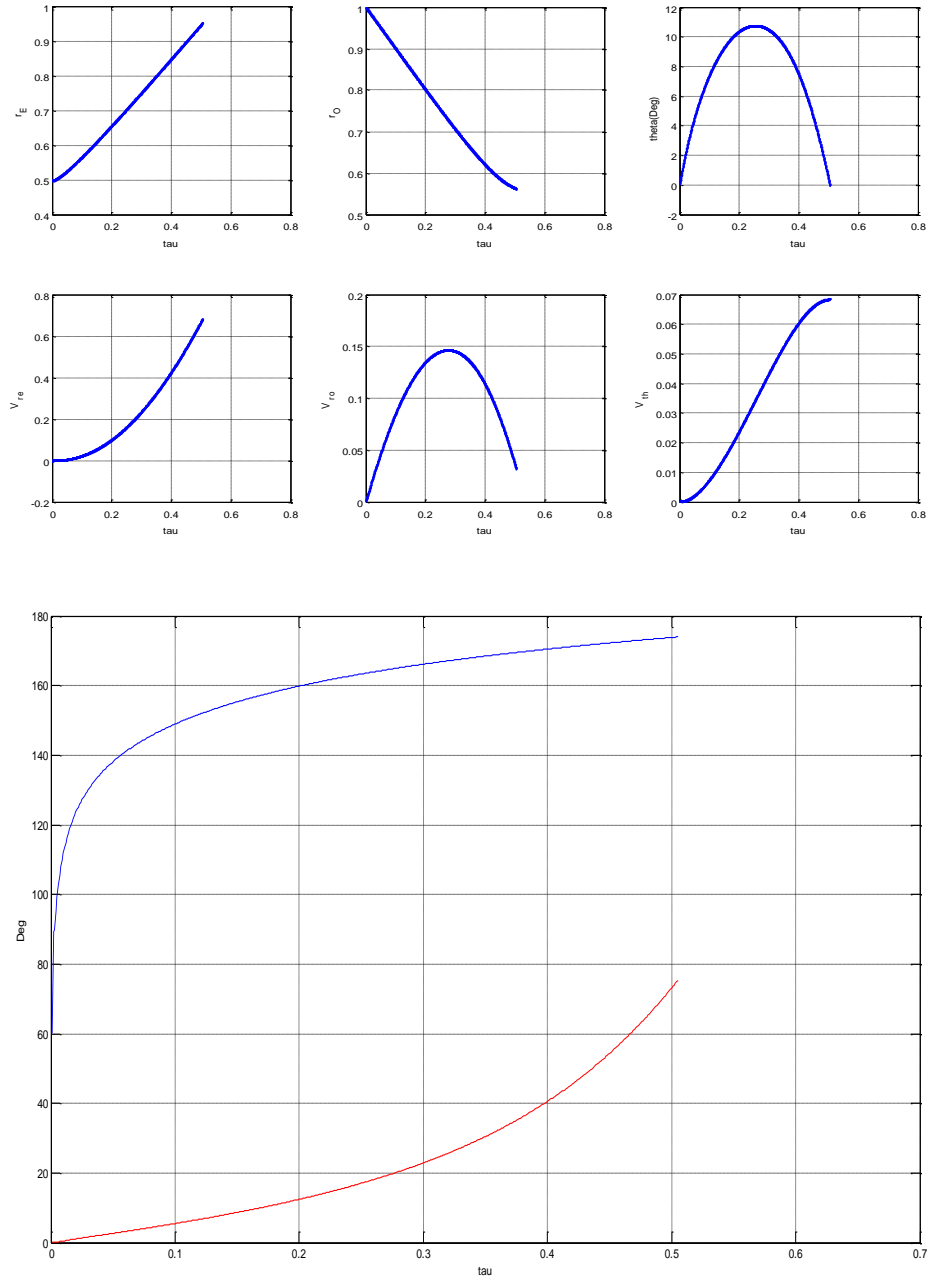


Figure A. 16: Time history of the States, Costates and Controls.

$$\alpha = 1, \xi = 120^\circ, r_{O_r} = 1$$

At the end point the rElay's control is $\varphi^*(0) = 180^\circ - 120^\circ = 60^\circ$

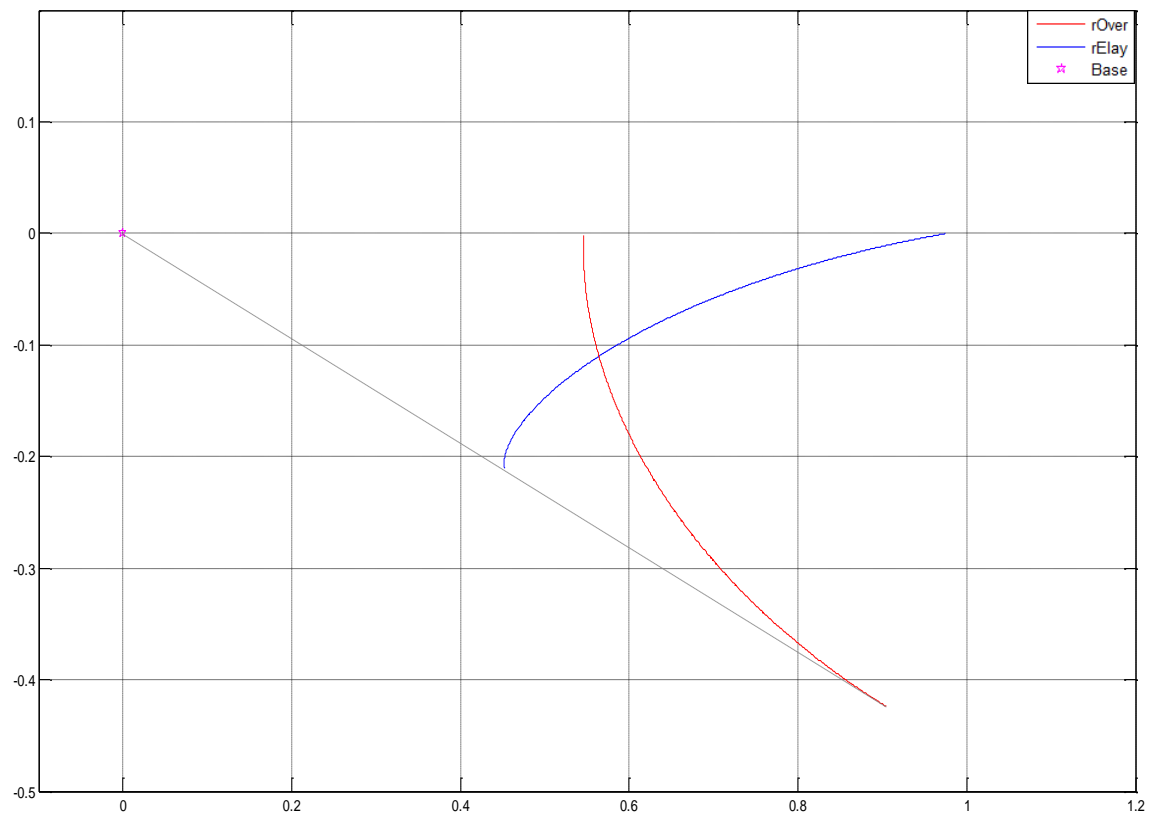


Figure A. 17: Optimal trajectories of Rover and Relay. $\alpha = 1$, $\xi = 150^\circ$, $r_{O_r} = 1$

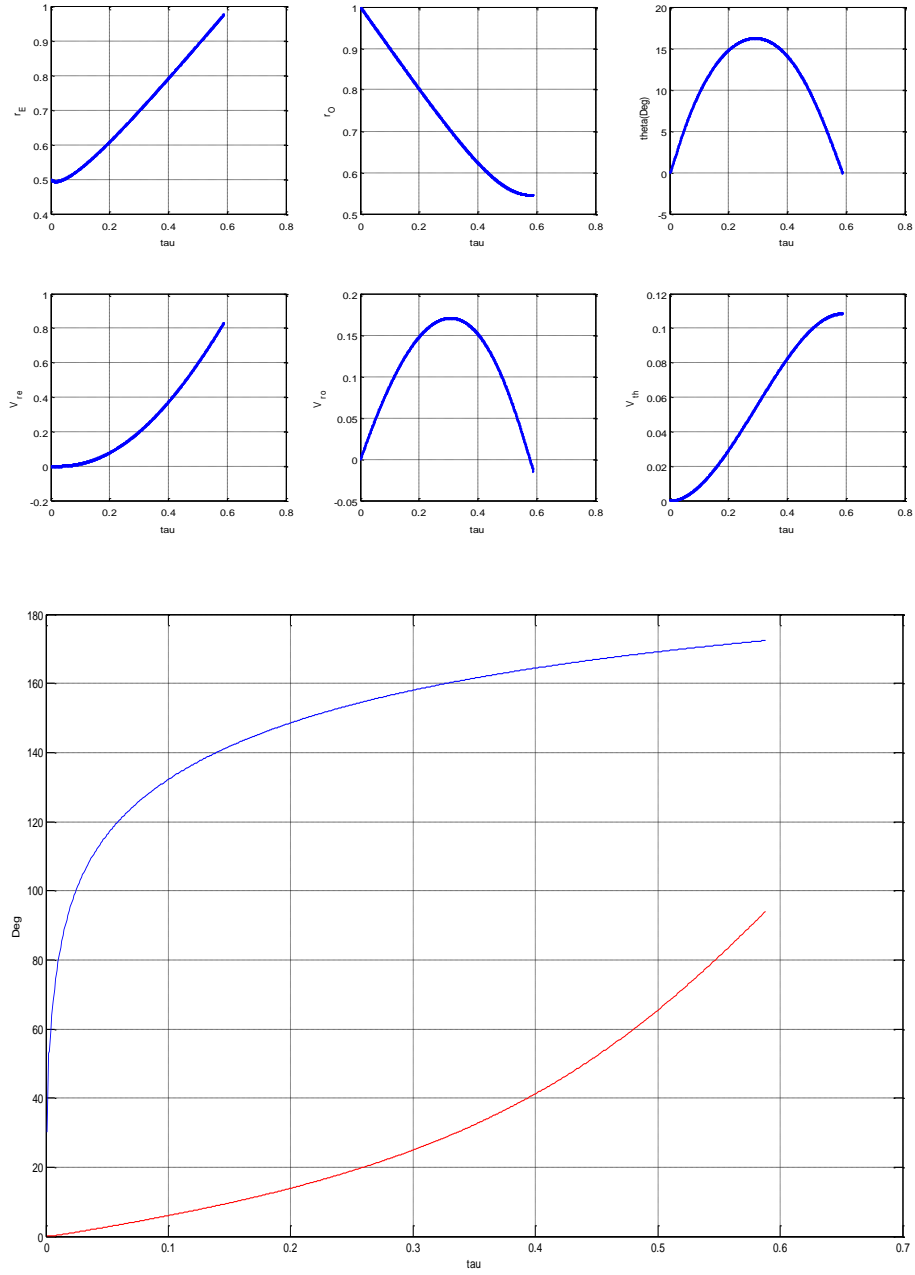


Figure A. 18: Time history of the States, Costates and Controls.

$$\alpha = 1, \xi = 150^\circ, r_{O_r} = 1$$

At the end point the rElay's control is $\varphi^*(0) = 180^\circ - 150^\circ = 30^\circ$

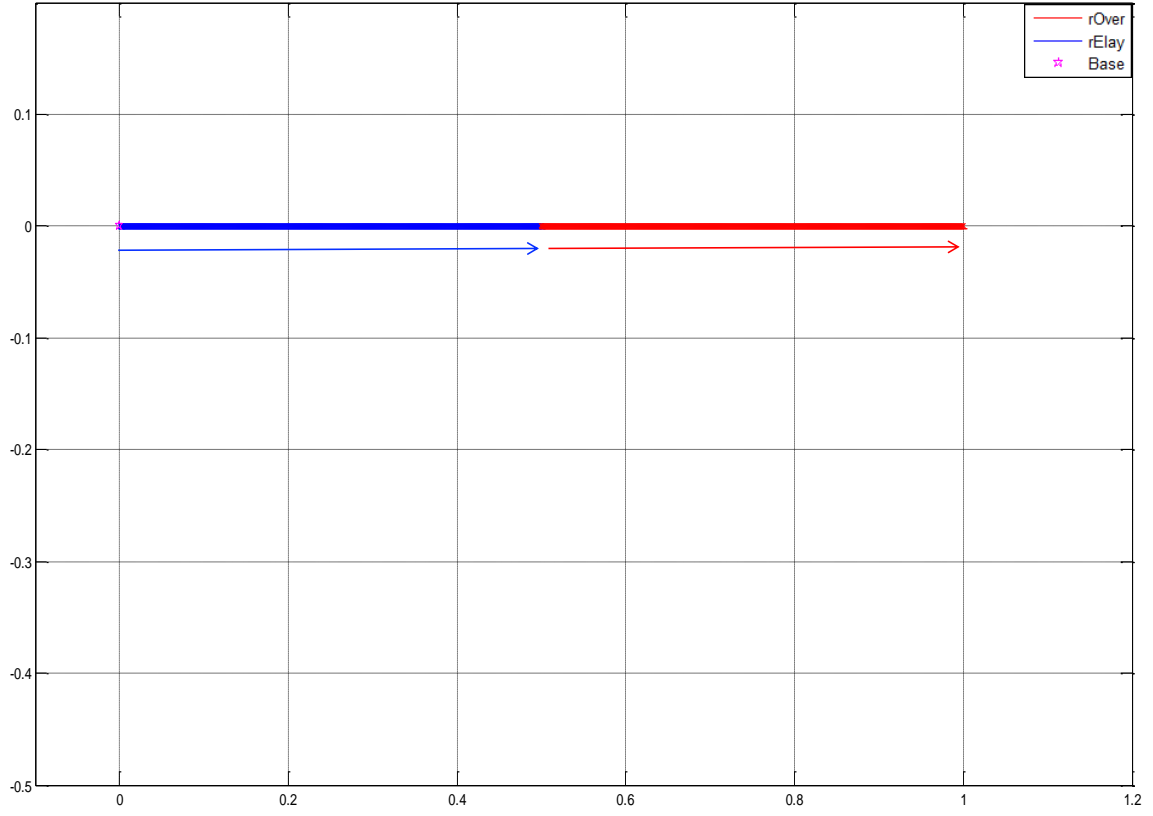


Figure A. 19: Optimal trajectories of Rover and Relay. $\alpha = 1$, $\xi = 180^\circ$, $r_{O_T} = 1$

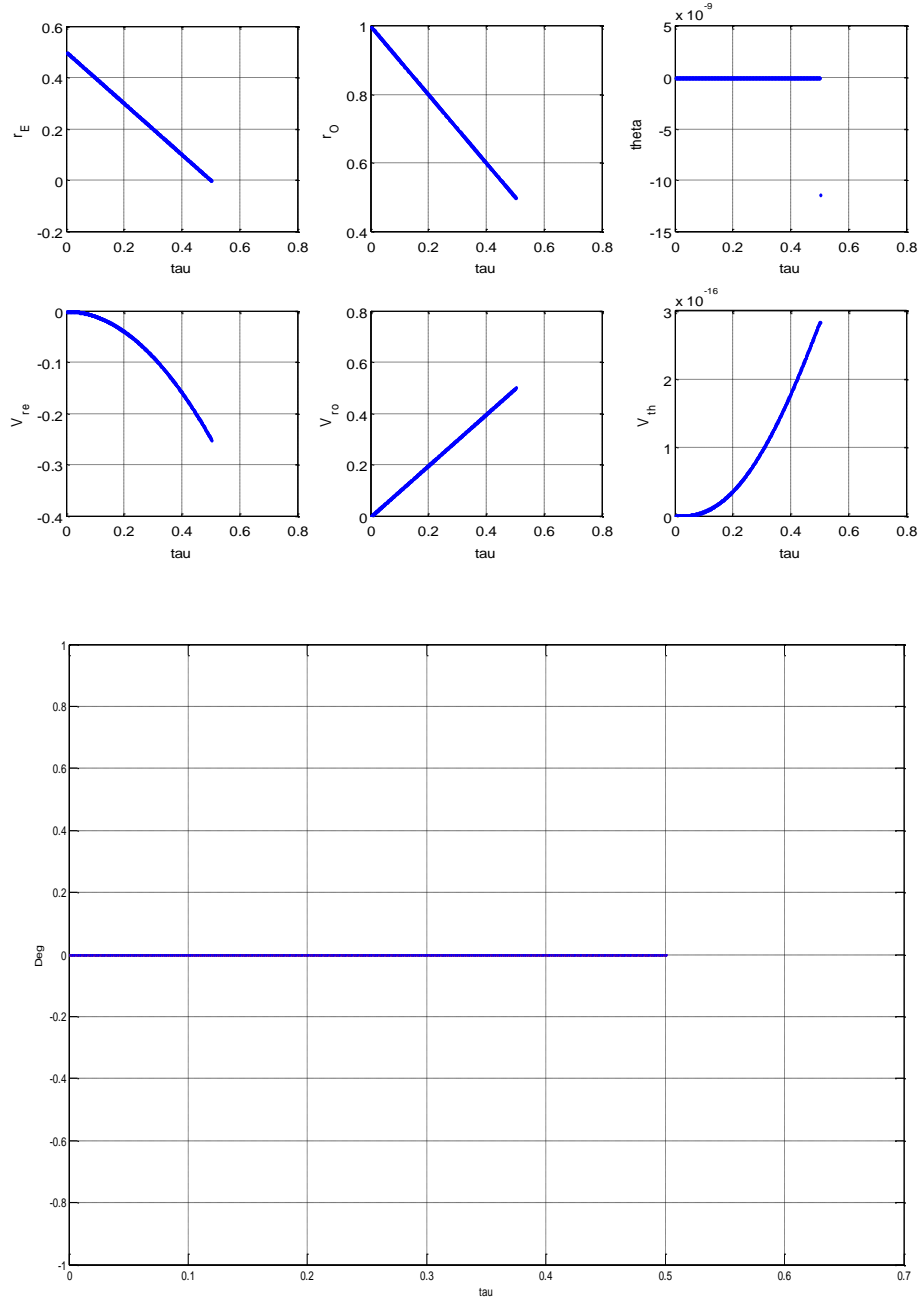


Figure A. 20: Time history of the States, Costates and Controls.

$$\alpha = 1, \quad \xi = 180^\circ, \quad r_{O_T} = 1$$

At the end point the rElay's control is $\varphi^*(0) = 180^\circ - 180^\circ = 0^\circ$

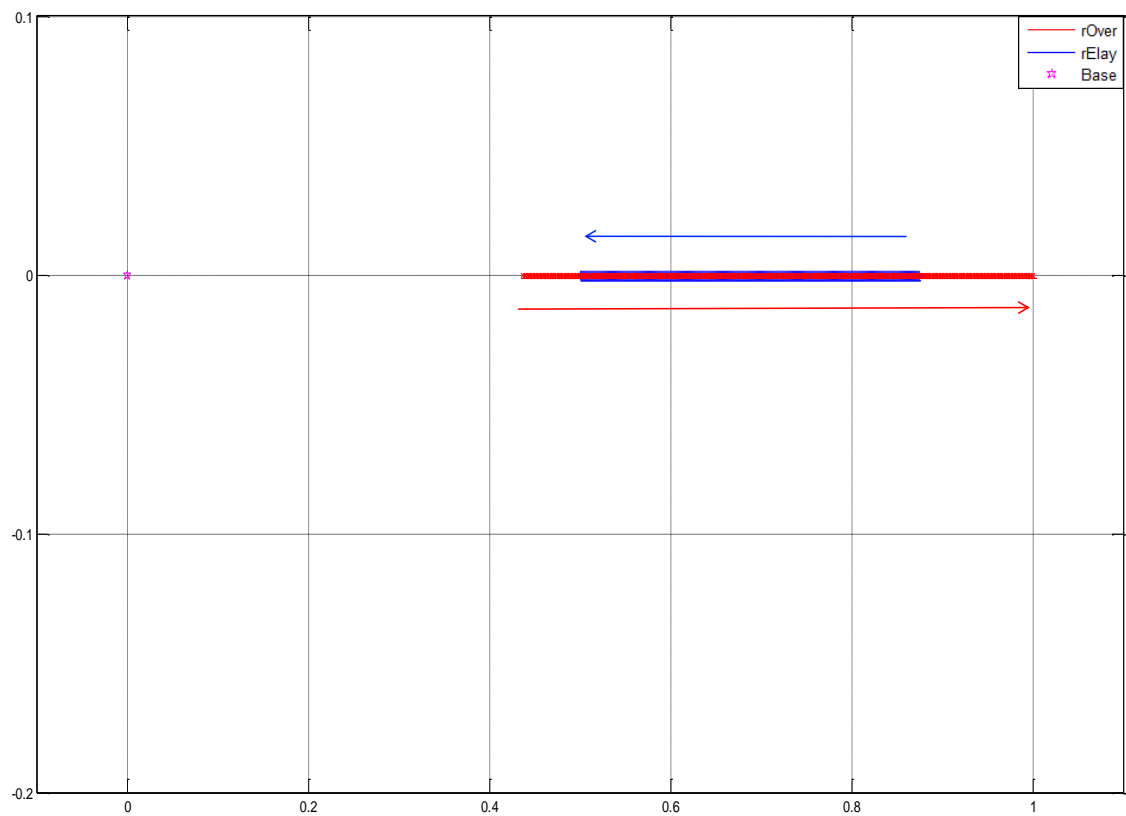


Figure A. 21: Optimal trajectories of Rover and Relay. $\alpha = 1.5$, $\xi = 0^\circ$, $r_{Or} = 1$

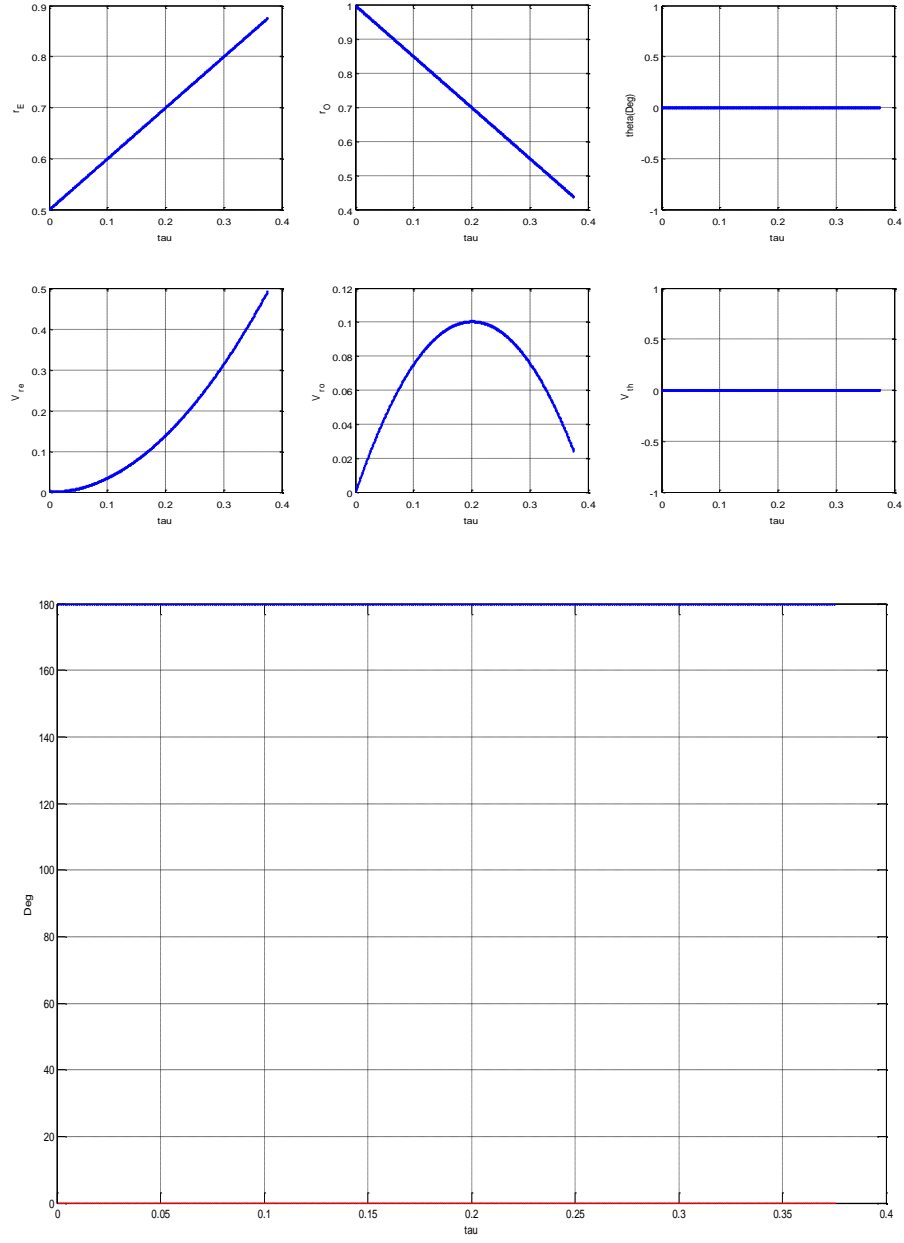


Figure A. 22: Time history of the States, Costates and Controls.

$$\alpha = 1.5, \quad \xi = 0^\circ, \quad r_{O_T} = 1$$

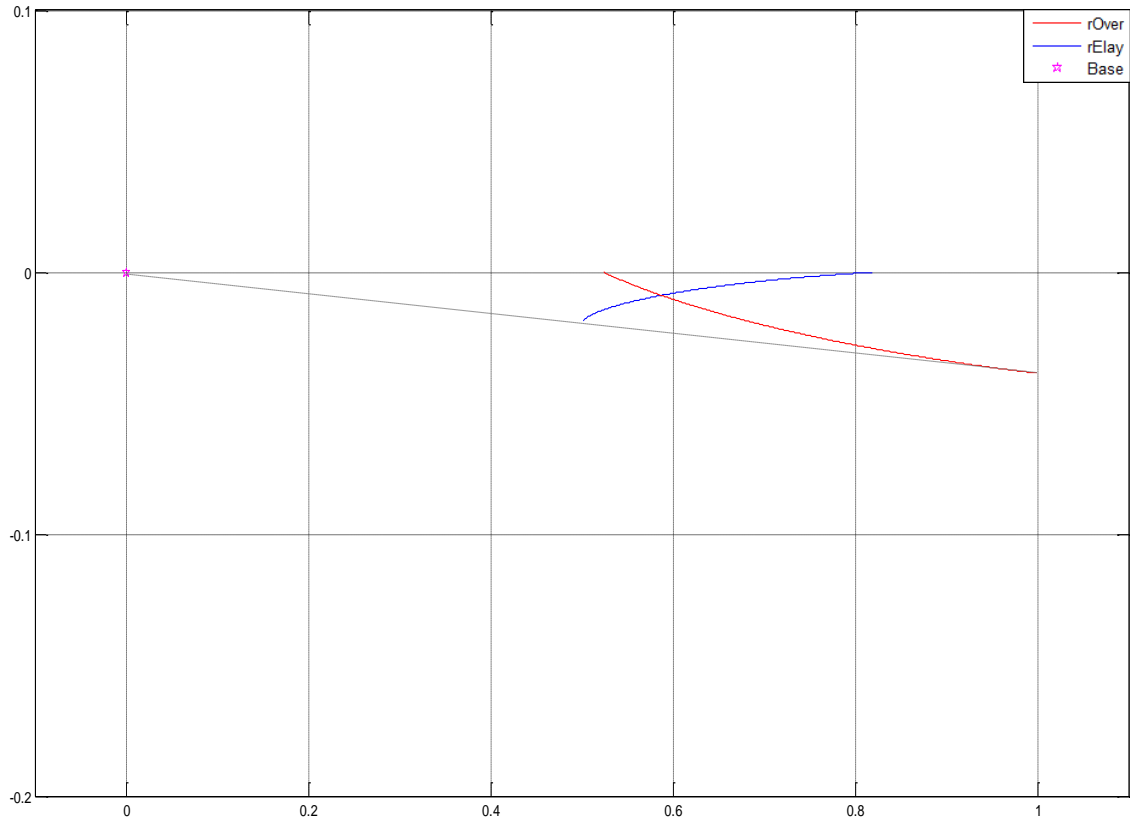


Figure A. 23: Optimal trajectories of Rover and Relay. $\alpha = 1.5$, $\xi = 30^\circ$, $r_{O_r} = 1$

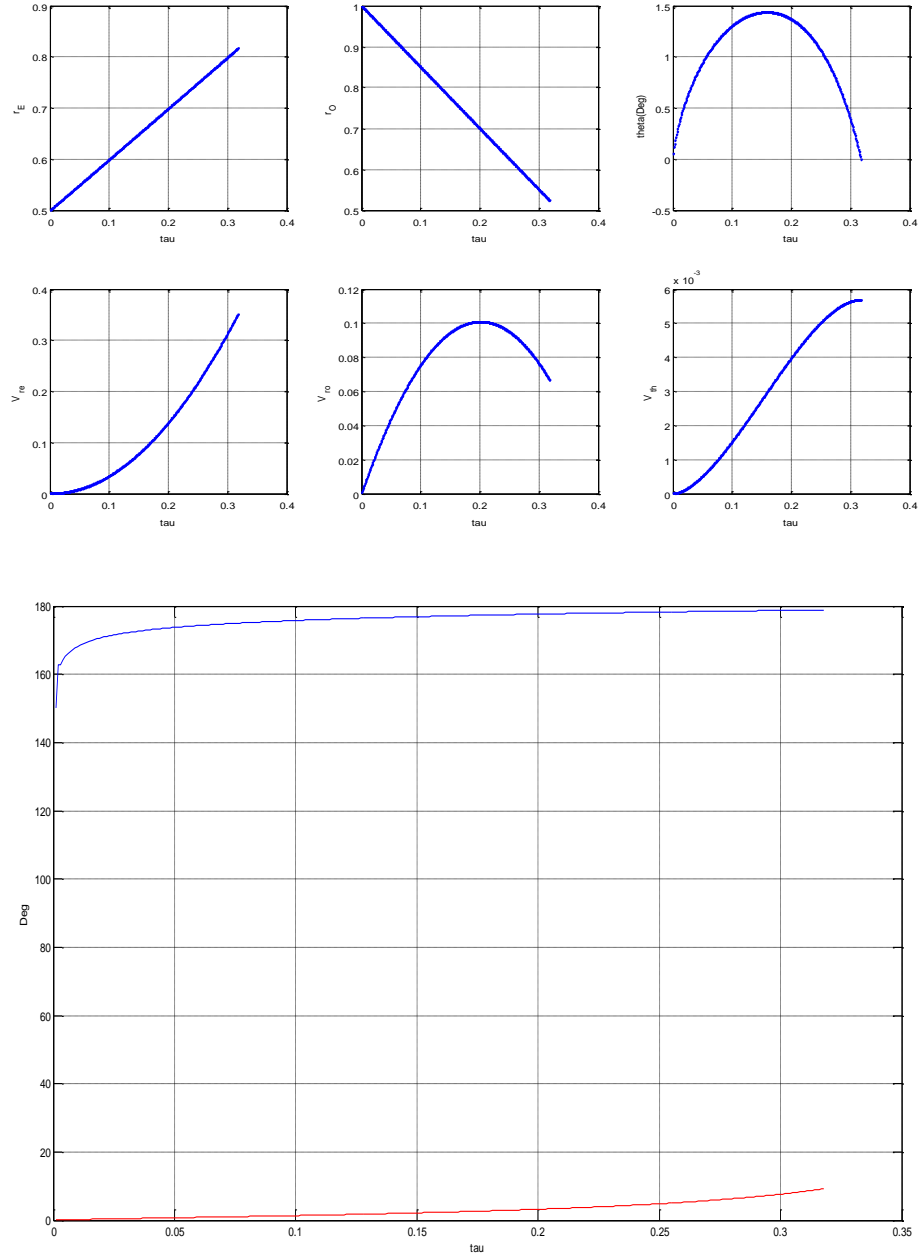


Figure A. 24: Time history of the States, Costates and Controls.

$$\alpha = 1.5, \xi = 30^\circ, r_{O_T} = 1$$

At the end point the rElay's control is $\varphi^*(0) = 180^\circ - 30^\circ = 150^\circ$

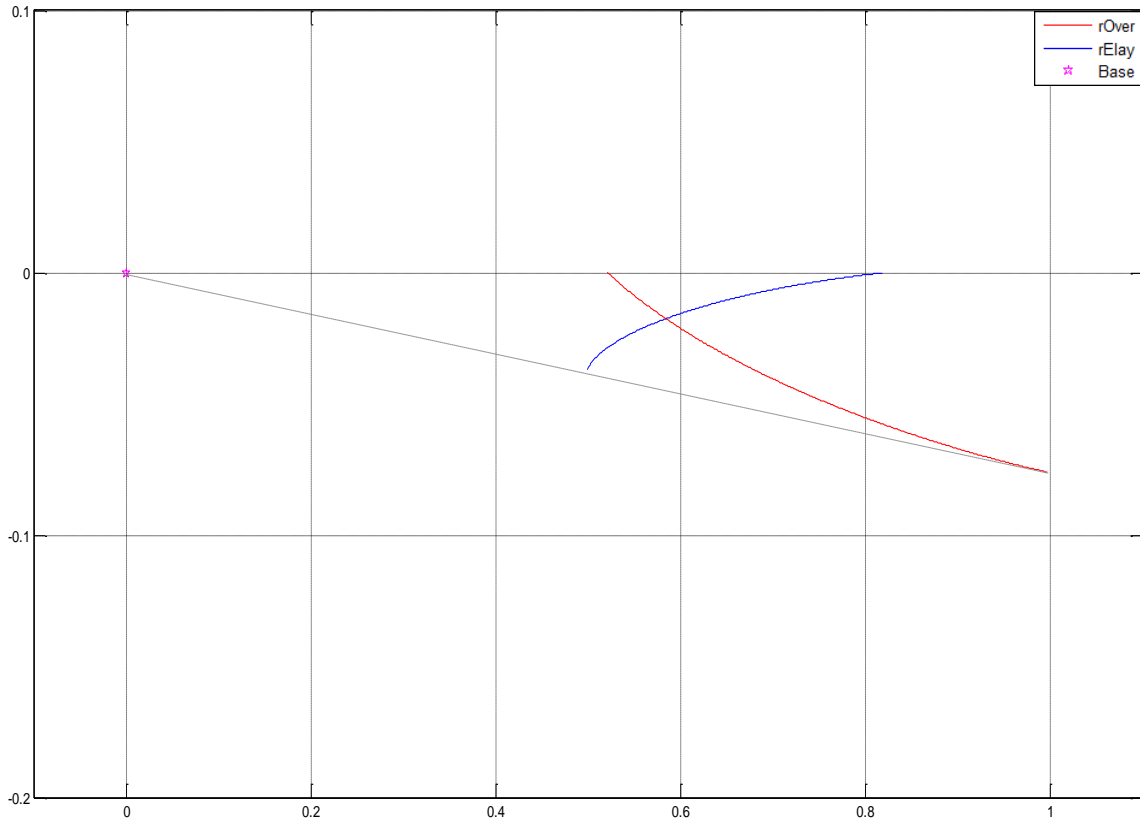


Figure A. 25: Optimal trajectories of Rover and Relay. $\alpha = 1.5$, $\xi = 60^\circ$, $r_{O_r} = 1$

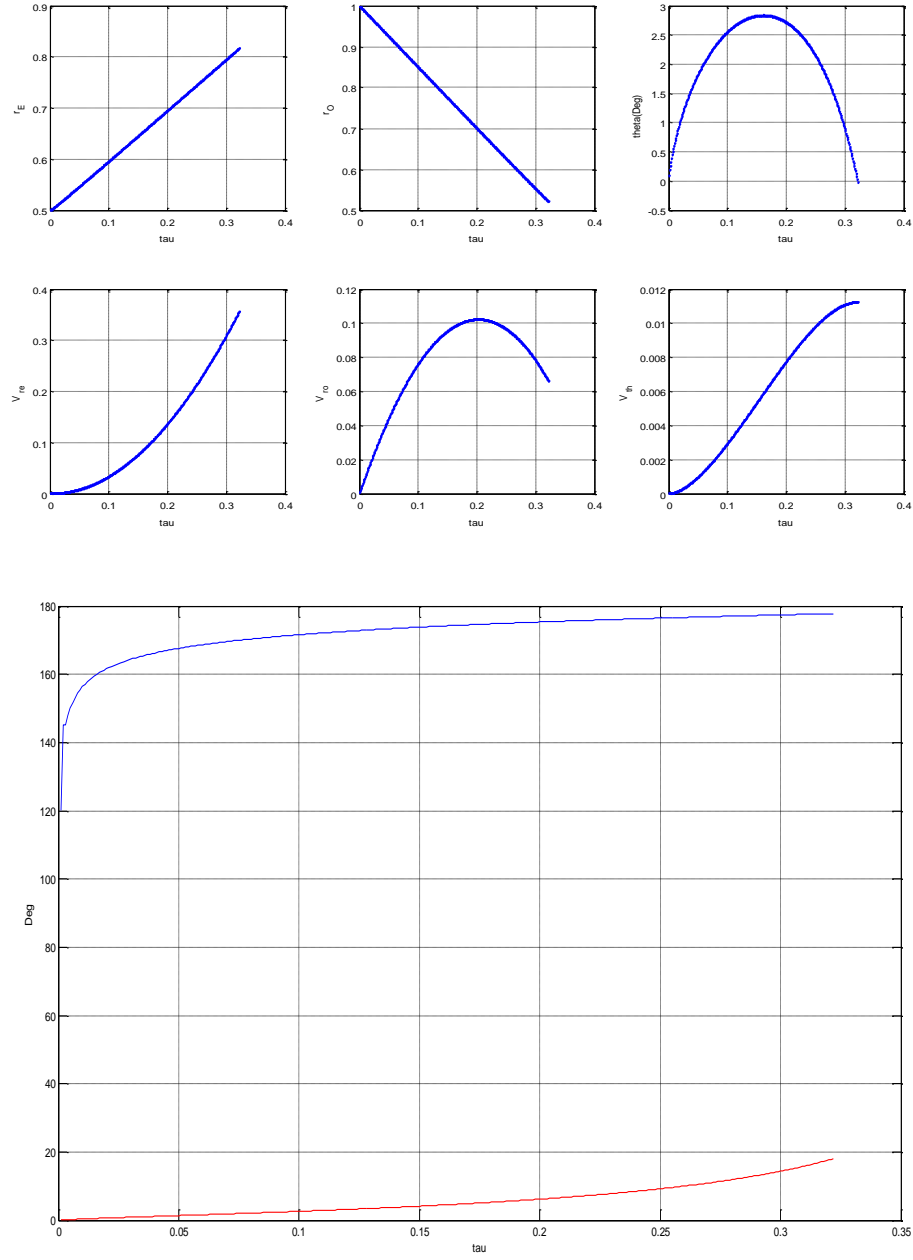


Figure A. 26: Time history of the States, Costates and Controls.

$$\alpha = 1.5, \xi = 60^\circ, r_{O_T} = 1$$

At the end point the rElay's control is $\varphi^*(0) = 120^\circ$

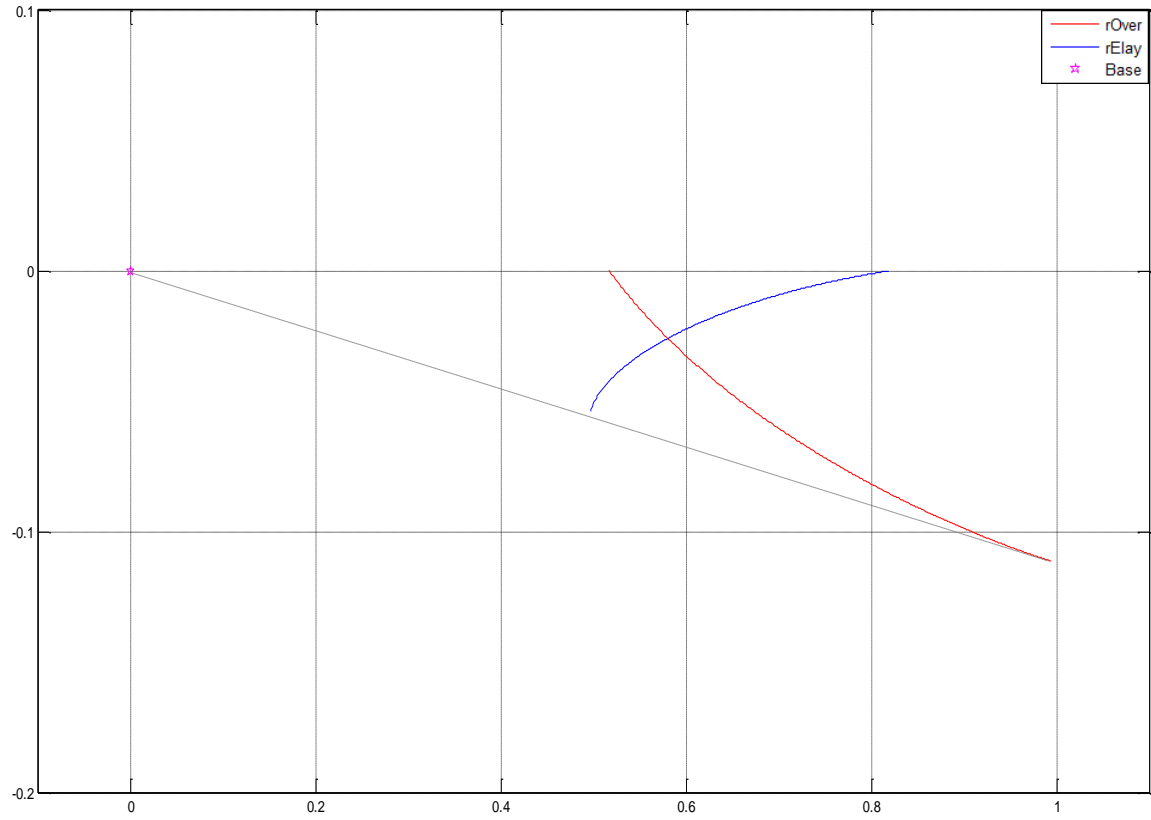


Figure A. 27: Optimal trajectories of Rover and Relay. $\alpha = 1.5$, $\xi = 90^\circ$, $r_{Or} = 1$

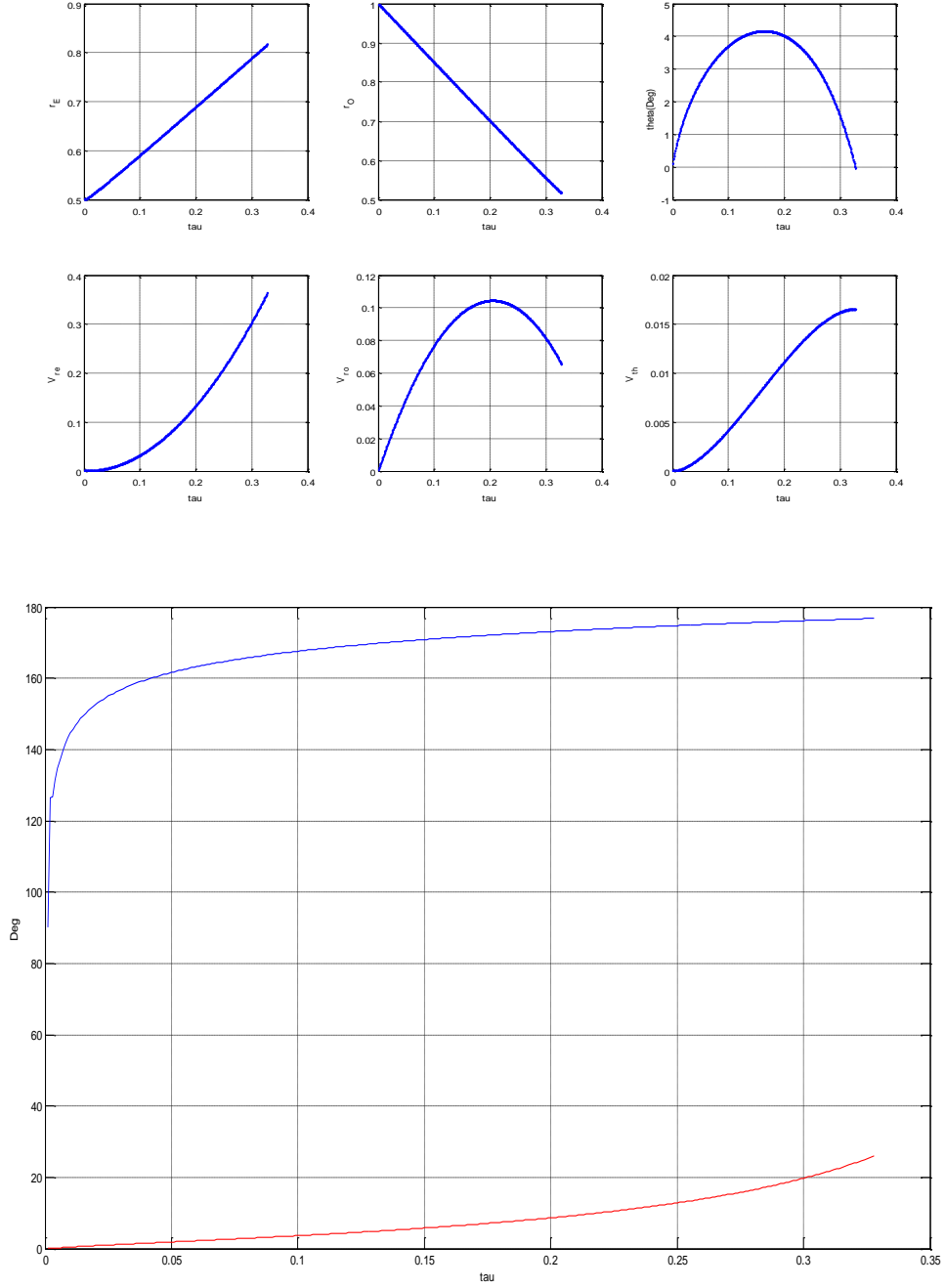


Figure A. 28: Time history of the States, Costates and Controls.

$$\alpha = 1.5, \xi = 90^\circ, r_{O_T} = 1$$

At the end point the rElay's control is $\varphi^*(0) = 90^\circ$

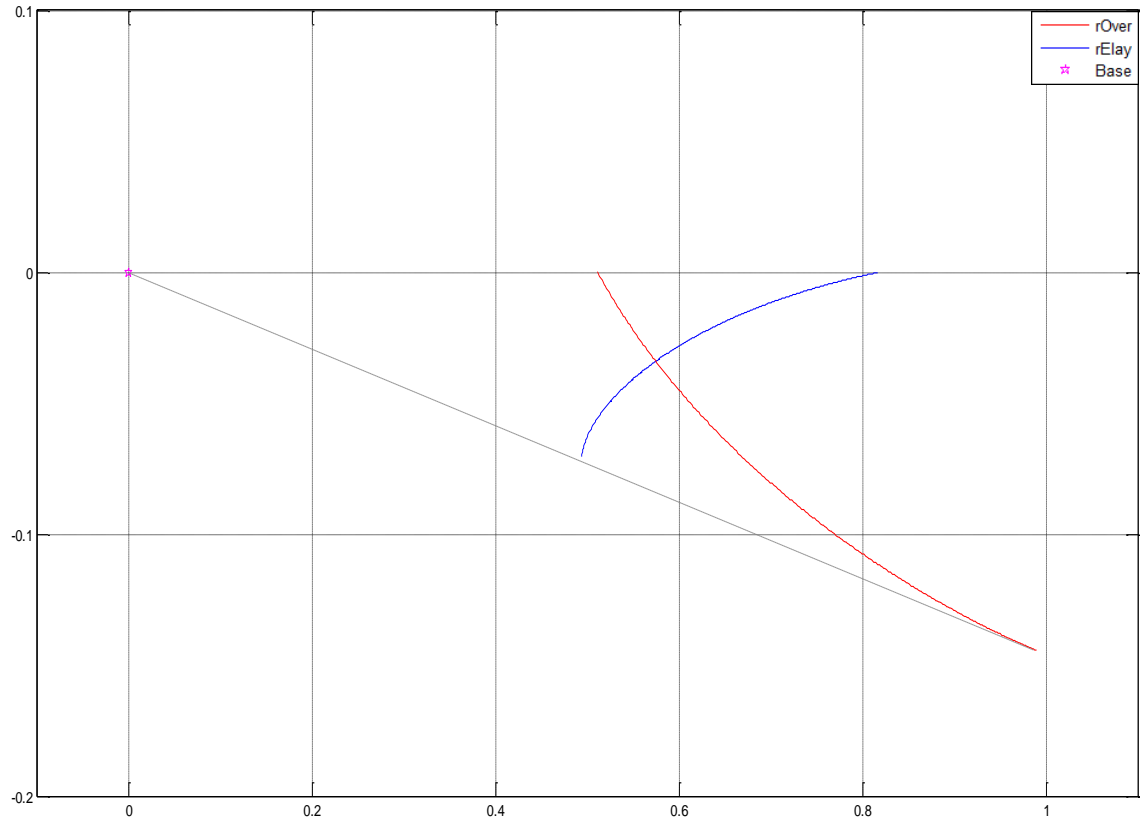


Figure A. 29: Optimal trajectories of Rover and Relay. $\alpha = 1.5$, $\xi = 120^\circ$, $r_{or} = 1$

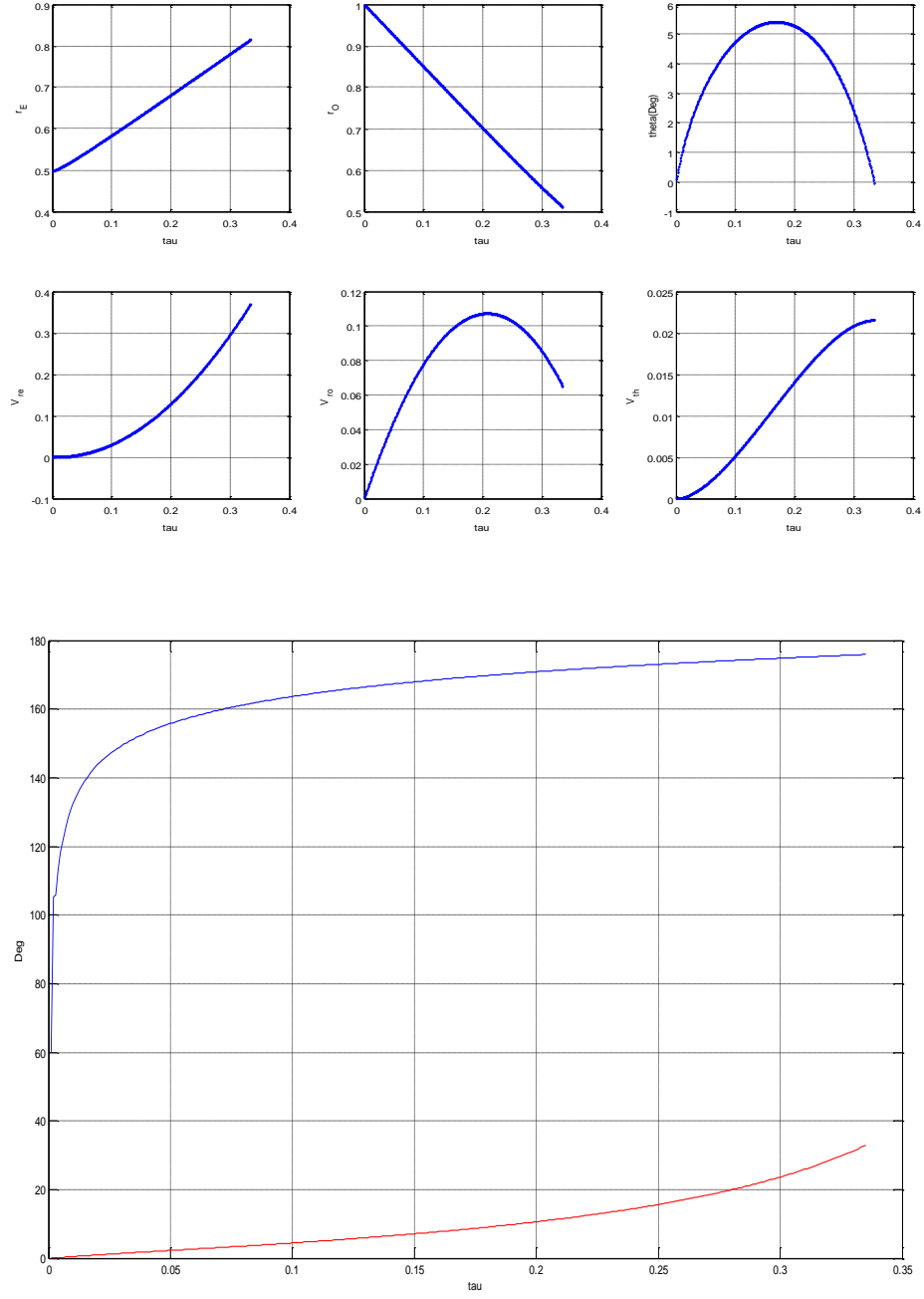


Figure A. 30: Time history of the States, Costates and Controls

$$\alpha = 1.5, \quad \xi = 120^\circ, \quad r_{O_T} = 1$$

At the end point the rElay's control is $\varphi^*(0) = 60^\circ$

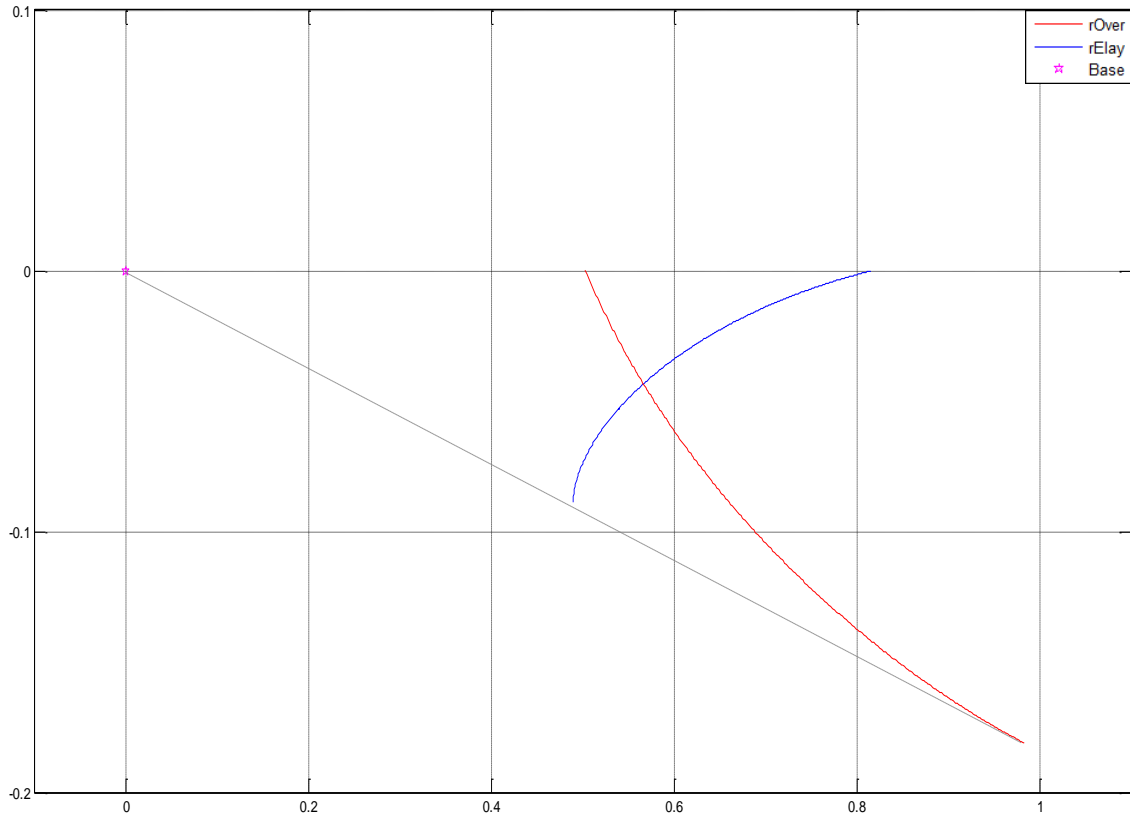


Figure A. 31: Optimal trajectories of Rover and Relay. $\alpha = 1.5$, $\xi = 150^\circ$, $r_{O_T} = 1$

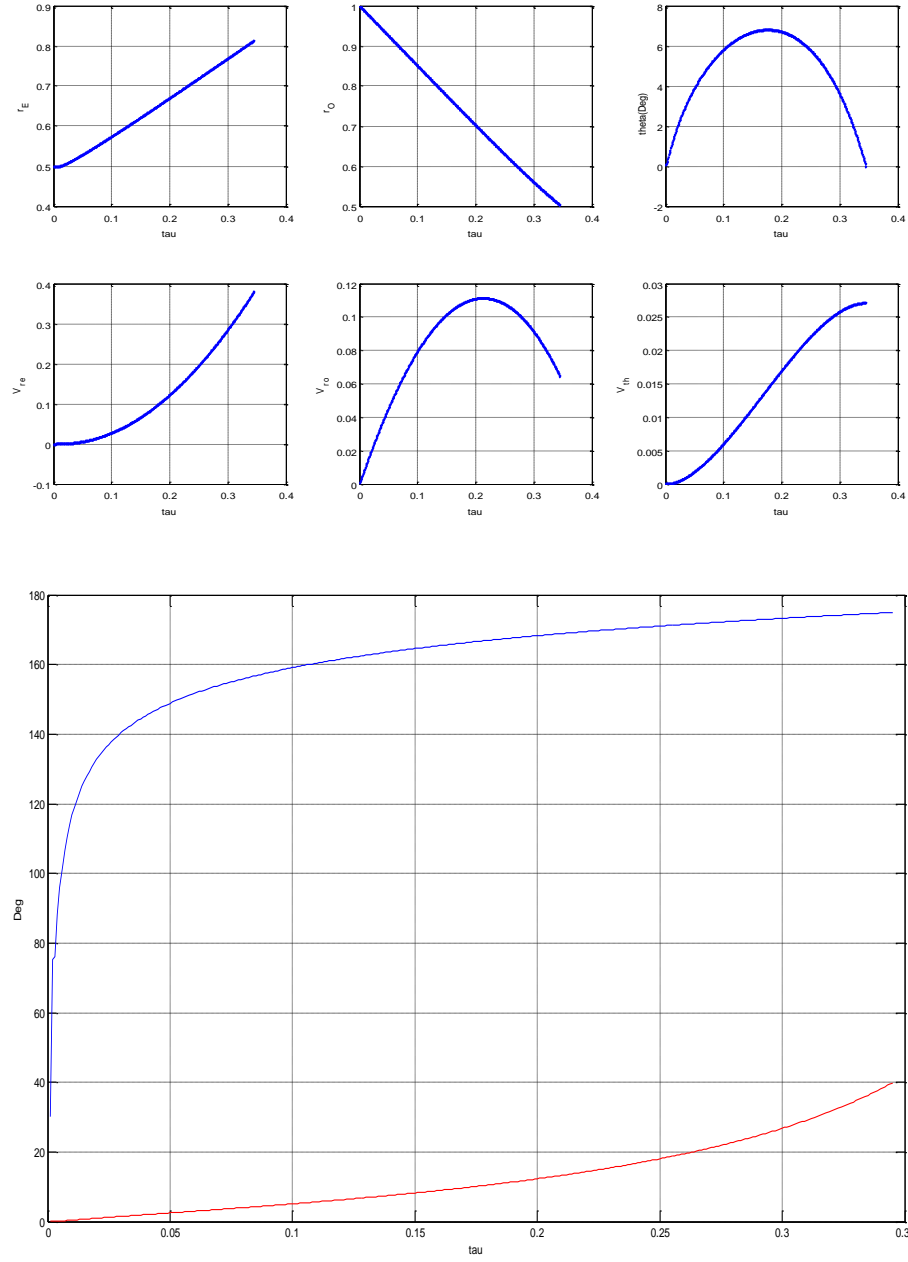


Figure A. 32: Time history of the States, Costates and Controls

$$\alpha = 1.5, \quad \xi = 150^\circ, \quad r_{O_T} = 1$$

At the end point the rElay's control is $\varphi^*(0) = 30^\circ$

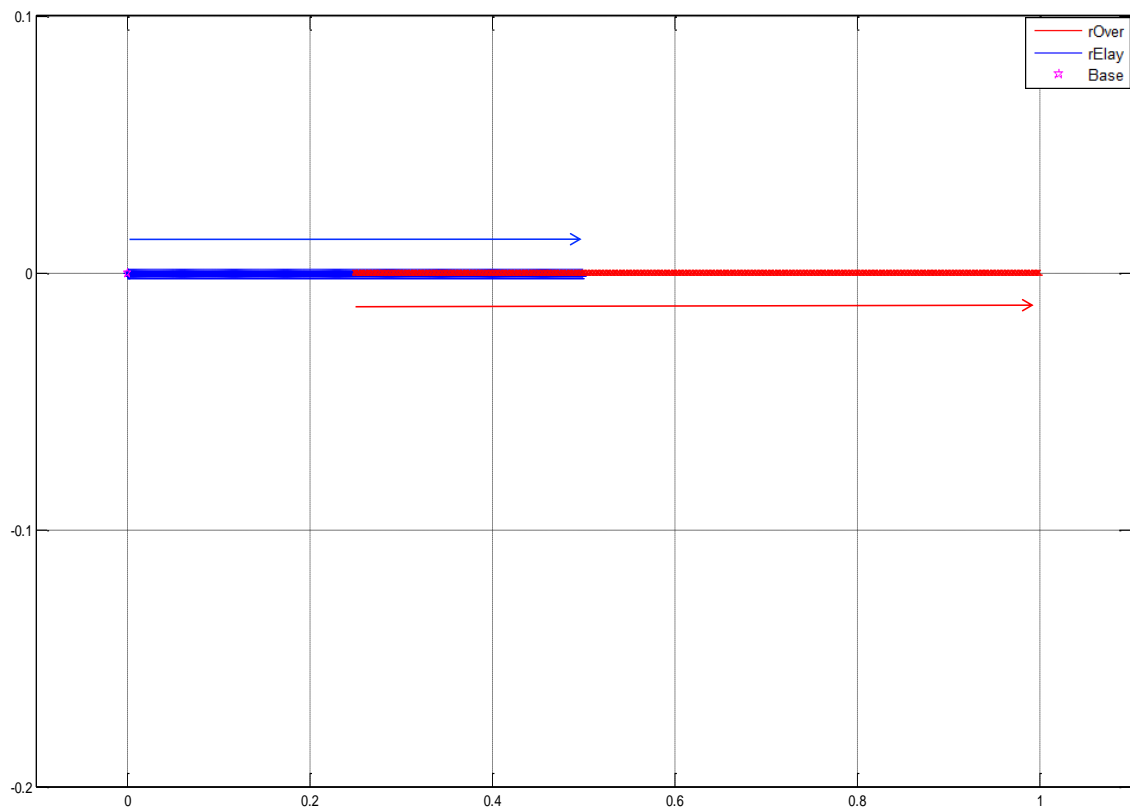


Figure A. 33: Optimal trajectories of Rover and Relay. $\alpha = 1.5$, $\xi = 180^\circ$, $r_{O_r} = 1$

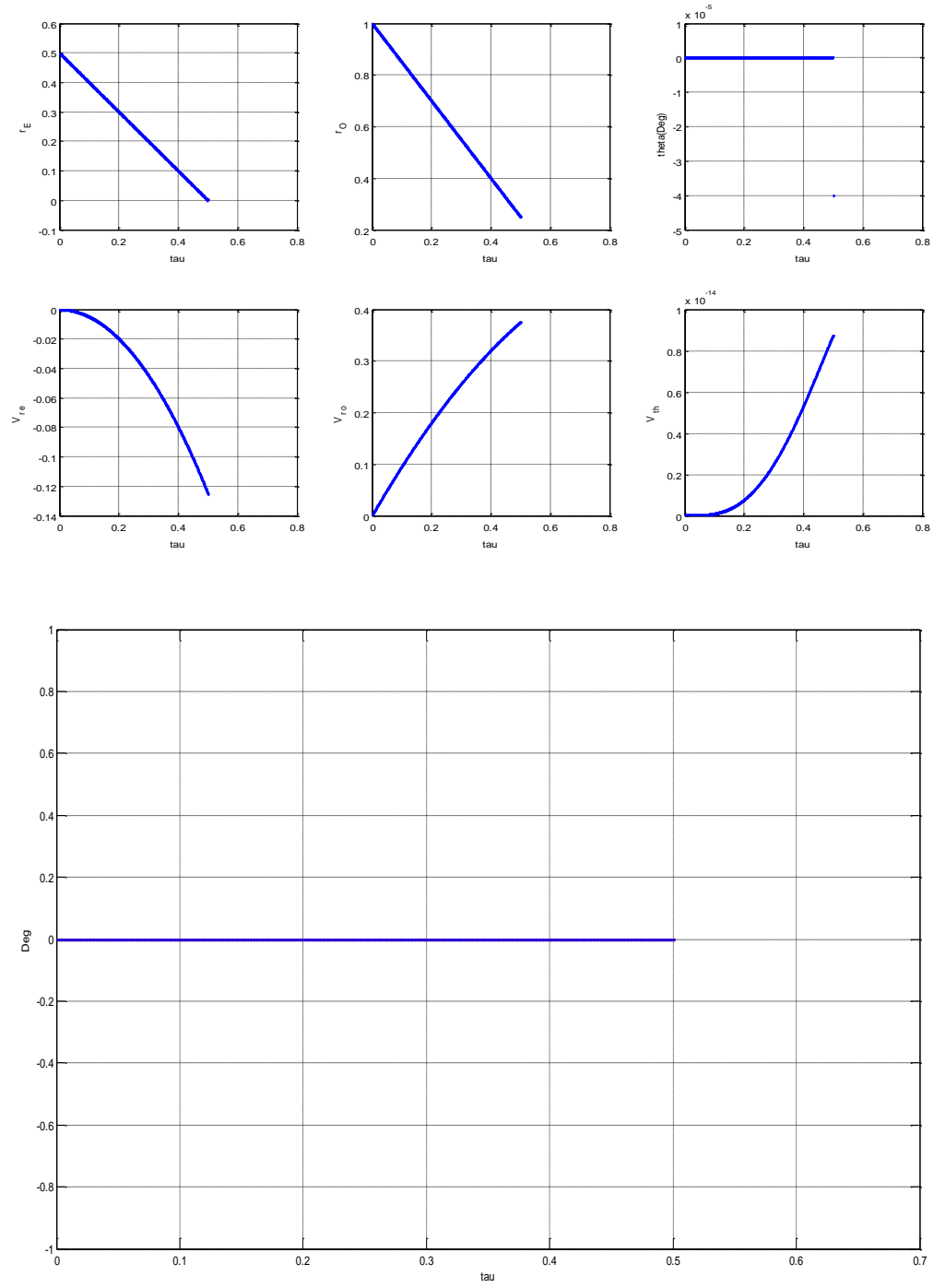


Figure A. 34: Time history of the States, Costates and Controls

$$\alpha = 1.5, \xi = 180^\circ, r_{O_r} = 1$$

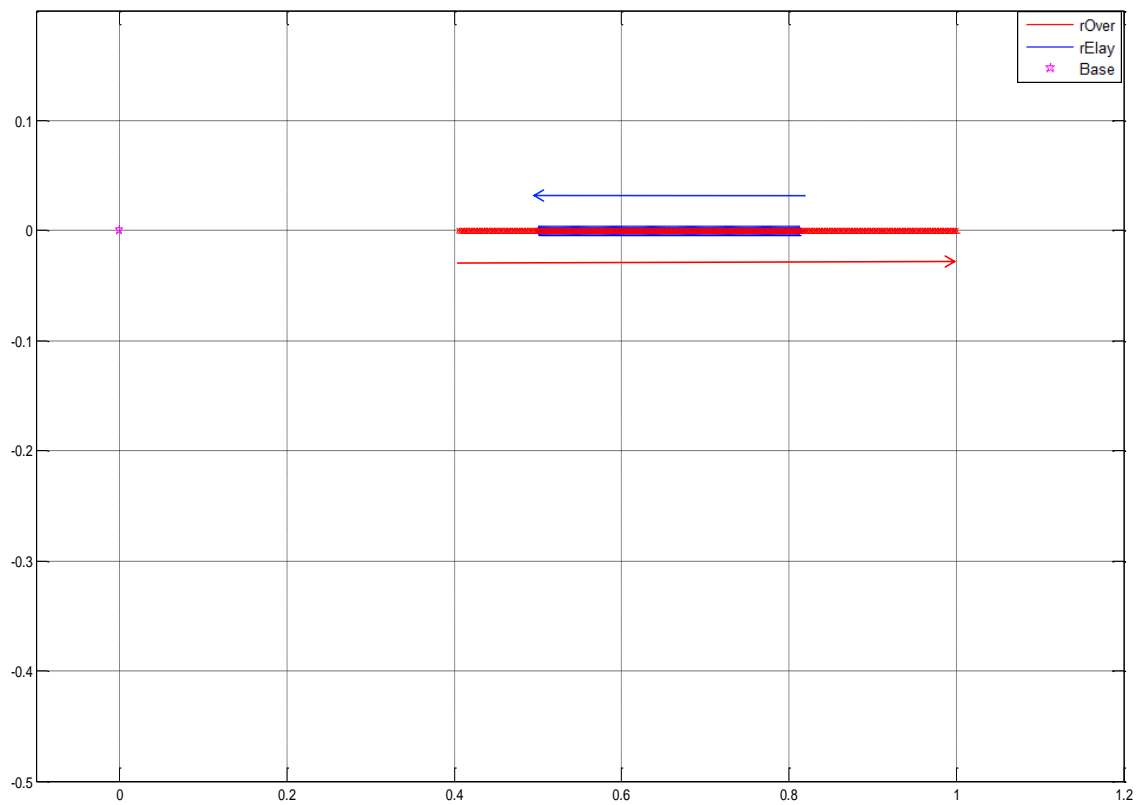


Figure A. 35: Optimal trajectories of Rover and Relay. $\alpha = 1.9$, $\xi = 0^\circ$, $r_{O_r} = 1$

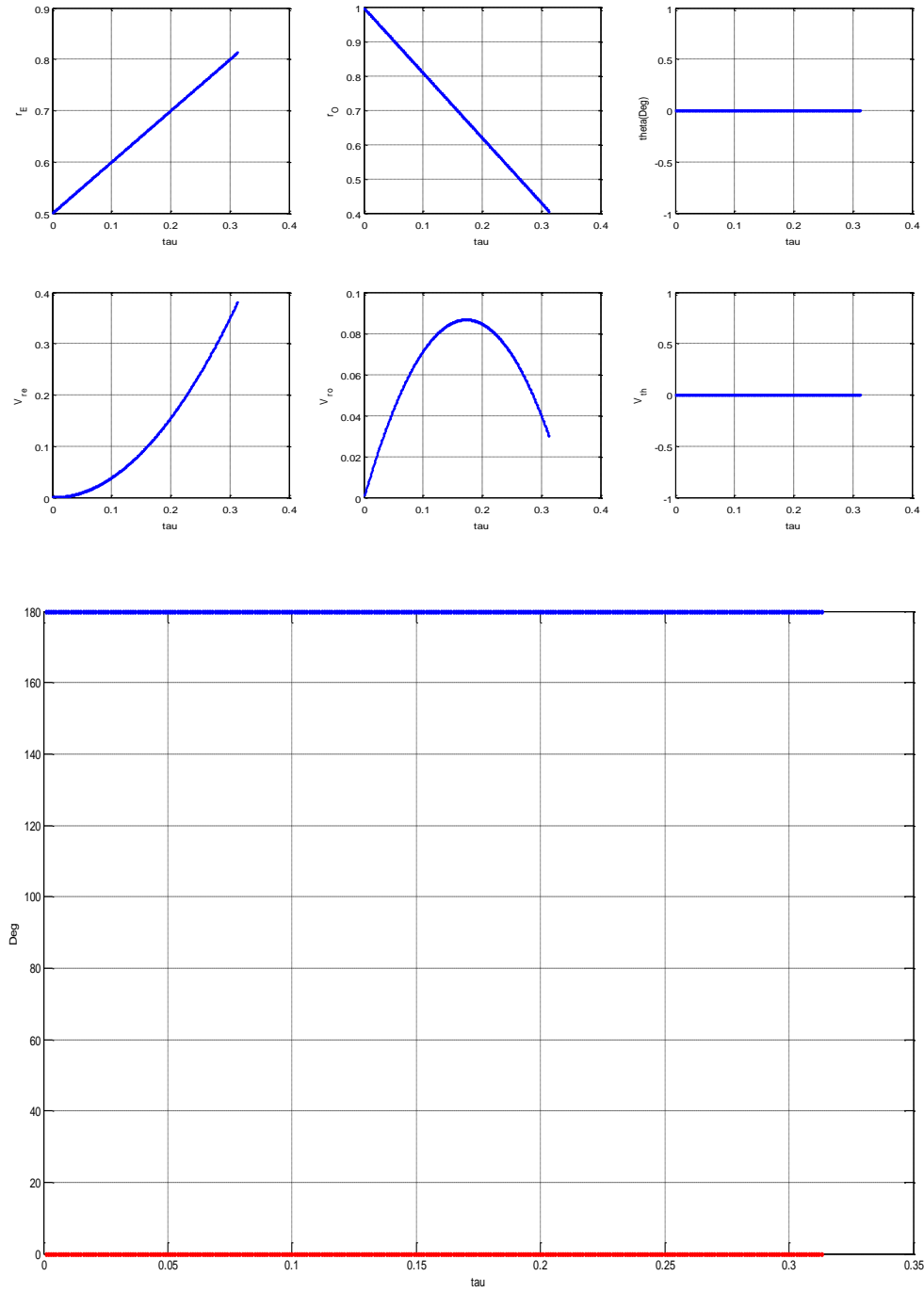


Figure A. 36: Time history of the States, Costates and Controls.

$$\alpha = 1.9, \quad \xi = 0^\circ, \quad r_{O_r} = 1$$

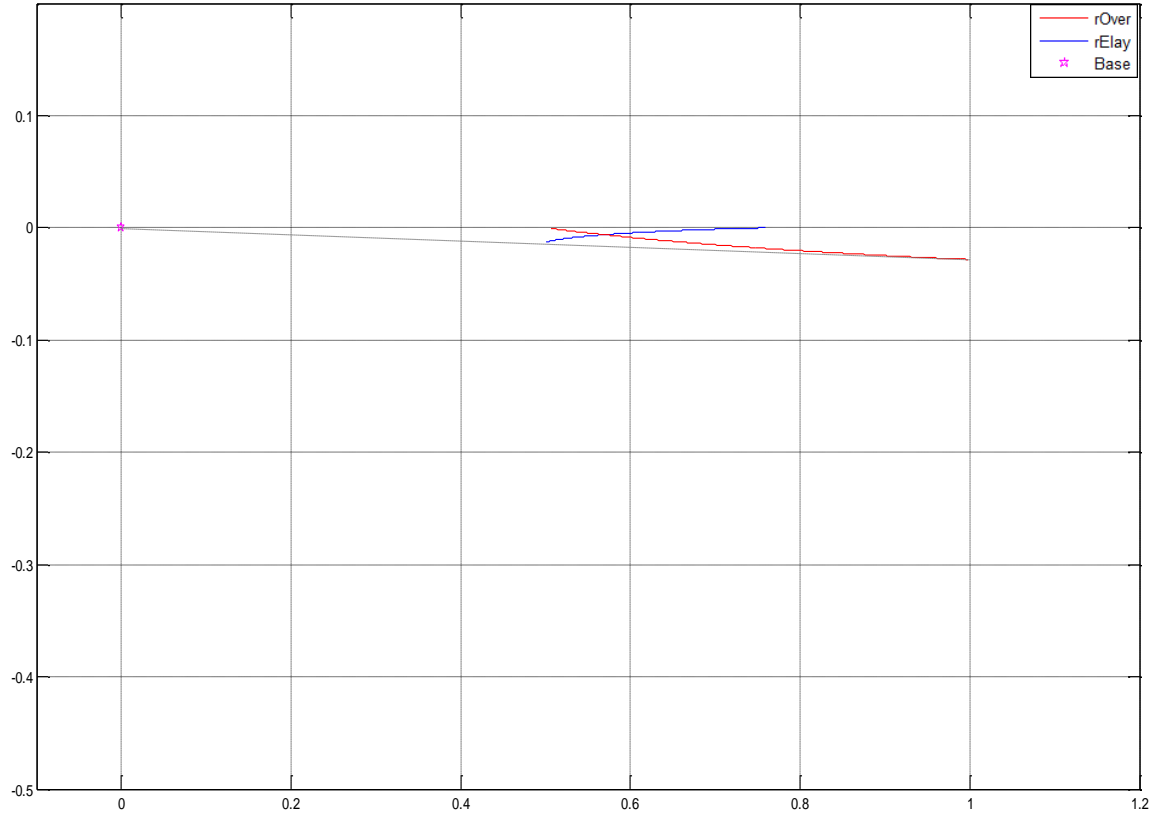


Figure A. 37: Optimal trajectories of Rover and Relay. $\alpha = 1.9$, $\xi = 30^\circ$, $r_{Or} = 1$

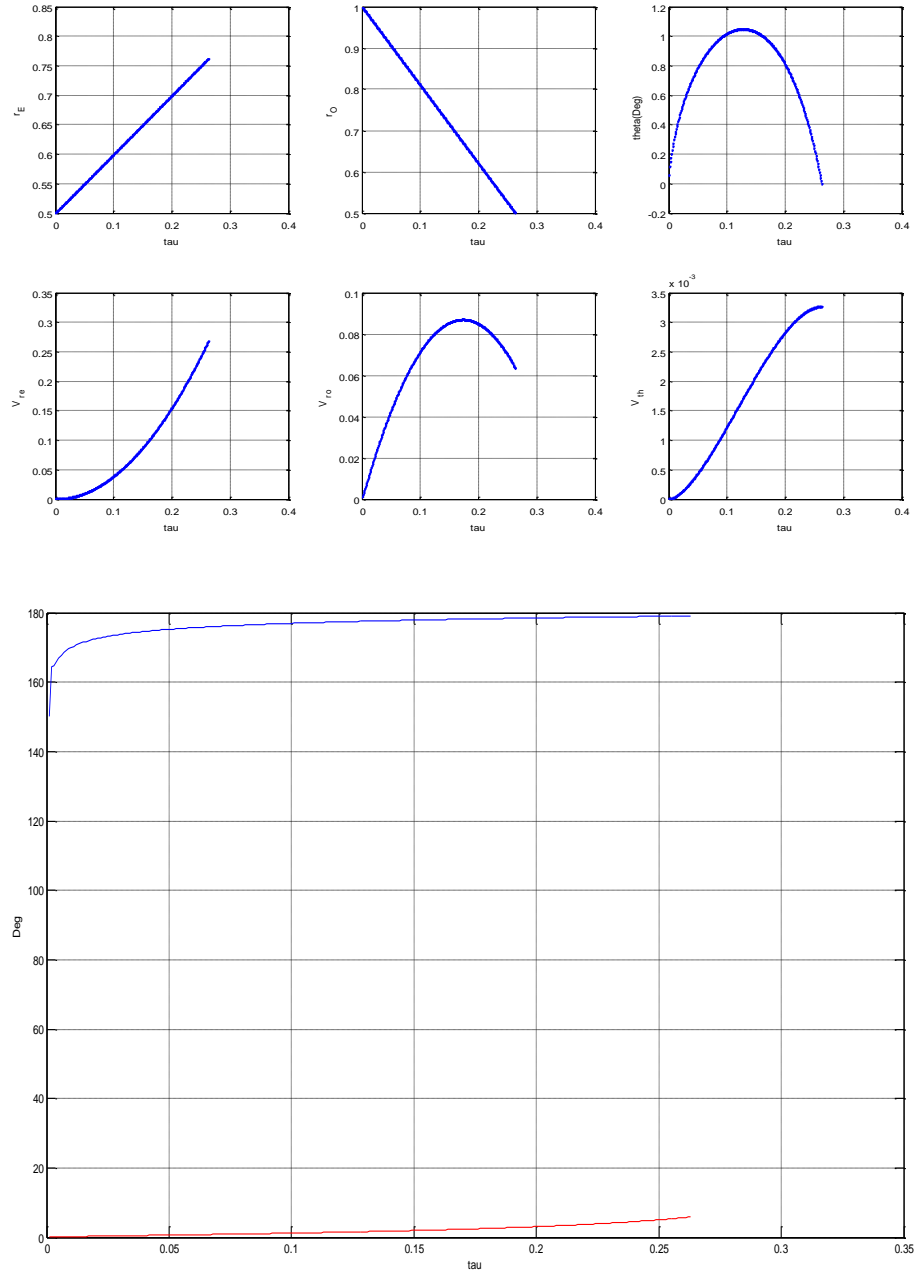


Figure A. 38: Time history of the States, Costates and Controls

$$\alpha = 1.9, \xi = 30^\circ, r_{O_T} = 1$$

At the end point the rElay's control is $\varphi^*(0) = 150^\circ$

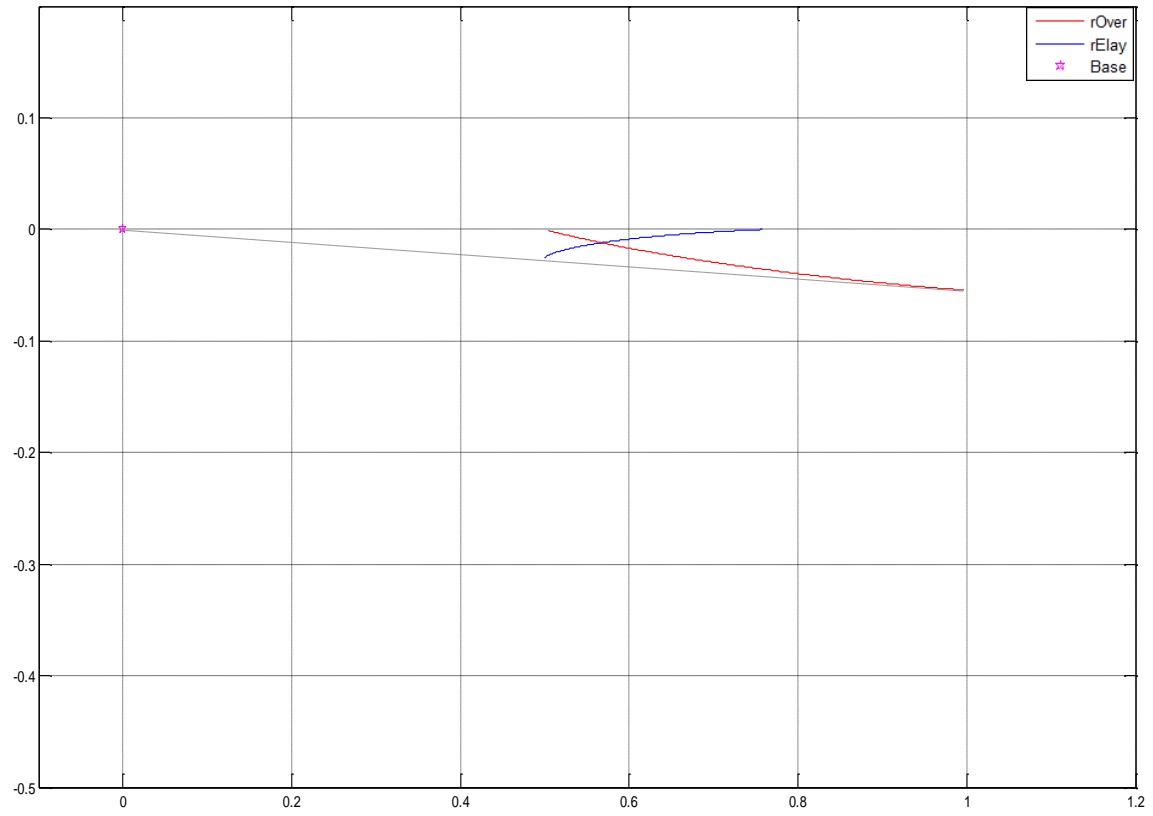


Figure A. 39: Optimal trajectories of Rover and Relay. $\alpha = 1.9$, $\xi = 60^\circ$, $r_{O_r} = 1$

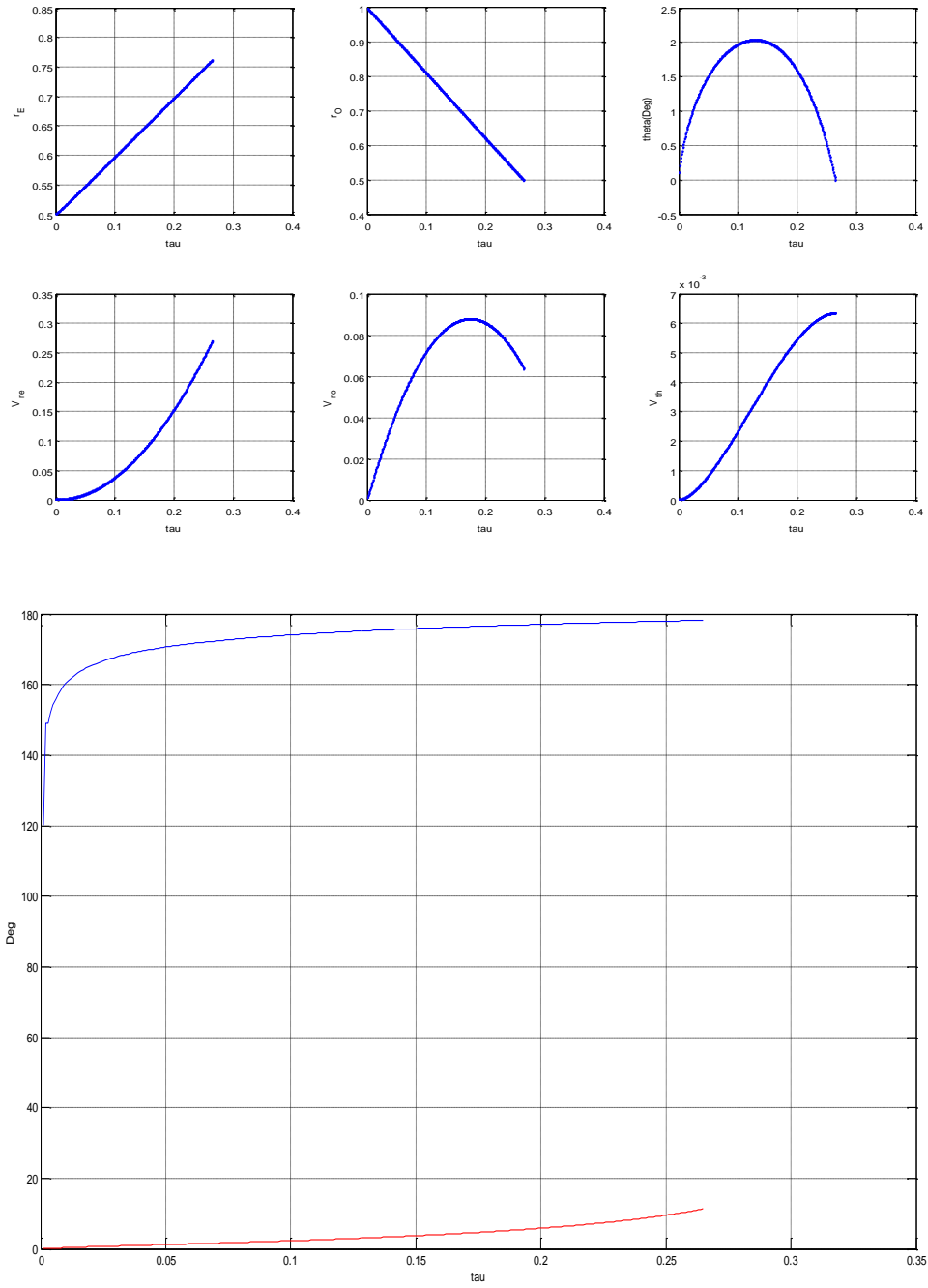


Figure A. 40: Time history of States, Costates and Controls. $\alpha = 1.9$, $\xi = 60^\circ$, $r_{O_r} = 1$

At the end point the rElay's control is $\varphi^*(0) = 120^\circ$

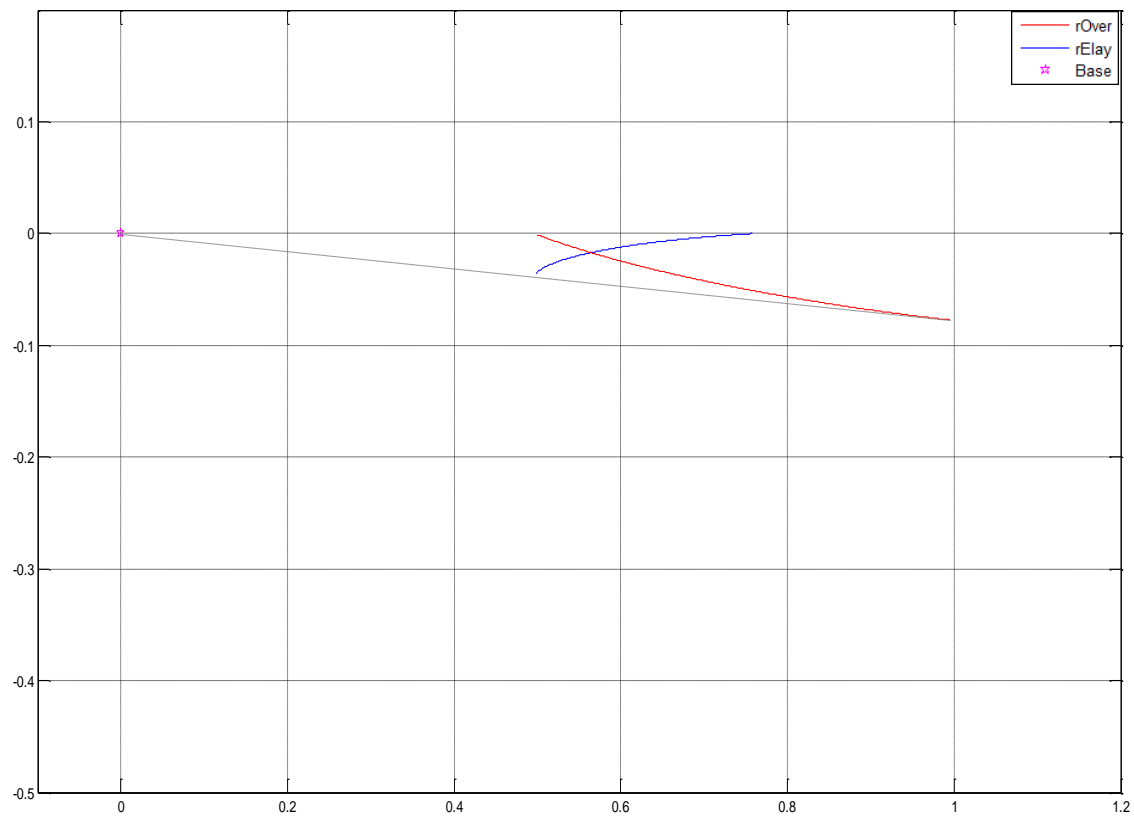


Figure A. 41: Optimal trajectories of Rover and Relay. $\alpha = 1.9$, $\xi = 90^\circ$, $r_{O_r} = 1$

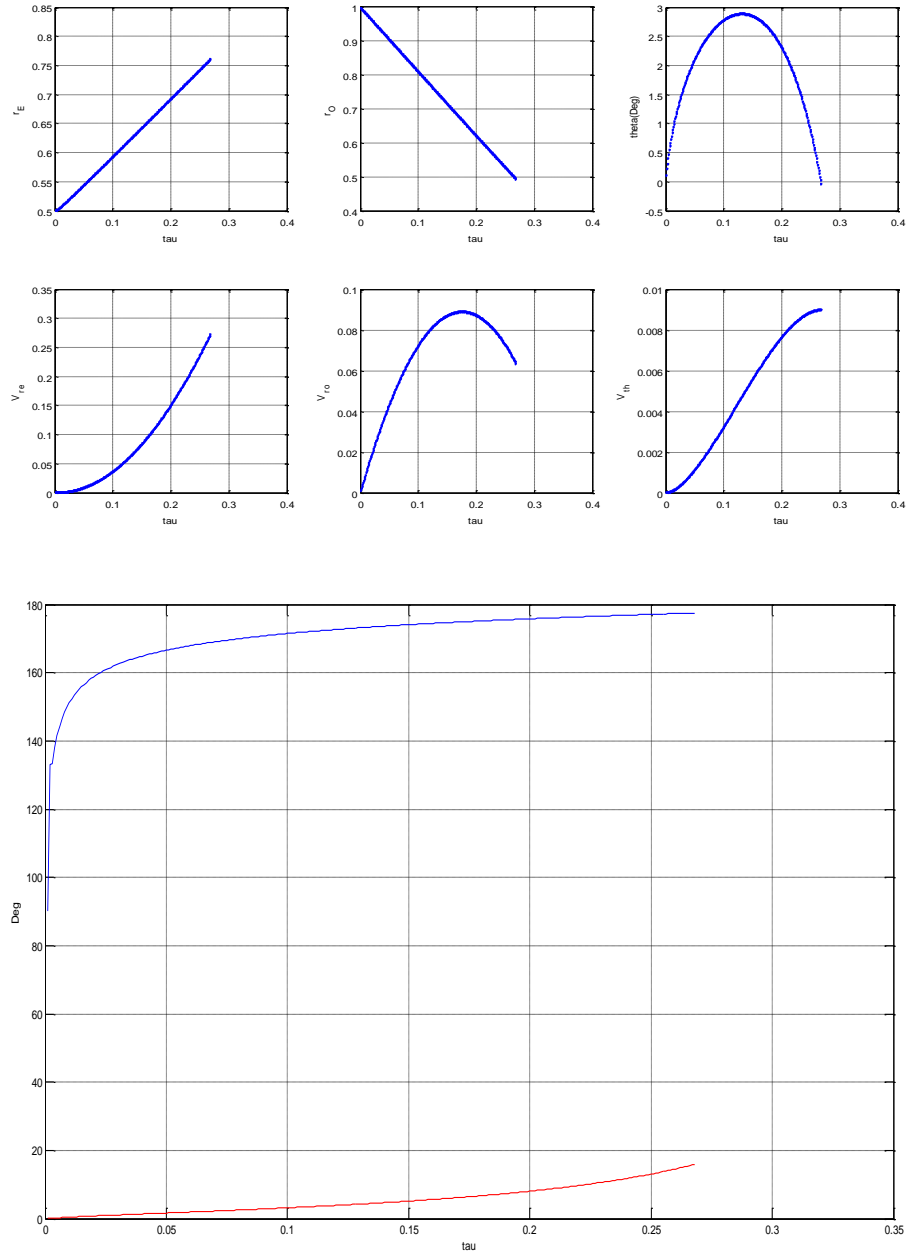


Figure A. 42: Time history of the States, Costates and Controls

$$\alpha = 1.9, \xi = 90^\circ, r_{O_r} = 1$$

At the end point the rElay's control is $\varphi^*(0) = 90^\circ$

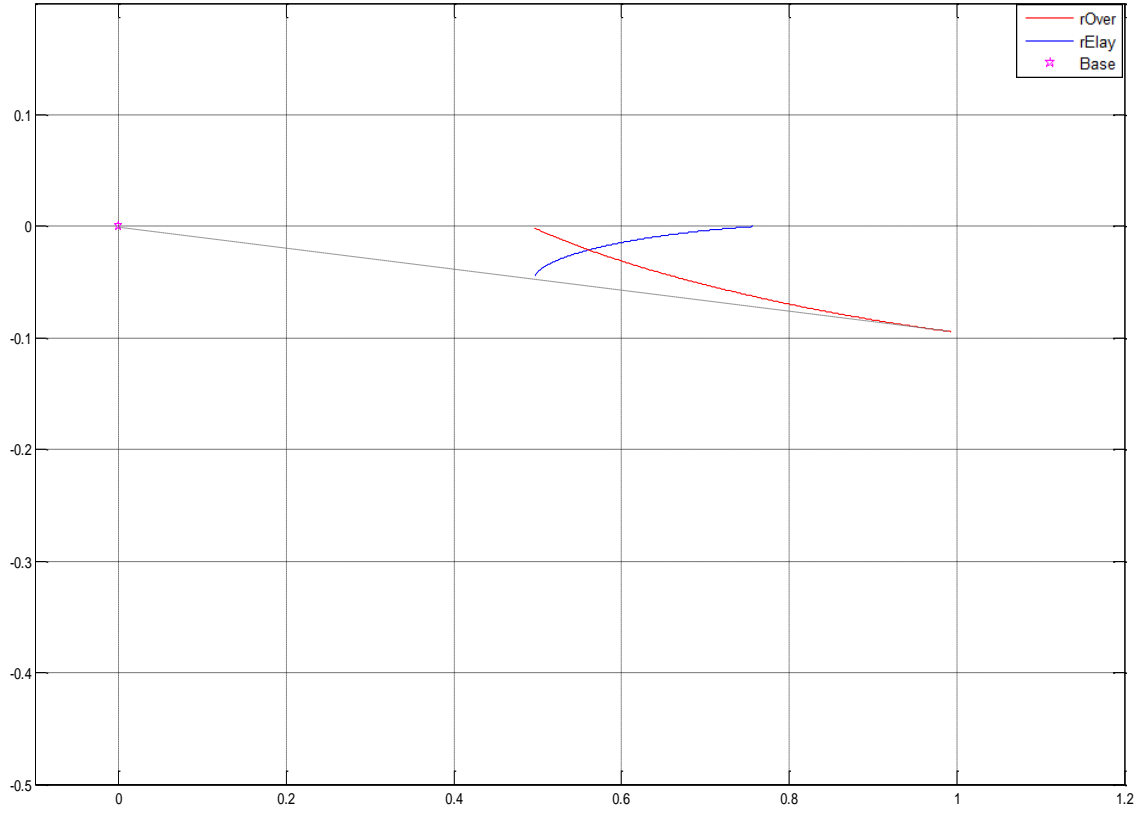


Figure A. 43: Optimal trajectories of Rover and Relay. $\alpha = 1.9$, $\xi = 120^\circ$, $r_{O_r} = 1$

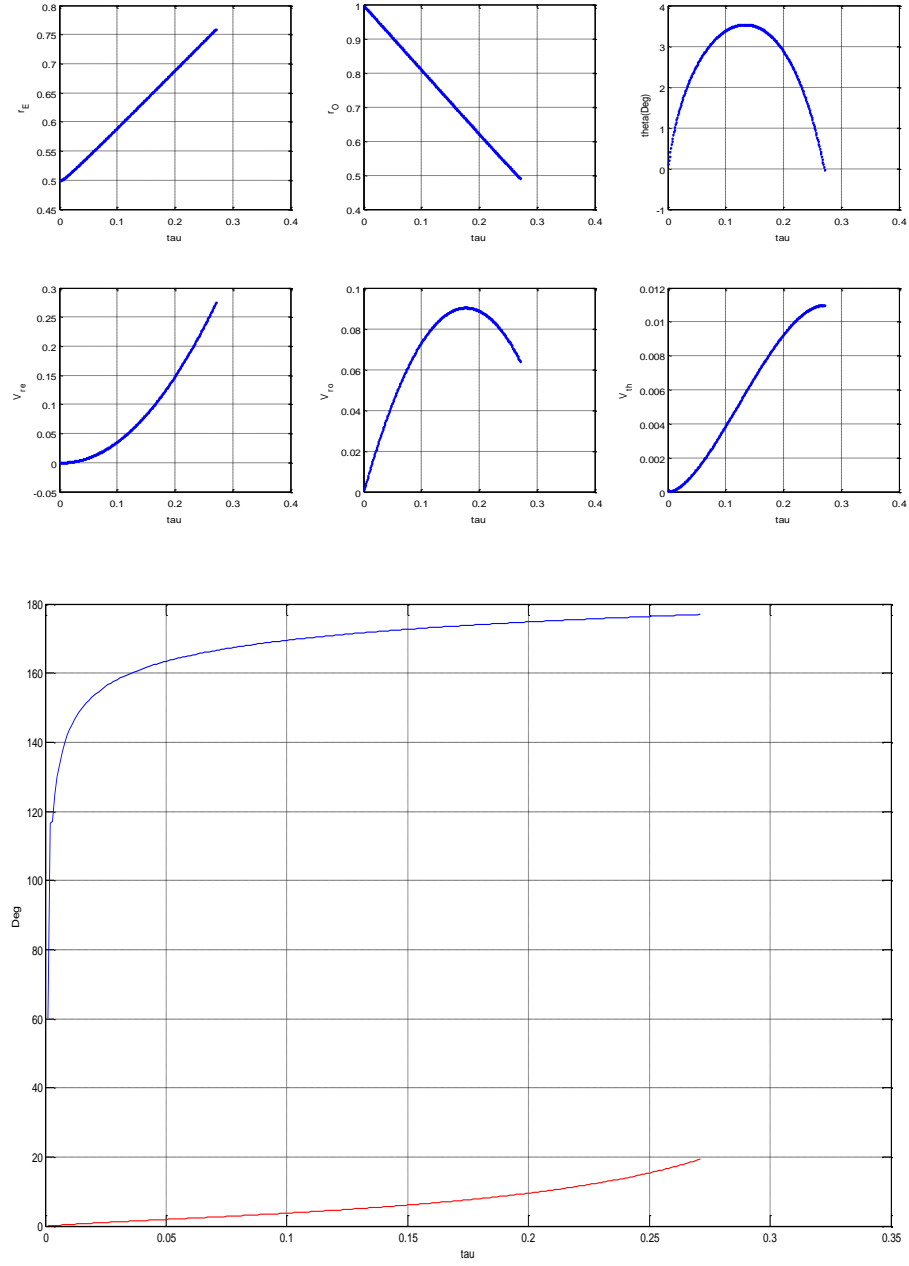


Figure A. 44: Time history of the States, Costates and Controls

$$\alpha = 1.9, \quad \xi = 120^\circ, \quad r_{O_T} = 1$$

At the end point the rElay's control is $\varphi^*(0) = 60^\circ$

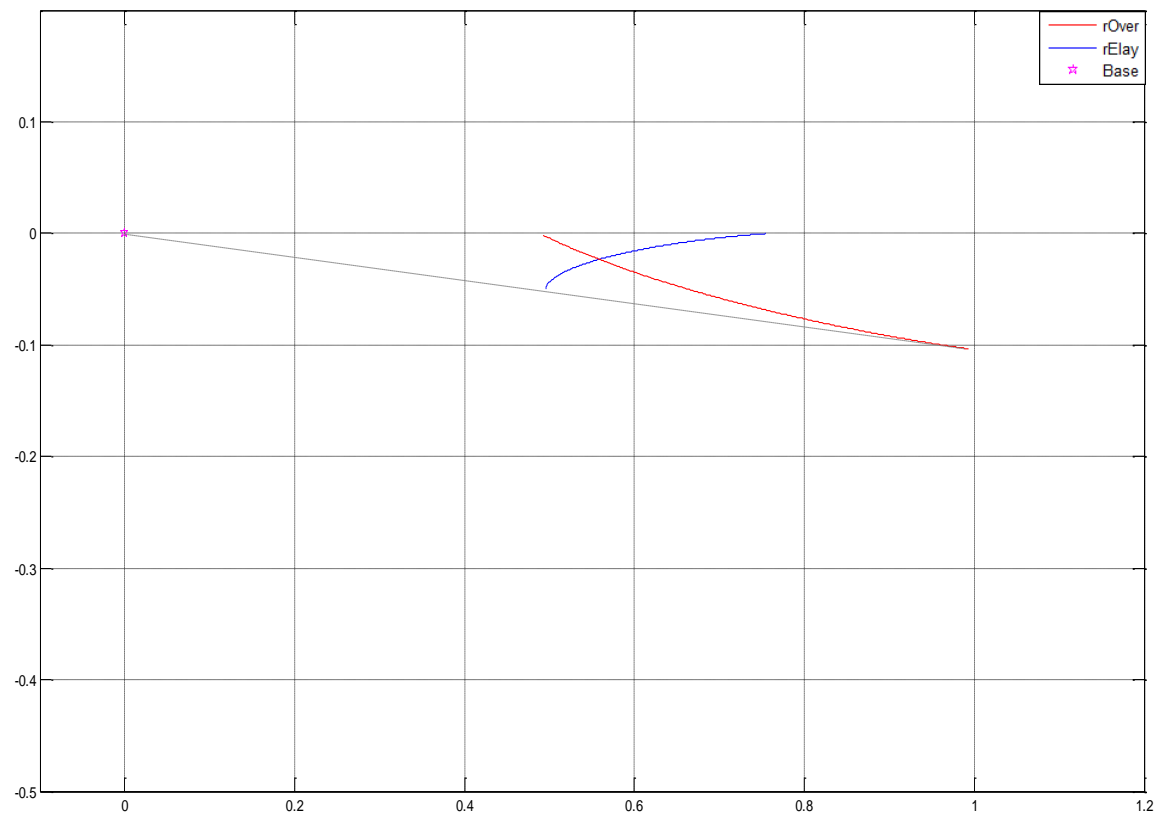


Figure A. 45: Optimal trajectories of Rover and Relay. $\alpha = 1.9$, $\xi = 150^\circ$, $r_{O_r} = 1$

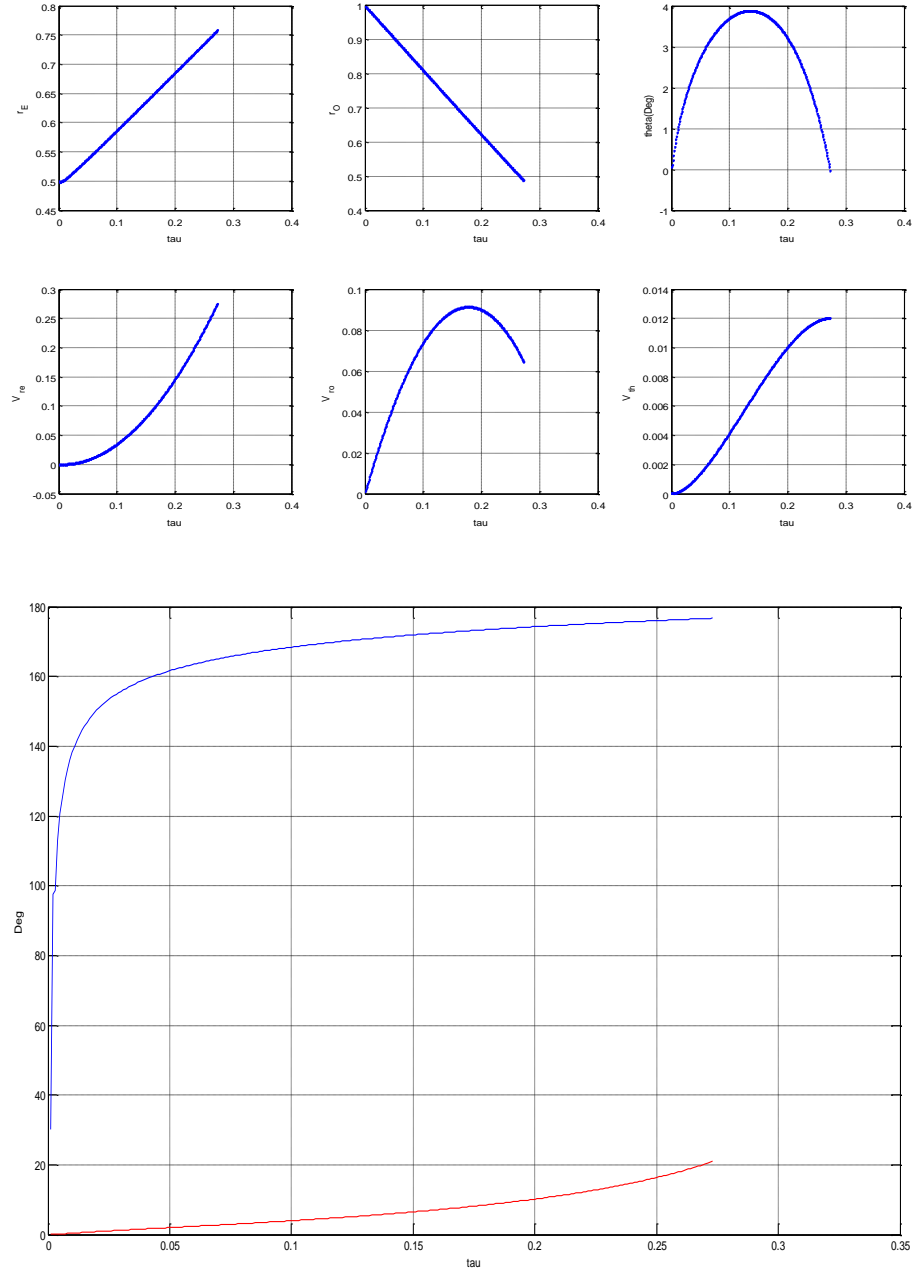


Figure A. 46: Time history of the States, Costates and Controls

$$\alpha = 1.9, \quad \xi = 150^\circ, \quad r_{O_T} = 1$$

At the end point the rElay's control is $\varphi^*(0) = 30^\circ$

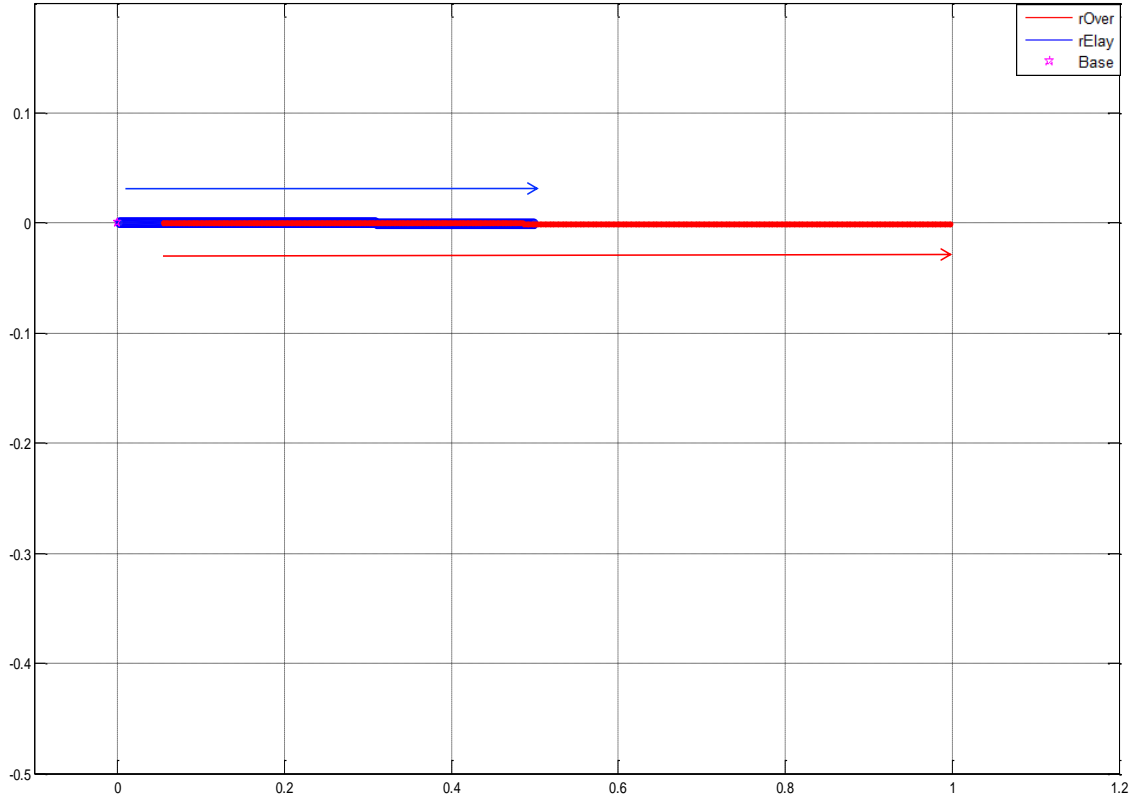


Figure A. 47: Optimal trajectories of Rover and Relay. $\alpha = 1.9$, $\xi = 180^\circ$, $r_{O_r} = 1$

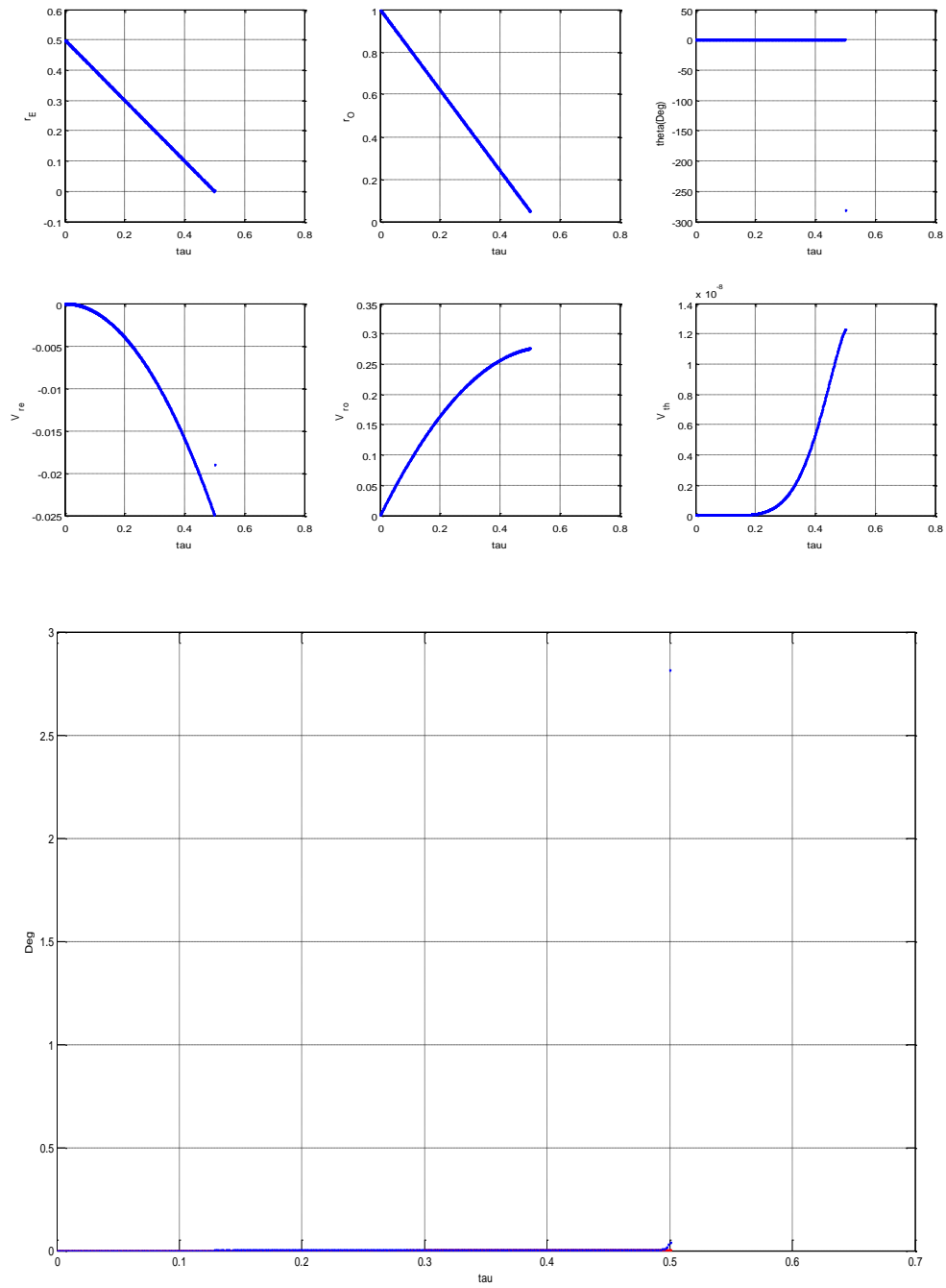


Figure A. 48: Time history of the States, Costates and Controls

$$\alpha = 1.9, \quad \xi = 180^\circ, \quad r_{O_r} = 1$$

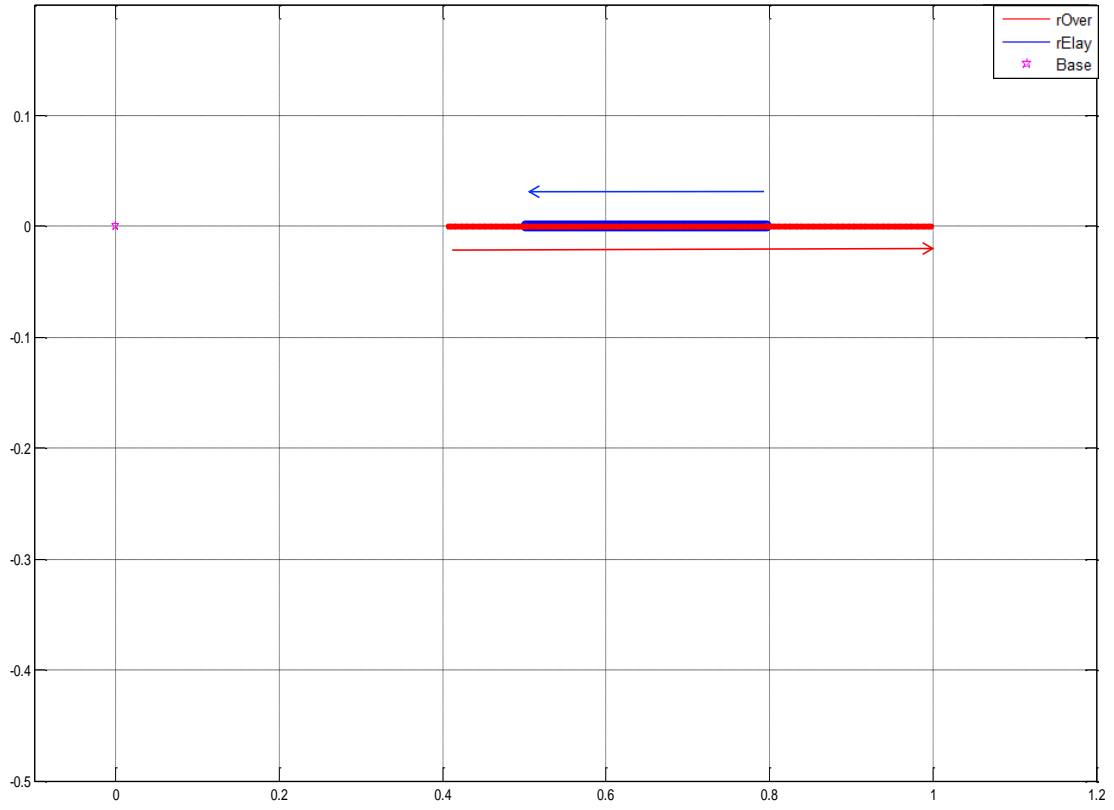


Figure A. 49: Optimal trajectories of Rover and Relay. $\alpha = 2$, $\xi = 0^\circ$, $r_{O_r} = 1$

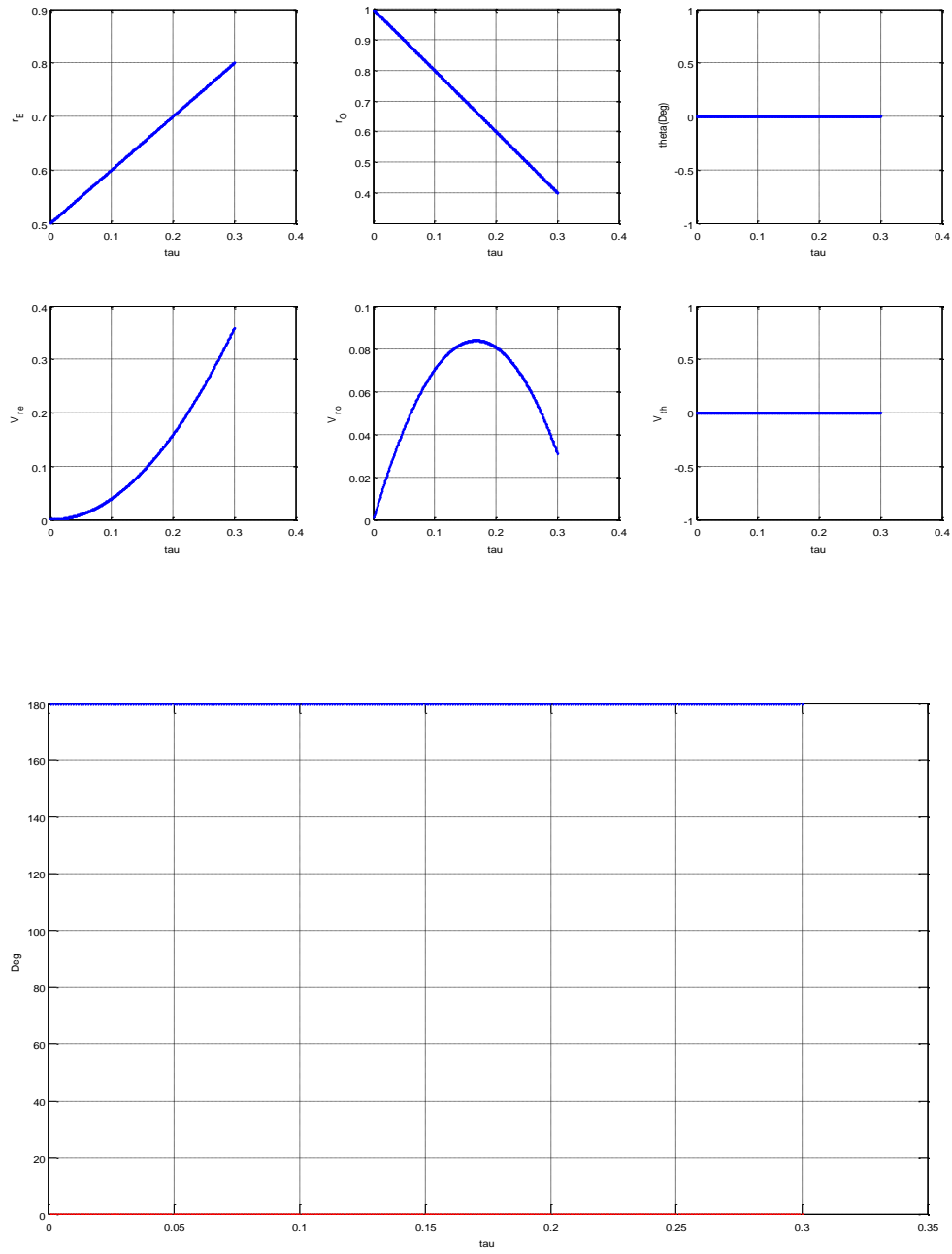


Figure A. 50: Time history of the States, Costates and Controls.

$$\alpha = 2, \xi = 0^\circ, r_{O_T} = 1$$

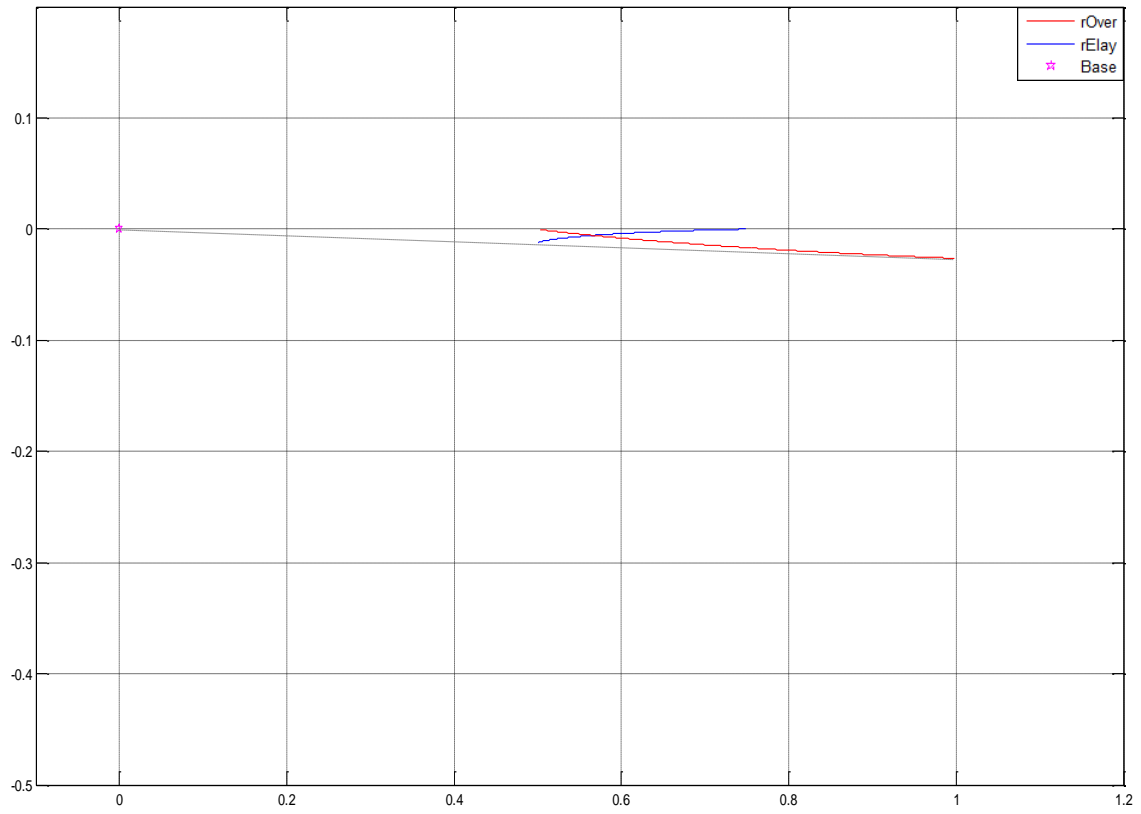


Figure A. 51: Optimal trajectories of Rover and Relay. $\alpha = 2$, $\xi = 30^\circ$, $r_{O_r} = 1$

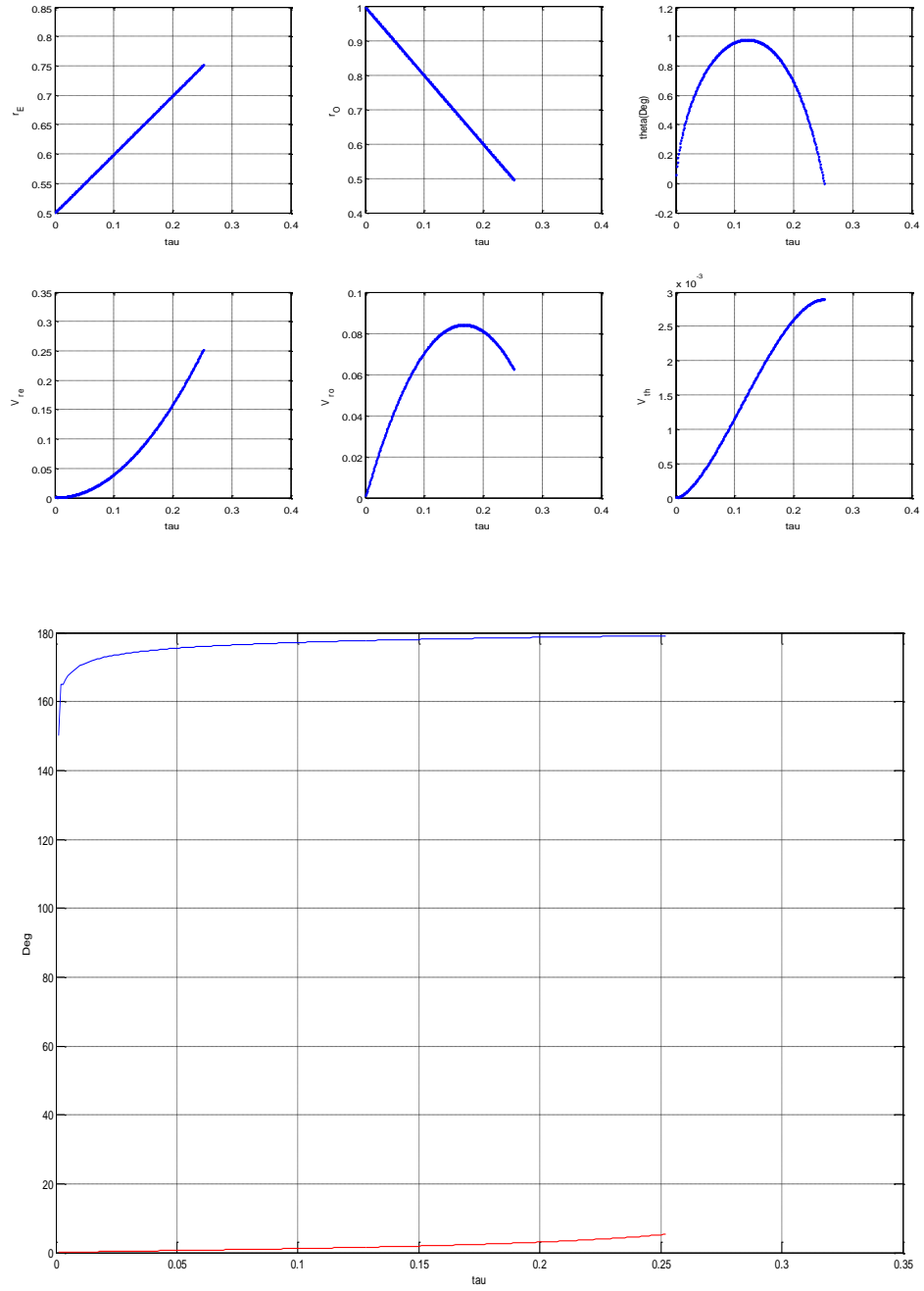


Figure A. 52: Time history of the States, Costates and Controls.

$$\alpha = 2, \xi = 30^\circ, r_{O_T} = 1$$

At the end point the rElay's control is $\varphi^*(0) = 150^\circ$

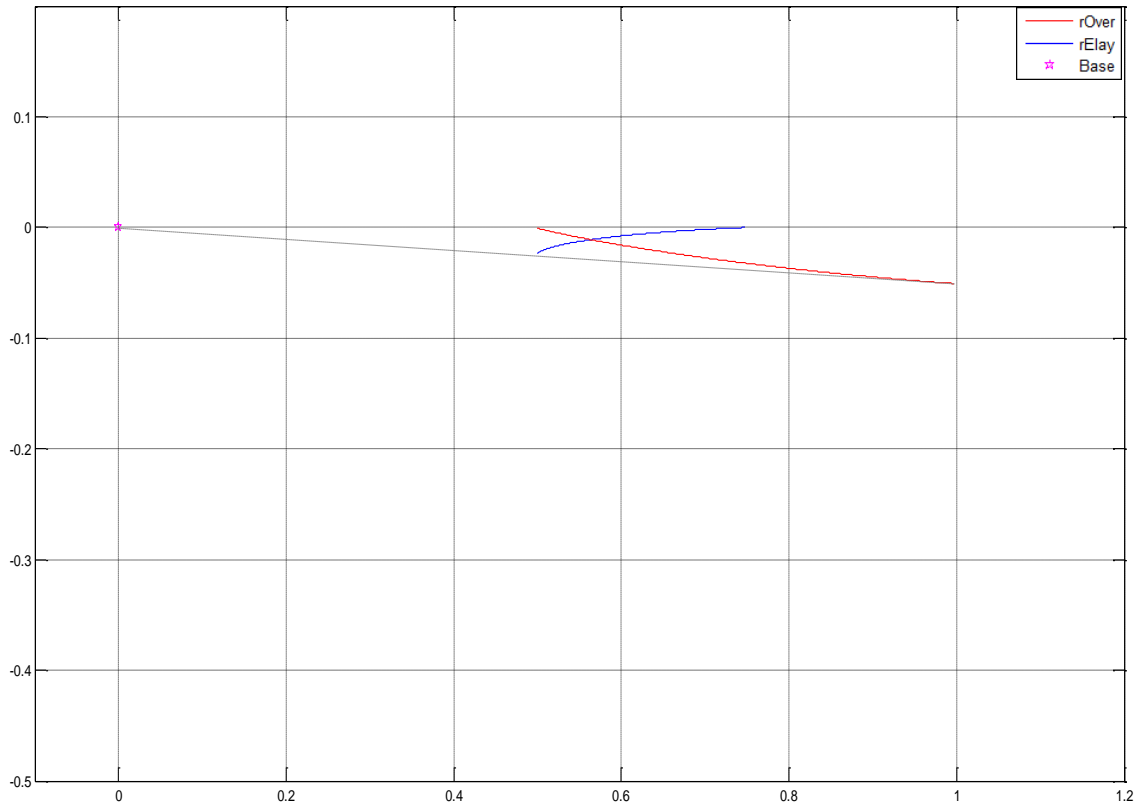


Figure A. 53: Optimal trajectories of Rover and Relay. $\alpha = 2$, $\xi = 60^\circ$, $r_{O_r} = 1$

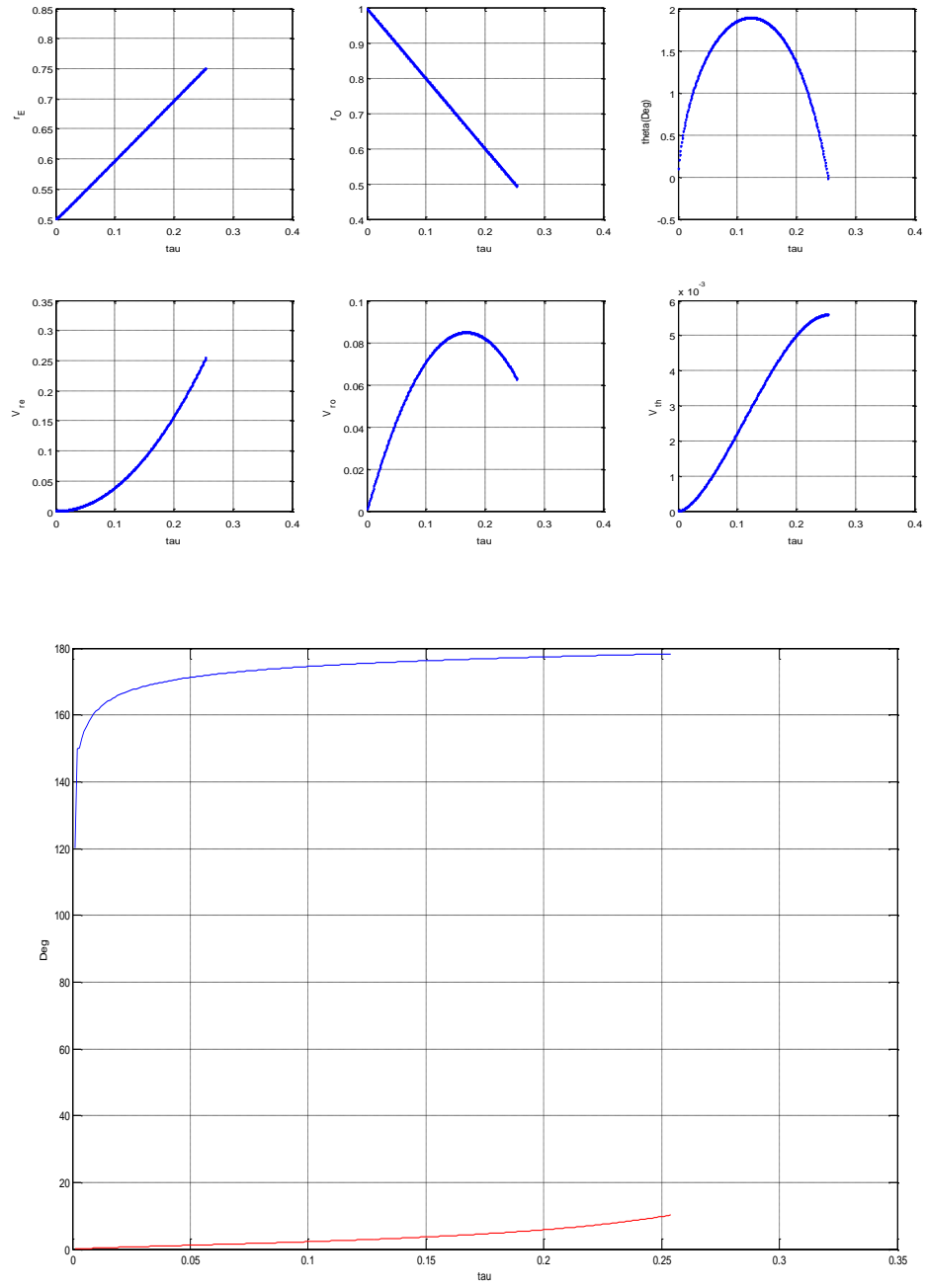


Figure A. 54: Time history of the States, Costates and Controls.

$$\alpha = 2, \quad \xi = 60^\circ, \quad r_{O_T} = 1$$

At the end point the rElay's control is $\varphi^*(0) = 120^\circ$

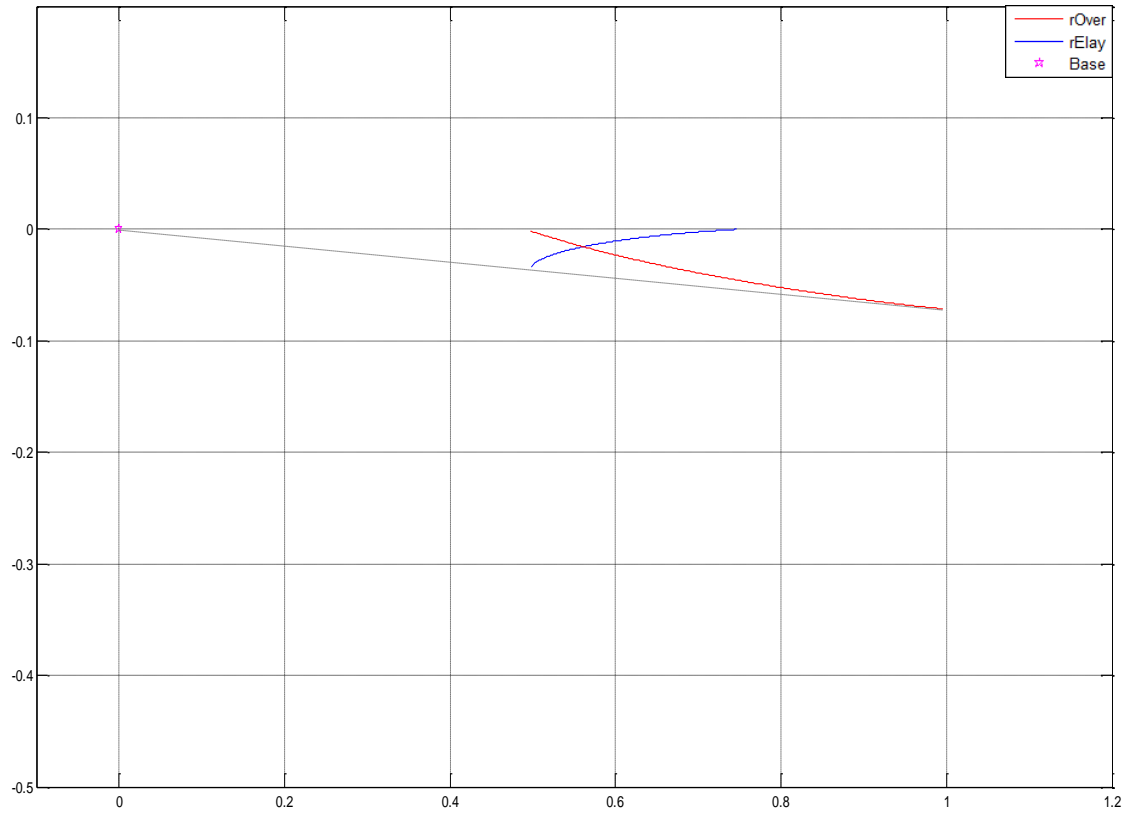


Figure A. 55: Optimal trajectories of Rover and Relay. $\alpha = 2$, $\xi = 90^\circ$, $r_{O_T} = 1$

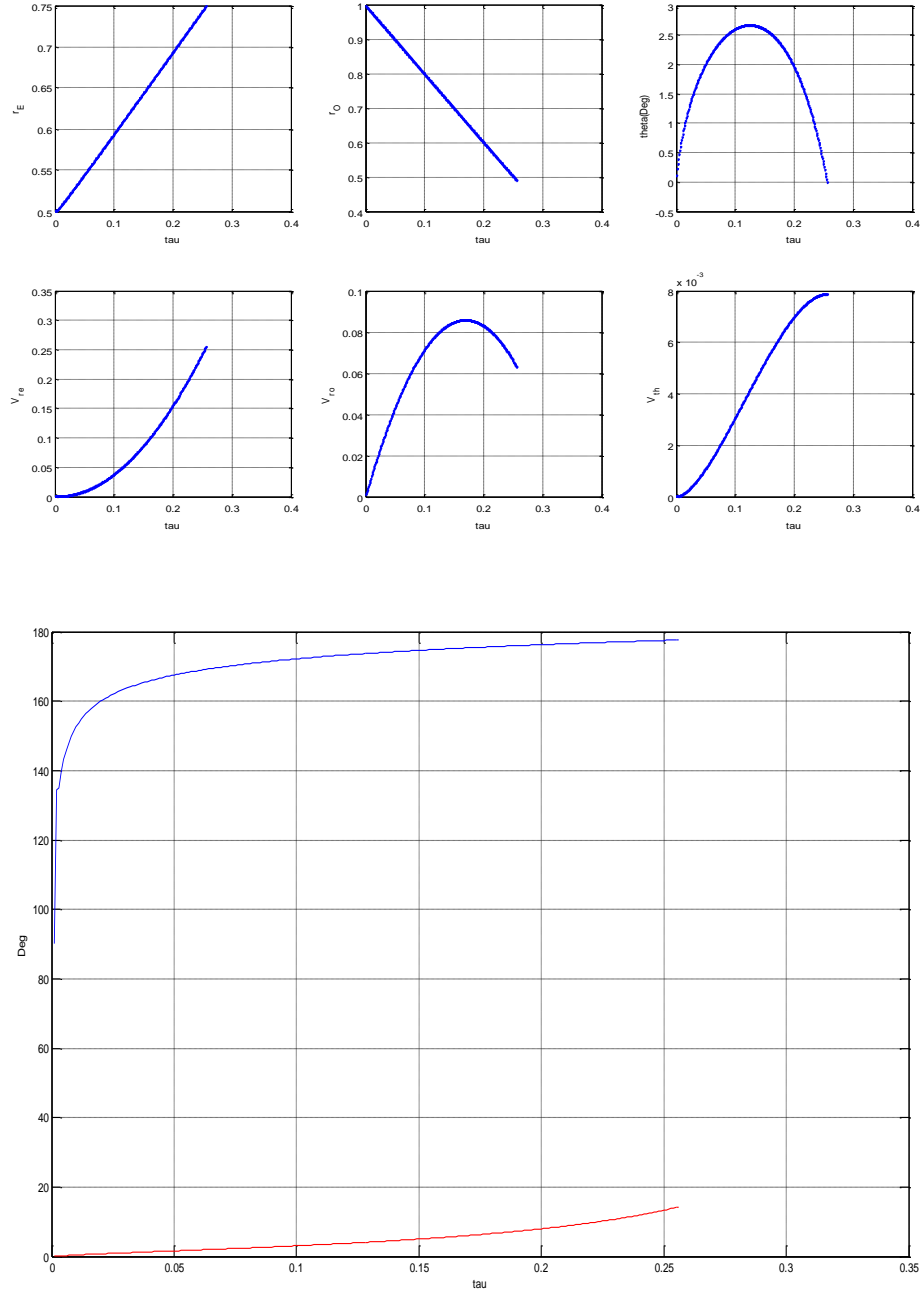


Figure A. 56: Time history of the States, Costates and Controls.

$$\alpha = 2, \quad \xi = 90^\circ, \quad r_{O_T} = 1$$

At the end point the rElay's control is $\varphi^*(0) = 90^\circ$

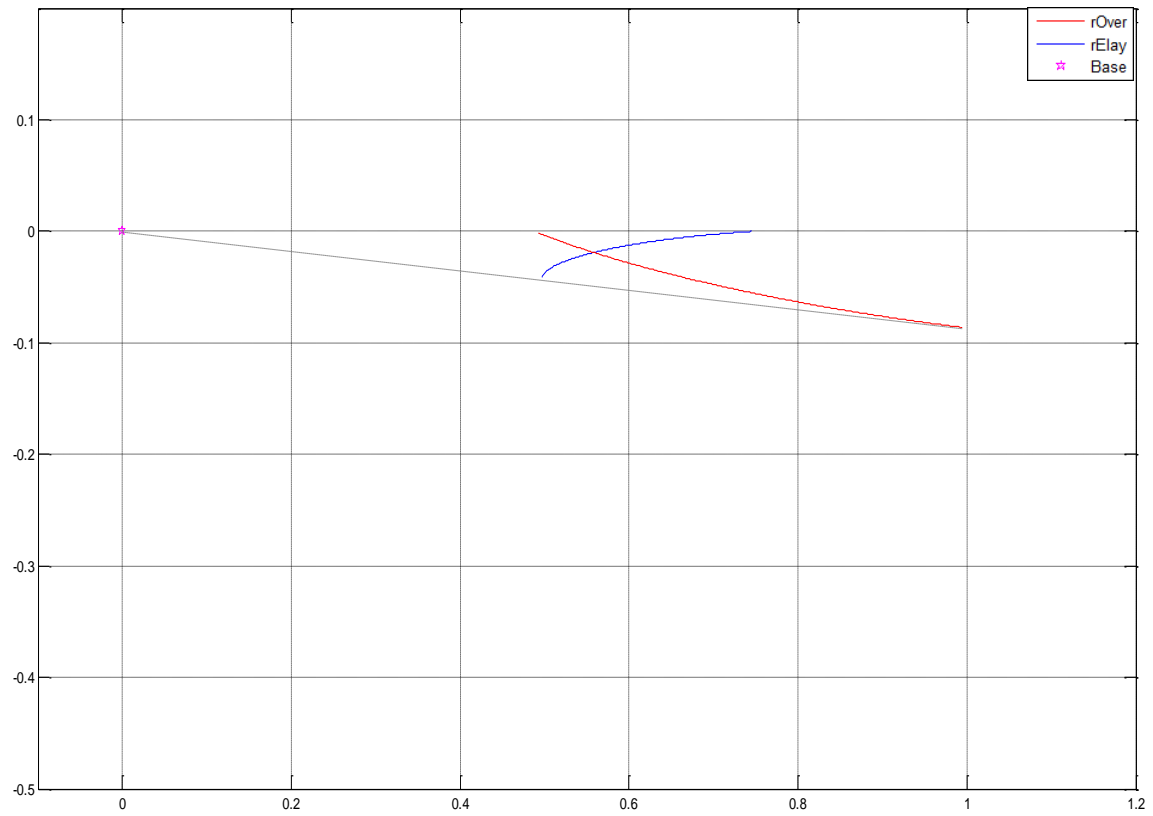


Figure A. 57: Optimal trajectories of Rover and Relay. $\alpha = 2$, $\xi = 120^\circ$, $r_{O_r} = 1$

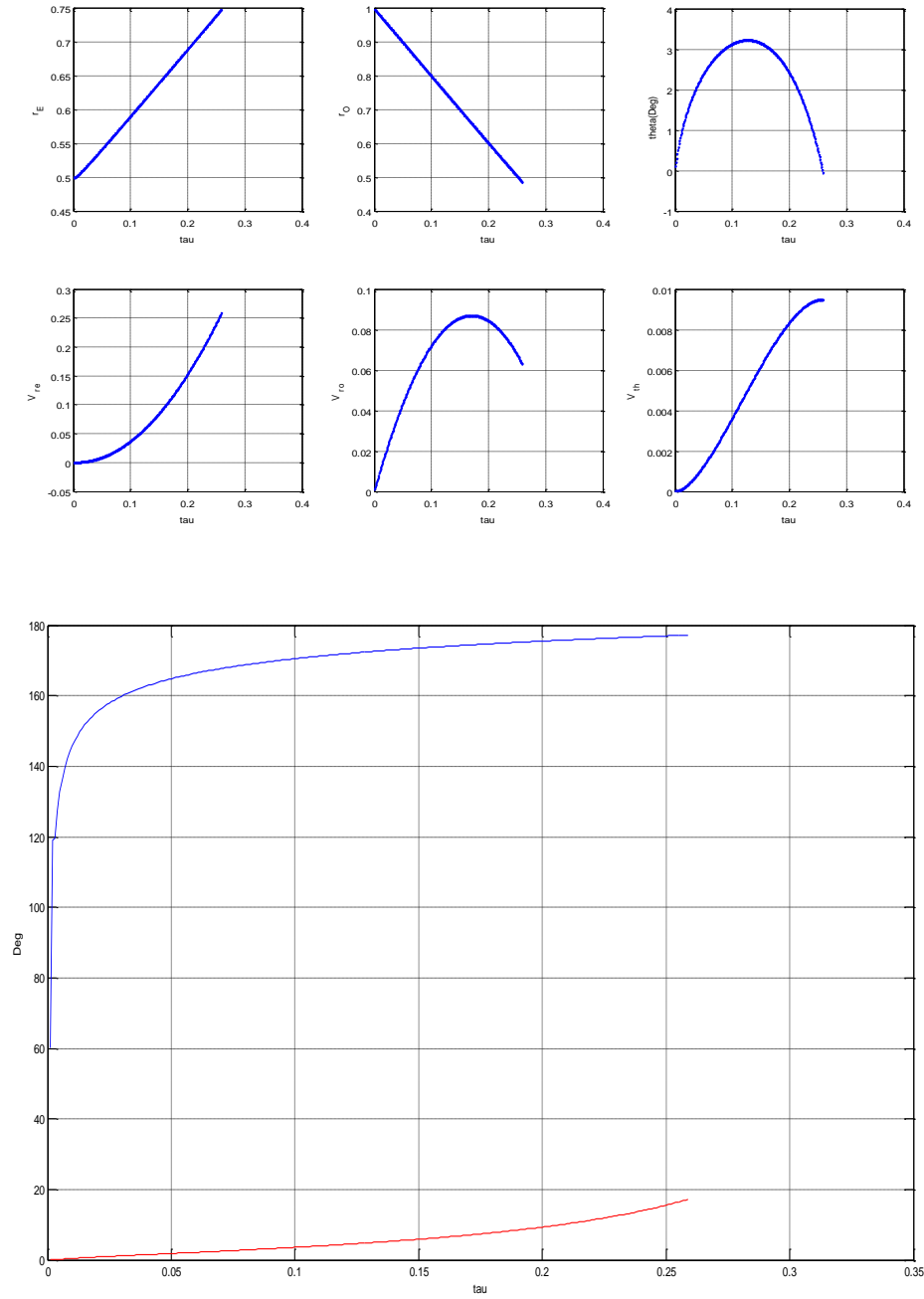


Figure A. 58: Time history of the States, Costates and Controls.

$$\alpha = 2, \quad \xi = 120^\circ, \quad r_{O_T} = 1$$

At the end point the rElay's control is $\varphi^*(0) = 60^\circ$

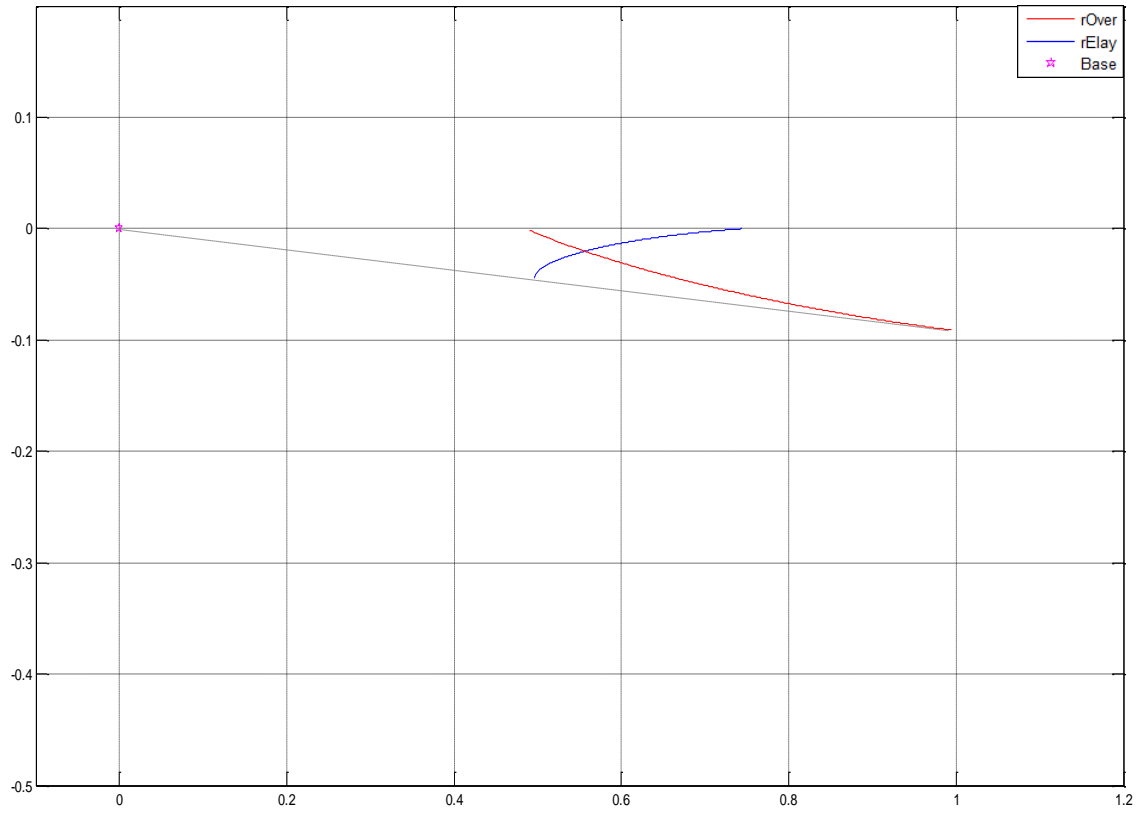


Figure A. 59: Optimal trajectories of Rover and Relay. $\alpha = 2$, $\xi = 150^\circ$, $r_{O_r} = 1$

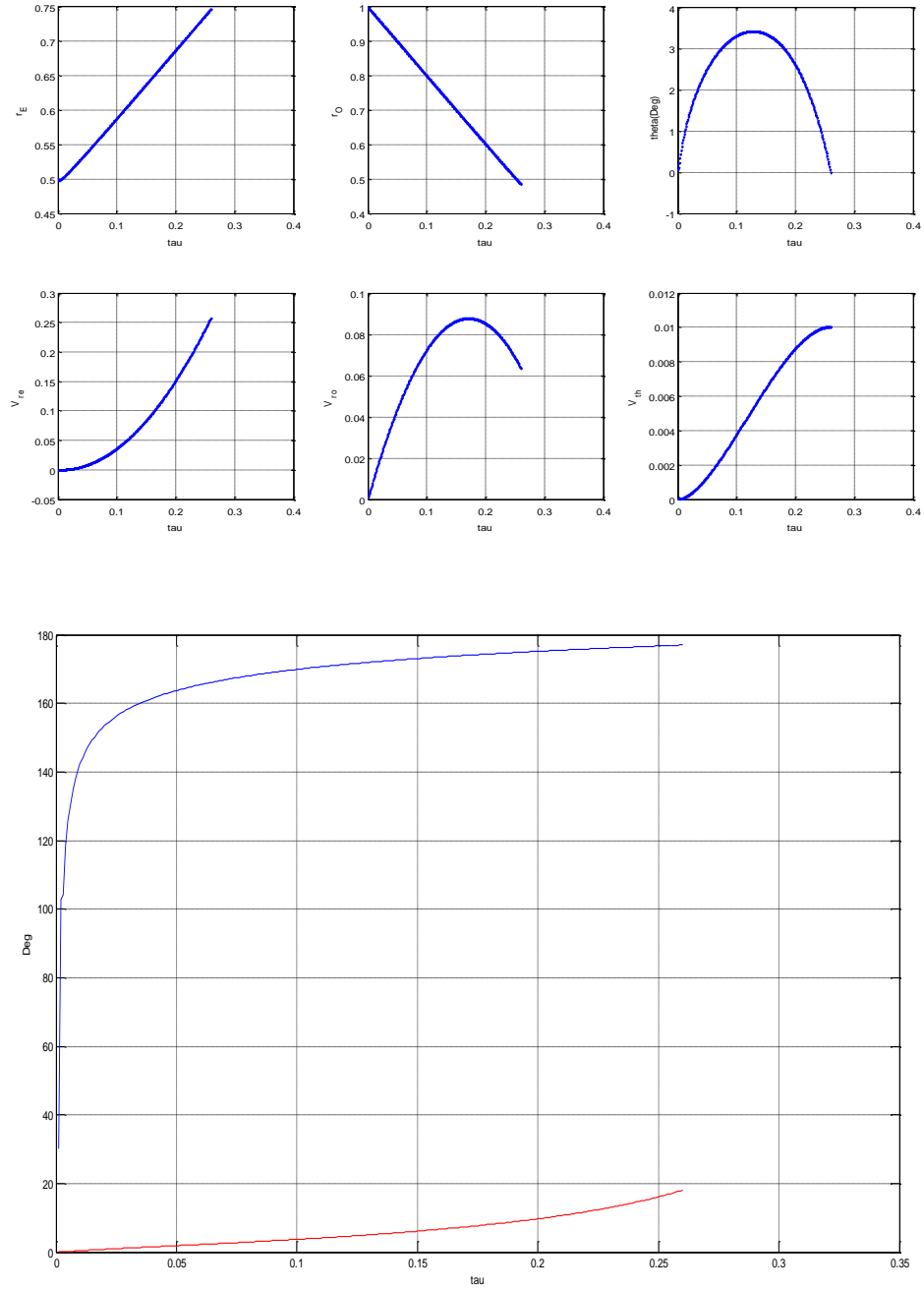


Figure A. 60: Time history of the States, Costates and Controls.

$$\alpha = 2, \xi = 150^\circ, r_{O_T} = 1$$

At the end point the rElay's control is $\varphi^*(0) = 30^\circ$

Appendix B – Geometry

An Elementary Euclidean Geometry Result:

It is well known that the locus of all points such that the sum of the distances from two fixed points is constant, is an ellipse. Thus, the following is of some interest.

Theorem 1 The Locus of all points such that the sum of the squares of the distances from two fixed points is constant, is a circle centered at the midpoint of the segment formed by the two fixed points. The radius of this circle is

$$R = \sqrt{d^2 - f^2}$$

where the sum of the squares of the distances is $2d^2$ and the distance between the fixed points is $2f$; obviously, $d \geq f$.

Proof:

Let the fixed points F_1 and F_2 be on the x -axis ($F_1 = (f, 0)$, $F_2 = (-f, 0)$) as shown in the figure below.

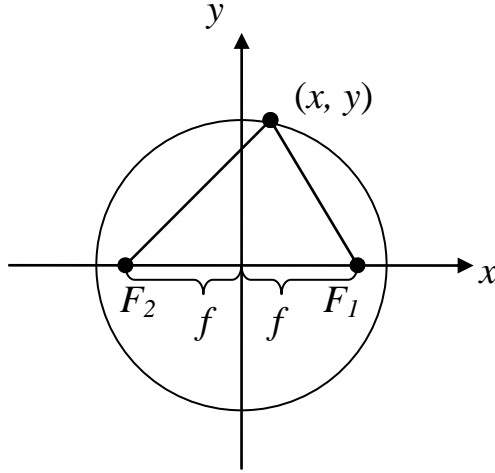


Figure B. 1: Schematic of Fixed Points Showing Isocost Circle

The sum of the squares of the distances is calculated as

$$\begin{aligned}
 2d^2 &= (f+x)^2 + y^2 + (f-x)^2 + y^2 \\
 &= 2f^2 + 2x^2 + 2y^2 \\
 \Rightarrow x^2 + y^2 &= d^2 - f^2
 \end{aligned}$$

This is the equation of a circle centered at the origin, whose radius is

$$R = \sqrt{d^2 - f^2}$$

□

This result appeared in [5].

Remark: The loci of constant costs, $2d^2$, are concentric circles where the minimum cost is found at the midpoint of the line formed by F_1 and F_2 , where $d = f$.

Extension: The Locus of all points such that the weighted sum of the squares of the distances from two fixed points is constant, is a circle centered on the segment formed by

the two fixed points and is at a distance of $(1 - 2\alpha)f$ from this segment's midpoint. The radius of this circle is

$$R = \sqrt{d^2 - 4\alpha(1 - \alpha)f^2}$$

where d^2 is the specified weighted sum of the squares of the distances, the distance between the fixed points is $2f$; and the weight is α ; if $\alpha < 0$ or $\alpha > 1$ this is true $\forall d > 0$, and if $0 \leq \alpha \leq 1$, $d > 2f\sqrt{\alpha(1 - \alpha)}$. Note: When the weight $\alpha = 1/2$, need $d > f$.

Proof: The weighted sum of the squares of the distances is calculated as

$$\begin{aligned} d^2 &= \alpha[(f + x)^2 + y^2] + (1 - \alpha)[(f - x)^2 + y^2] \\ &= \alpha f^2 + \alpha x^2 + 2\alpha fx + \alpha y^2 + (1 - \alpha)f^2 + (1 - \alpha)x^2 - 2(1 - \alpha)fx + (1 - \alpha)y^2 \\ &= f^2 + x^2 + y^2 - 2fx(1 - 2\alpha) \\ &= [x - (1 - 2\alpha)f]^2 + f^2 + y^2 - (1 - 2\alpha)^2 f^2 \\ \Rightarrow [x - (1 - 2\alpha)f]^2 + y^2 &= d^2 - 4\alpha(1 - \alpha)f^2 \end{aligned}$$

□

Appendix C – New Parameterization of Family of “Endpoints”

Each “sweet spot” on the line $r_E = \frac{1}{2}r_O$ is encapsulated in a small hemispherical terminal manifold, as shown in Fig.C.1

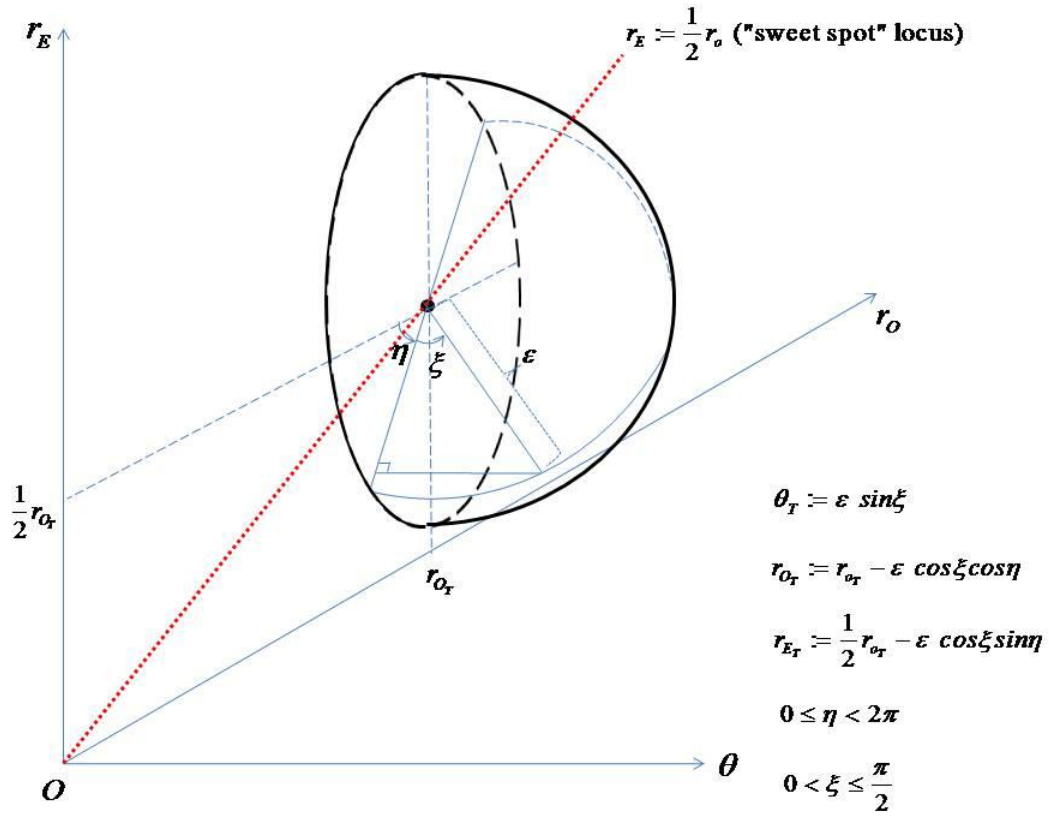


Figure C. 1: End States' Manifold

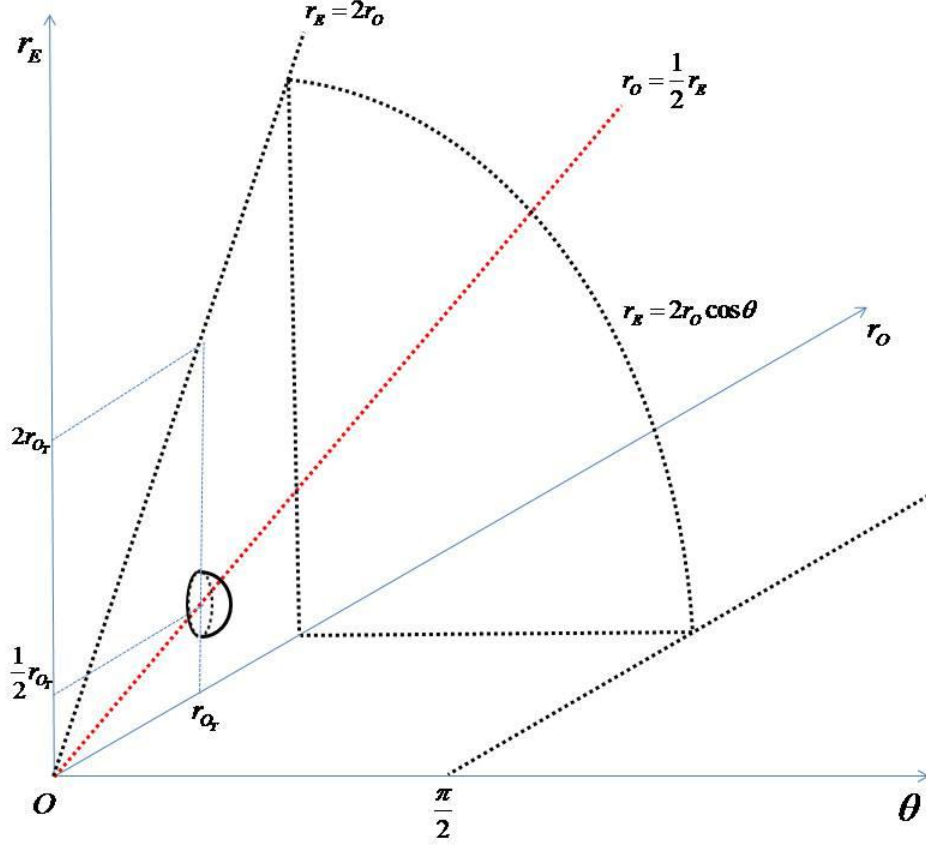


Figure C. 2: State Space

Consider the family of “sweet spots” $\left(\frac{1}{2}r_{o_r}, r_{o_r}, 0\right)$ which is parameterized by $r_{o_r}, r_{o_r} > 0$.

As in the optimal control case, we back off from “sweet spots” and the retrograde integration of the characteristics equations is initiated from end states $(r_{E_T}, r_{o_T}, \theta_T)$ on a hemispherical manifold, as shown in Fig.C.1, where

$$\theta_T = \varepsilon \sin \xi$$

$$r_{o_T} := r_{o_r} - \varepsilon \cos \xi \cos \eta$$

$$r_{E_T} := \frac{1}{2} r_{o_T} - \varepsilon \cos \xi \sin \eta$$

$$0 \leq \eta < 2\pi$$

$$0 < \xi \leq \frac{\pi}{2}$$

The end states associated with the “sweet spot” $\left(\frac{1}{2} r_{o_T}, r_{o_T}, 0 \right)$ reside on a hemispherical terminal manifold, as shown in Fig.C.2, where the state space of the differential game is illustrated.

Without loss of generality we confine our attention to $r_{o_T} = 1$. The family of optimal trajectories is thus parameterized by $0 < \xi \leq \frac{\pi}{2}$ and $0 \leq \eta < 2\pi$. The retrograde integration stops when $r_E = 2r_o \cos \theta$.

The optimal control of the rElay at $t=T$ is given by the solution of the end game where the end state is $r_{E_T}, r_{o_T}, \theta_T$. It is

$$\left. \begin{aligned} \cos(\varphi^*(T)) &= \frac{r_{o_T} \cos \theta_T - 2r_{E_T}}{\sqrt{4r_{E_T}^2 + r_{o_T}^2 - 4r_{E_T} r_{o_T} \cos \theta_T}}, \\ \sin(\varphi^*(T)) &= \frac{r_{o_T} \sin \theta_T}{\sqrt{4r_{E_T}^2 + r_{o_T}^2 - 4r_{E_T} r_{o_T} \cos \theta_T}}, \end{aligned} \right\} \quad (26)$$

provided that the end state is not $r_{E_T} = \frac{1}{2} r_{o_T}$, $\theta_T = 0$.

Similarly, the optimal control of the rOver at $t=T$ given by the solution of the end game is

$$\left. \begin{aligned} \cos(\psi^*(T)) &= \frac{r_{O_T} - r_{E_T} \cos \theta_T}{\sqrt{r_{E_T}^2 + r_{O_T}^2 - 2r_{E_T} r_{O_T} \cos \theta_T}}, \\ \sin(\psi^*(T)) &= \frac{r_{E_T} \sin \theta_T}{\sqrt{r_{E_T}^2 + r_{O_T}^2 - 2r_{E_T} r_{O_T} \cos \theta_T}}, \end{aligned} \right\} \quad (27)$$

provided that the end state is not $r_{E_T} = r_{O_T}$, $\theta_T = 0$; when this is the case, from first principles we conclude that the rOver's control $\psi^*(T) = 0$.

Similar to the solution of the optimal control problem, the “sweet spot” is $r_{E_T} = \frac{1}{2} r_{O_T}$, $\theta_T = 0$. This however is problematic, because the respective rElay and rOver terminal controls given by eqs. (26) and (27) cannot be computed. Therefore, similar to the optimal control problem, one backs off and one considers the terminal states on the hemisphere shown in Fig.C.1.

The end states on the small hemisphere around the “sweet spot” are parameterized as follows.

$$\left. \begin{aligned}
\theta_T &:= \varepsilon \sin \xi \\
r_{O_T} &:= r_{o_T} - \varepsilon \cos \xi \cos \eta \\
r_{E_T} &:= \frac{1}{2} r_{o_T} - \varepsilon \cos \xi \sin \eta \\
0 &\leq \eta < 2\pi \\
0 &\leq \xi < \frac{\pi}{2} \\
0 &< \varepsilon = 1, \text{ fixed}
\end{aligned} \right\} \quad (28)$$

The optimal controls at $t=T$ for end states on the hemispherical terminal manifold are obtained by inserting eqs. (28) into the terminal control eqs. (26) and (27).

We calculate

$$\begin{aligned}
4r_{E_T}^2 + r_{O_T}^2 - 4r_{E_T} r_{O_T} \cos \theta_T &\approx 4 \left(\frac{1}{4} r_{o_T}^2 + \varepsilon^2 \cos^2 \xi \sin^2 \eta - \varepsilon r_{o_T} \cos \xi \sin \eta \right) \\
&\quad + r_{o_T}^2 + \varepsilon^2 \cos^2 \xi \cos^2 \eta - 2\varepsilon r_{o_T} \cos \xi \cos \eta \\
&\quad - 4 \left(\frac{1}{2} r_{o_T} - \varepsilon \cos \xi \sin \eta \right) (r_{o_T} - \varepsilon \cos \xi \cos \eta) \left(1 - \frac{1}{2} \varepsilon^2 \sin^2 \xi \right) \\
&= \varepsilon^2 \left[r_{o_T}^2 \sin^2 \xi + 3 \cos^2 \xi \sin^2 \eta + \cos^2 \xi - 2 \cos^2 \xi \sin 2\eta \right]
\end{aligned}$$

$$\begin{aligned}
r_{O_T} \sin \theta_T &\approx \varepsilon r_{O_T} \sin \xi \\
r_{O_T} \cos \theta_T - 2r_{E_T} &\approx \varepsilon \cos \xi (2 \sin \eta - \cos \eta)
\end{aligned}$$

Inserting these expressions into the rElay's terminal control eqs. (26) yields

$$\begin{aligned}
\cos(\varphi^*(T)) &= \frac{\cos \xi (2 \sin \eta - \cos \eta)}{\sqrt{r_{o_T}^2 \sin^2 \xi + 3 \cos^2 \xi \sin^2 \eta + \cos^2 \xi - 2 \cos^2 \xi \sin 2\eta}} \\
\sin(\varphi^*(T)) &= \frac{r_{O_T} \sin \xi}{\sqrt{r_{o_T}^2 \sin^2 \xi + 3 \cos^2 \xi \sin^2 \eta + \cos^2 \xi - 2 \cos^2 \xi \sin 2\eta}}
\end{aligned}$$

Next,

$$\begin{aligned}
r_{E_T}^2 + r_{O_T}^2 - 2r_{E_T} r_{O_T} \cos \theta_T &\approx \frac{1}{4} r_{o_T}^2 + \varepsilon^2 \cos^2 \xi \sin^2 \eta - \varepsilon r_{o_T} \cos \xi \sin \eta + r_{o_T}^2 + \varepsilon^2 \cos^2 \xi \cos^2 \eta \\
&\quad - 2\varepsilon r_{o_T} \cos \xi \cos \eta \\
&\quad - 2 \left(\frac{1}{2} r_{o_T} - \varepsilon \cos \xi \sin \eta \right) \left(r_{o_T} - \varepsilon \cos \xi \cos \eta \right) \left(1 - \frac{1}{2} \varepsilon^2 \sin^2 \xi \right) \\
&= \frac{1}{4} r_{o_T}^2 + \varepsilon r_{o_T} \cos \xi (\sin \eta - \cos \eta) \\
&\quad + \varepsilon^2 \left(\frac{1}{2} r_{o_T}^2 \sin^2 \xi + \cos^2 \xi - 2 \cos^2 \xi \sin \eta \cos \eta \right) \\
&\approx \frac{1}{4} r_{o_T}^2
\end{aligned}$$

$$\begin{aligned}
r_{O_T} - r_{E_T} \cos \theta_T &= \frac{1}{2} r_{o_T} + \varepsilon \cos \xi (\sin \eta - \cos \eta) + \frac{1}{4} \varepsilon^2 r_{o_T} \sin^2 \xi \approx \frac{1}{2} r_{o_T} \\
r_{E_T} \sin \theta_T &= \varepsilon \left(\frac{1}{2} r_{o_T} - \varepsilon \cos \xi \sin \eta \right) \sin \xi \approx \frac{1}{2} \varepsilon r_{o_T} \sin \xi \\
&\rightarrow \cos(\psi^*(T)) \approx 1, \sin(\psi^*(T)) \approx 0
\end{aligned}$$

Inserting these expressions into the rOver's terminal control eqs. (27) yields

Using these controls at time $t=T$, we obtain

$$\begin{aligned}
\dot{r}_E &= \frac{\cos \xi (2 \sin \eta - \cos \eta)}{\sqrt{r_{o_T}^2 \sin^2 \xi + 3 \cos^2 \xi \sin^2 \eta + \cos^2 \xi - 2 \cos^2 \xi \sin 2 \eta}}, \dot{r}_O = \alpha \\
\dot{\theta} &= \frac{\varepsilon \alpha \sin \xi (r_{o_T} - 2 \varepsilon \cos \xi \sin \eta)}{r_{o_T}^2} \\
&\quad - \frac{r_{o_T} \sin \xi}{\left(\frac{1}{2} r_{o_T} - \varepsilon \cos \xi \sin \eta \right) \sqrt{r_{o_T}^2 \sin^2 \xi + 3 \cos^2 \xi \sin^2 \eta + \cos^2 \xi - 2 \cos^2 \xi \sin 2 \eta}}
\end{aligned}$$

We note that $r_E \uparrow$ if $0 < \eta < \pi$ and $r_E \downarrow$ if $\pi < \eta < 2\pi$, that is, $r_E \uparrow$ if $r_E < \frac{r_{o_T}}{2}$ and $r_E \downarrow$ if

$r_E > \frac{r_{o_T}}{2}$, $\dot{\theta} < 0$. Hence, the trajectory heads toward the locus of “sweet spots”

s.t. $r_O \uparrow$.

The above differential equations allow us to propagate the state to time $T - \Delta T$:

$$r_E(T - \Delta T) = \frac{1}{2}r_{o_T} - \varepsilon \cos \xi \sin \eta - \frac{\cos \xi (2 \sin \eta - \cos \eta)}{\sqrt{r_{o_T}^2 \sin^2 \xi + 3 \cos^2 \xi \sin^2 \eta + \cos^2 \xi - 2 \cos^2 \xi \sin 2 \eta}} \cdot \Delta T$$

$$r_O(T - \Delta T) = r_{o_T} - \varepsilon \cos \xi \cos \eta - \alpha \cdot \Delta T$$

$$\theta(T - \Delta T) = \varepsilon \sin \xi + \frac{r_{o_T} \sin \xi}{\left(\frac{1}{2}r_{o_T} - \varepsilon \cos \xi \sin \eta \right) \sqrt{r_{o_T}^2 \sin^2 \xi + 3 \cos^2 \xi \sin^2 \eta + \cos^2 \xi - 2 \cos^2 \xi \sin 2 \eta}} \cdot \Delta T - \frac{\varepsilon \alpha \sin \xi (r_{o_T} - 2 \varepsilon \cos \xi \sin \eta)}{r_{o_T}^2} \cdot \Delta T$$

To propagate the characteristics/co-states to time $T - \Delta T$ ($\tau = \Delta T$), we proceed as follows.

Recall

$$\begin{aligned}\frac{d}{d\tau}V_{r_E} &= 4r_E - 2r_O \cos \theta + \frac{V_\theta^2}{r_E^2 \sqrt{r_E^2 V_{r_E}^2 + V_\theta^2}}, \quad V_{r_E}(0) = 0 \\ \frac{d}{d\tau}V_{r_O} &= 2r_O - 2r_E \cos \theta - \alpha \frac{V_\theta^2}{r_O^2 \sqrt{r_O^2 V_{r_O}^2 + V_\theta^2}}, \quad V_{r_O}(0) = 0 \\ \frac{d}{d\tau}V_\theta &= 2r_E r_O \sin \theta, \quad V_\theta(0) = 0, \quad 0 \leq \tau \leq T\end{aligned}$$

Now, on the one hand,

$$\sin \varphi^* = \frac{V_\theta}{\sqrt{r_E^2 V_{r_E}^2 + V_\theta^2}}$$

and on the other hand, we have calculated the terminal rElay's control

$$\sin(\varphi_T^*(\theta_T, r_{O_T}, r_{E_T})) = \frac{r_{O_T} \sin \xi}{\sqrt{r_{O_T}^2 \sin^2 \xi + 3 \cos^2 \xi \sin^2 \eta + \cos^2 \xi - 2 \cos^2 \xi \sin 2\eta}}$$

Similarly, on the one hand

$$\sin \psi^* = \frac{V_\theta}{\sqrt{r_O^2 V_{r_O}^2 + V_\theta^2}}$$

and on the other hand, we have calculated the rOver's terminal control

$$\sin(\psi_T^*(\theta_T, r_{O_T}, r_{E_T})) \approx 0$$

Thus, the limits

$$\lim_{V_\theta, V_{r_E} \rightarrow \infty} \frac{V_\theta}{\sqrt{r_E^2 V_{r_E}^2 + V_\theta^2}}, \quad \lim_{V_\theta, V_{r_E} \rightarrow \infty} \frac{V_\theta}{\sqrt{r_O^2 V_{r_O}^2 + V_\theta^2}}$$

exist.

\Rightarrow

$$\left. \frac{V_\theta}{\sqrt{r_E^2 V_{r_E}^2 + V_\theta^2}} \right|_{\tau=0} = 0$$

$$\left. \frac{V_\theta}{\sqrt{r_O^2 V_{r_O}^2 + V_\theta^2}} \right|_{\tau=0} = 0$$

\Rightarrow at $\tau=0$

$$\frac{d}{d\tau} V_{r_E} = 2(2r_E - r_O \cos \theta), \quad V_{r_E}(0) = 0$$

$$\frac{d}{d\tau} V_{r_O} = 2(2r_O - r_E \cos \theta), \quad V_{r_O}(0) = 0$$

$\Rightarrow V_{r_E}(\Delta T)$

$$= 2 \left[r_{o_r} - 2\varepsilon \cos \xi \sin \eta - \left(r_{o_r} - \frac{1}{2} r_{o_r} \varepsilon^2 \sin^2 \xi - \varepsilon \cos \xi \cos \eta + \frac{1}{2} \varepsilon^3 \cos \xi \sin^2 \xi \cos \eta \right) \right]$$

$$= 2\varepsilon \Delta T \left(\frac{1}{2} r_{o_r} \varepsilon \sin^2 \xi - 2 \cos \xi \sin \eta + \cos \xi \cos \eta - \frac{1}{2} \varepsilon^2 \cos \xi \sin^2 \xi \cos \eta \right)$$

$V_{r_O}(\Delta T)$

$$= 2 \left[r_{o_r} - \varepsilon \cos \xi \cos \eta - \left(\frac{1}{2} r_{o_r} - \frac{1}{4} r_{o_r} \varepsilon^2 \sin^2 \xi - \varepsilon \cos \xi \sin \eta + \frac{1}{2} \varepsilon^3 \cos \xi \sin^2 \xi \sin \eta \right) \right]$$

$$= \Delta T \left(r_{o_r} - 2\varepsilon \cos \xi \cos \eta + \frac{1}{2} r_{o_r} \varepsilon^2 \sin^2 \xi + 2\varepsilon \cos \xi \sin \eta + \varepsilon^3 \cos \xi \sin^2 \xi \sin \eta \right)$$

$V_\theta(\Delta T)$

$$= 2\varepsilon \sin \xi \Delta T \left(\frac{1}{2} r_{o_r}^2 - \frac{1}{2} \varepsilon r_{o_r} \cos \xi \cos \eta - r_{o_r} \varepsilon \cos \xi \sin \eta + \varepsilon^2 \cos \xi \sin \eta \cos \eta \right)$$

From this point on, the retrograde integration of the characteristics' eqs.(10) is undertaken.

We show the family of optimal trajectories in an (x,y) plane where

$$x(t) = r_E(t) \cos(\theta(t)), \quad y(t) = r_E(t) \sin(\theta(t)).$$

Appendix D – Suboptimal Solution

Suboptimal solutions are useful in their own right and provide insight into the optimal control problem and differential game

Geometric Approach

Using a geometric approach provides a suboptimal but easily implementable solution of the differential game. This approach is suboptimal because the rElay and the rOver each momentarily assume that the other player is stationary when determining their optimal control.

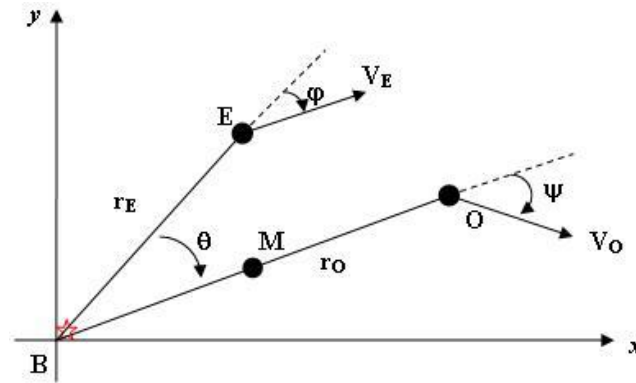


Figure D. 1: Schematic of Relay System Showing the Midpoint

The geometry of the engagement forms a triangle with vertices E , B and O representing the respective locations of the rElay, Base and rOver (see Figure D.1). Let M be the midpoint between the rOver and the Base. Simply rotating the schematic in Figure

D.1 provides an equivalent schematic (see Figure D.2) which is similar to the one analyzed in Appendix A.

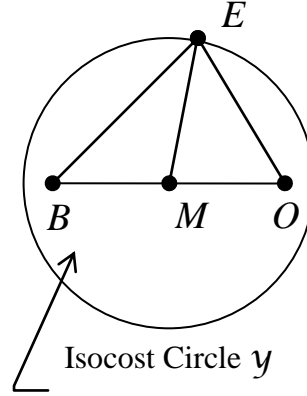


Figure D. 2: Schematic of Relay System Showing Isocost Circle

If the rOver were stationary, the loci of constant instantaneous costs

$$\gamma = \overline{EO}^2 + \overline{BE}^2$$

for the rElay are concentric circles centered at the midpoint and the midpoint is the rElay location which minimizes the cost.[2] The rElay is on the circumference of said circles, and the instantaneous cost γ is determined by the position of the rElay. This means that the gradient vector for minimizing cost is in the radial direction. Therefore, the optimal strategy of the rElay is to head toward the midpoint M .

The optimal control of the rElay is determined using the triangle $\triangle BEM$. The distance between E and M is determined using the law of cosines (just as in determining the distance between E and O before). The control angle φ is then found indirectly by finding its supplementary angle using the law of sines. However, due to an inherent

ambiguity in the law of sines, the control law is specified for three cases: (1) φ is acute, (2) φ is 90° and (3) φ is obtuse.

$$\varphi^* = \begin{cases} \sin^{-1} \left(\frac{r_o \sin \theta}{\sqrt{4r_E^2 + r_o^2 - 4r_E r_o \cos \theta}} \right) & \text{for } r_E < \frac{r_o \cos \theta}{2} \\ \frac{\pi}{2} & \text{for } r_E = \frac{r_o \cos \theta}{2} \\ \pi - \sin^{-1} \left(\frac{r_o \sin \theta}{\sqrt{4r_E^2 + r_o^2 - 4r_E r_o \cos \theta}} \right) & \text{for } r_E > \frac{r_o \cos \theta}{2} \end{cases} \quad (29)$$

This ambiguity can be bypassed by using an inverse cosine function in place of the inverse sine, i.e.

$$\varphi^* = \cos^{-1} \left(\frac{r_o \cos \theta - 2r_E}{\sqrt{4r_E^2 + r_o^2 - 4r_E r_o \cos \theta}} \right) \quad (30)$$

$$\psi^* = \varphi^* - \theta \quad (31)$$

Note that these rElay strategies are independent of the planning horizon T .

Once E , B and O are collinear, reducing the rElay velocity eliminates the need for excessive control use. However, the rElay might never actually arrive at the midpoint due to a short planning horizon T , or the maximizing efforts of a fast rOver. If the rOver used a suboptimal control strategy (which would usually be the case in practice), the rElay may be able to always arrive at the midpoint and consistently match the motion of the midpoint; this is a singular trajectory.

An additional one-sided optimization problem is obtained when the rOver's point of view is taken, namely, the rElay is stationary and the rOver works to maximize the cost functional.

$$\mathcal{Y} = \int_0^T (2r_E^2 + r_O^2 - 2r_E r_O \cos \theta) dt$$

The rOver will run away from the rElay.

Numerical Results

Guided by the suboptimal solution and the solution of the one – sided optimal control problem, the differential game is solved using Isaacs method [2], namely, the retrograde integration of the characteristics' equations (10). In the figures below, the spatial results are shown. The following numerical results show the solution of the differential game where $T = 0.25$, $\alpha = 1$, $r_{E_0} = .5$, $r_{O_0} = 1$ and $\theta_0 = \frac{\pi}{6}$.

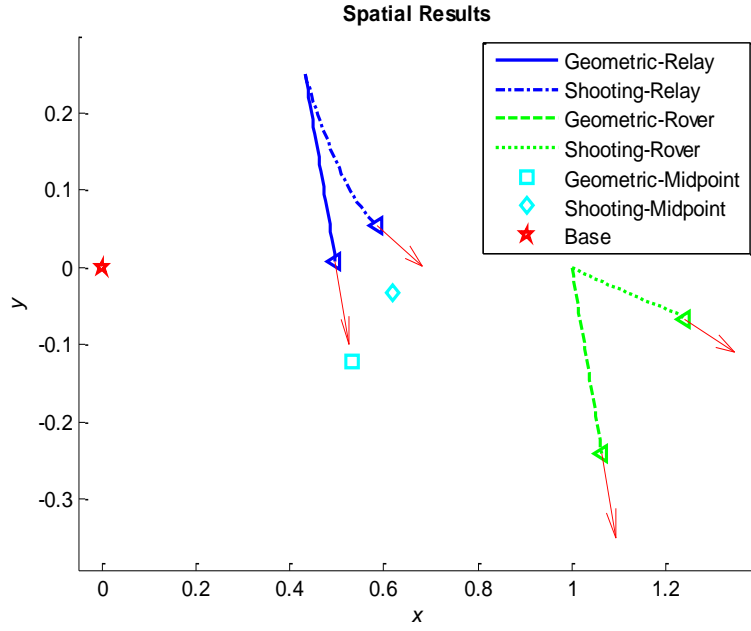


Figure D. 3: Relative Spatial Results for $T = .25$, $\alpha = 1$, $r_{E_0} = .5$, $r_{O_0} = 1$ and $\theta_0 = \frac{\pi}{6}$

The following numerical results show the solution of the min-max problem where $T = .49$, $\alpha = 1$, $r_{O_0} = 1$ and $\theta_0 = \frac{\pi}{3}$.

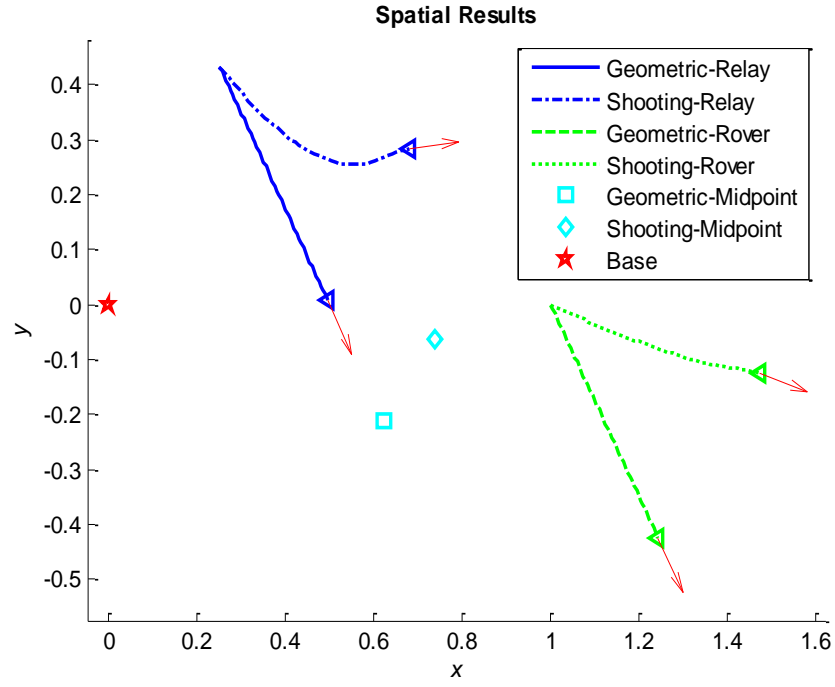


Figure D. 4: Relative Spatial Results for $T = 1$, $\alpha = 1$, $r_{E_0} = .5$, $r_{O_0} = 1$ and $\theta_0 = \frac{\pi}{3}$

Bibliography

- [1] Goldenberg, D., Lin, J., Morse, A. S., Rosen, B. E., and Yang, Y. R., “Towards Mobility as a Network Control Primitive,” *Mobihoc '04*, ACM, 24-26 May 2004
- [2] Isaacs, R.: Differential Games – a mathematical theory with application to warfare and pursuit, control and optimization. SIAM 1965
- [3] L. S. Pontryagin, V. G. Boltyanskii, R. V. Gamkrelidze, and E. F. Mishchenko, *The Mathematical Theory of Optimal Processes*, John Wiley, 1962
- [4] Polya, G. : How to Solve It, Princeton University Press, 1973
- [5] V. Gutenmacher and N. B. Vasilyev, *Lines and Curves*, Birkhäuser Boston, 2004, pp. 23-24
- [6] Pachter, M., J. Hansen, D. Jacques and P. Blue: “Optimal Guidance of a Relay Aircraft to Extend Small Unmanned Aircraft Range”, *International Journal of Micro Air Vehicles*, to appear.
- [7] John H. Hansen, “Optimal Guidance of a Relay MAV for ISR Support Beyond Line-Of-Sight”, AFIT thesis, 2008

REPORT DOCUMENTATION PAGE				Form Approved OMB No. 074-0188	
<p>The public reporting burden for this collection of information is estimated to average 1 hour per response, including the time for reviewing instructions, searching existing data sources, gathering and maintaining the data needed, and completing and reviewing the collection of information. Send comments regarding this burden estimate or any other aspect of the collection of information, including suggestions for reducing this burden to Department of Defense, Washington Headquarters Services, Directorate for Information Operations and Reports (0704-0188), 1215 Jefferson Davis Highway, Suite 1204, Arlington, VA 22202-4302. Respondents should be aware that notwithstanding any other provision of law, no person shall be subject to a penalty for failing to comply with a collection of information if it does not display a currently valid OMB control number.</p> <p>PLEASE DO NOT RETURN YOUR FORM TO THE ABOVE ADDRESS.</p>					
1. REPORT DATE (DD-MM-YYYY) 16 06 2011		2. REPORT TYPE Master's Thesis		3. DATES COVERED (From – To) March 2010 – June 2011	
TITLE AND SUBTITLE A Relay-Rover Differential Game				5a. CONTRACT NUMBER	
				5b. GRANT NUMBER	
				5c. PROGRAM ELEMENT NUMBER	
6. AUTHOR(S) Youngdong Choi, Captain, ROKAF				5d. PROJECT NUMBER	
				5e. TASK NUMBER	
				5f. WORK UNIT NUMBER	
7. PERFORMING ORGANIZATION NAMES(S) AND ADDRESS(S) Air Force Institute of Technology Graduate School of Engineering and Management (AFIT/ENY) 2950 Hobson Way, Building 640 WPAFB OH 45433-8865				8. PERFORMING ORGANIZATION REPORT NUMBER AFIT/GAE/ENY/11-J06	
9. SPONSORING/MONITORING AGENCY NAME(S) AND ADDRESS(ES) AFRL/RBCA Tele:(703)255-8680 Phillip Chandler Wright Patterson AFB, OH 45433 Email:chandler@wpafb.af.mil				10. SPONSOR/MONITOR'S ACRONYM(S) AFOSR	
				11. SPONSOR/MONITOR'S REPORT NUMBER(S)	
12. DISTRIBUTION/AVAILABILITY STATEMENT APPROVED FOR PUBLIC RELEASE; DISTRIBUTION UNLIMITED.					
13. SUPPLEMENTARY NOTES This material is declared a work of the U.S. Government and is not subject to copyright protection in the United States.					
14. ABSTRACT Guidance laws are developed to optimally position a relay Micro-UAV (MAV) to provide an operator at the base with real-time Intelligence, Surveillance, and Reconnaissance (ISR) by relaying communication and video signals when the rover MAV performing the ISR mission is out of radio contact range with the base. The ISR system is comprised of two MAVs, the Relay and the Rover, and a Base. The Relay strives to minimize the radio frequency (RF) power required for maintaining communications, while the Rover performs the ISR mission, which may maximize the required RF power. The optimal control of the Relay MAV entails the solution of a differential game. Suboptimal solutions are also analyzed to gain insight into the solution of the differential game. One suboptimal approach investigated envisages the Rover to momentarily remain stationary and solves for the optimal path for the Relay to minimize the RF power requirement during the planning horizon. The one – sided optimal control problem is solved. Another suboptimal approach is based upon the geometry of the system: The midpoint between the Rover and the Base is the location which minimizes the RF power required, so the Relay heads toward that point—assuming that the Rover is stationary. At the same time, to maximize the required RF power, the Rover runs away from the Relay.					
15. SUBJECT TERMS Differential Game, Optimal Control, End Game Control, MAV, Isaacs method					
16. SECURITY CLASSIFICATION OF:			17. LIMITATION OF ABSTRACT UU	18. NUMBER OF PAGES 161	19a. NAME OF RESPONSIBLE PERSON Dr. Meir, Pachter
a. REPORT U	b. ABSTRACT U	c. THIS PAGE U			19b. TELEPHONE NUMBER (Include area code) (937) 255-3636, ext 7247 (meir.pachter@afit.edu)

Standard Form 298 (Rev. 8-98)
Prescribed by ANSI Std. Z39-18